# ENHANCED SOLAR STILL PERFORMANCE USING MIX WETTABILITY SURFACE COVER AND THERMOELECTRIC COOLING SYSTEM

NURSYAHIRAH BINTI MOHD SHATAR

FACULTY OF ENGINEERING
UNIVERSITI MALAYA
KUALA LUMPUR

2023

# ENHANCED SOLAR STILL PERFORMANCE USING MIX WETTABILITY SURFACE COVER AND THERMOELECTRIC COOLING SYSTEM

**NURSYAHIRAH BINTI MOHD SHATAR**

**THESIS SUBMITTED IN FULFILMENT OF THE REQUIREMENTS FOR THE DEGREE OF DOCTOR OF PHILOSOPHY**

**FACULTY OF ENGINEERING**
**UNIVERSITI MALAYA**
**KUALA LUMPUR**

**2023**

**UNIVERSITI MALAYA**

**ORIGINAL LITERARY WORK DECLARATION**

Name of Candidate: NURSYAHIRAH BINTI MOHD SHATAR

Matric No: S2101051/1

Name of Degree: DOCTOR OF PHILOSOPHY

Title of Dissertation: ENHANCED SOLAR STILL PERFORMANCE USING MIX WETTABILITY SURFACE COVER AND THERMOELECTRIC COOLING SYSTEM

Field of Study: ENERGY (NEC 521: MECHANICS AND METAL WORK)

I do solemnly and sincerely declare that:

(1) I am the sole author/writer of this Work;
(2) This Work is original;
(3) Any use of any work in which copyright exists was done by way of fair dealing and for permitted purposes and any excerpt or extract from, or reference to or reproduction of any copyright work has been disclosed expressly and sufficiently and the title of the Work and its authorship have been acknowledged in this Work;
(4) I do not have any actual knowledge nor do I ought reasonably to know that the making of this work constitutes an infringement of any copyright work;
(5) I hereby assign all and every rights in the copyright to this Work to the Universiti Malaya ("UM"), who henceforth shall be owner of the copyright in this Work and that any reproduction or use in any form or by any means whatsoever is prohibited without the written consent of UM having been first had and obtained;
(6) I am fully aware that if in the course of making this Work I have infringed any copyright whether intentionally or otherwise, I may be subject to legal action or any other action as may be determined by UM.

Candidate's Signature Date: 26/12/2023

Subscribed and solemnly declared before,

Witness's Signature Date: 26/12/2023

Name:

Designation:

**ENHANCED SOLAR STILL PERFORMANCE USING MIX WETTABILITY SURFACE COVER AND THERMOELECTRIC COOLING SYSTEM**

## ABSTRACT

Water purification using renewable energy sources is prevalent to produce clean water for human consumption and sanitation. Solar still is a water distillation method that uses solar energy as a heat source to produce fresh water. Selection of a solar still condensing cover material remains a challenge, particularly for enhancing the condensate formation and collection. Therefore, this research proposed the application of a mixed wettability surface on the solar still condensing cover. A water-based silicone coating is used on a glass cover with different surface areas. Furthermore, utilisation of thermoelectric water-cooling system with varying cooling power was included to further enhance the rate of condensation on the solar still cover. Comparison in solar still performance between the use of mix wettability cover and other commonly used cover materials which includes uncoated glass, polycarbonate (PC) and acrylic (PMMA) with thermoelectric cooling was conducted. For solar still without cover cooling, the addition of coating showed improvement to the solar still productivity with the highest freshwater output at 30% coated surface area. For solar still using water cooling without thermoelectric, the productivity was enhanced by 10% and 26% for glass cover and mixed wettability cover, respectively but reduced by 21% and 22% for solar still using PC and PMMA cover, respectively when subjected to low solar radiation. Increasing the thermoelectric cooling power from 12 W to 36 W increased the solar still productivity for glass and mix wettability cover to 76% and 126%, respectively compared to the reference solar still. However, PMMA and PC covers had lower productivity compared to the reference solar still by up to -48% and -82%, respectively. A detailed analysis on the energy, exergy, environment and economic of the solar still using mix wettability cover and thermoelectric cooling showed that the system had an energy and exergy efficiency of

14.3% and 4.3%, respectively using 36 W cooling power. While the cost per litre, $CO_2$ mitigation, enviro-economic and exergo-economic was found to be 0.036 $/L, 2.97 tonnes $CO_2$, $ 83.21 and 4.64 kWh/$, respectively. Hence, the research outcome highlights the superior performance of using mix wettability surface combined with thermoelectric cooling for solar still application.

**Keywords:** Cover material, Desalination, Mix wettability surface, Solar still, Thermoelectric cooling

**PENINGKATAN PRESTASI ALAT PENYULINGAN SOLAR MENGGUNAKAN PERMUKAAN CAMPURAN KEBOLEHBASAHAN DAN SISTEM PENYEJUKAN TERMOELEKTRIK**

## ABSTRAK

Pembersihan air menggunakan sumber tenaga boleh diperbaharui adalah lazim untuk menghasilkan air bersih bagi kegunaan manusia dan sanitasi. Alat penyulingan solar merupakan kaedah penyulingan air yang menggunakan tenaga suria sebagai sumber haba untuk menghasilkan air tawar. Pemilihan bahan penutup pemeluwapan bagi alat penyulingan solar masih menjadi cabaran, terutamanya untuk meningkatkan pembentukan dan pengumpulan kondensat. Oleh itu, penyelidikan ini mencadangkan penggunaan permukaan kebolehbasahan campuran pada penutup pemeluwapan alat penyulingan solar. Salutan silikon berasaskan air digunakan pada penutup kaca dengan luas permukaan yang berbeza. Tambahan pula, penggunaan sistem penyejukan air termoelektrik dengan kuasa penyejukan yang berbeza ditambah untuk meningkatkan lagi kadar pemeluwapan pada penutup alat penyulingan solar. Perbandingan dalam prestasi alat penyulingan solar menggunakan penutup kebolehbasahan campuran dan bahan penutup lain yang biasa digunakan termasuk kaca yang tidak disalut, polikarbonat (PC) dan akrilik (PMMA) dengan pengunaan penyejukan termoelektrik telah dijalankan. Bagi alat penyulingan solar tanpa penyejukan penutup, penambahan salutan menunjukkan peningkatan kepada produktiviti alat penyulingan solar dengan pengeluaran air tawar tertinggi pada 30% keluasan permukaan bersalut. Untuk alat penyulingan solar menggunakan penyejukan air tanpa termoelektrik, produktiviti telah dipertingkatkan sebanyak 10% dan 26% untuk penutup kaca dan penutup kebolehbasahan campuran, masing-masing tetapi dikurangkan sebanyak 21% dan 22% untuk alat penyulingan solar yang menggunakan penutup PC dan PMMA, masing-masing apabila digunakan pada sinaran suria yang rendah. Meningkatkan kuasa penyejukan termoelektrik daripada 12 W

kepada 36 W meningkatkan produktiviti alat penyulingan solar untuk kaca dan penutup kebolehbasahan campuran masing-masing kepada 76% dan 126% berbanding alat penyulingan solar rujukan. Walau bagaimanapun, penutup PMMA dan PC mempunyai produktiviti yang lebih rendah berbanding alat penyulingan solar rujukan, sehingga -48% dan -82%. Analisis terperinci mengenai tenaga, exergy, alam sekitar dan ekonomi bagi alat penyulingan solar menggunakan penutup kebolehbasahan campuran dan penyejukan termoelektrik menunjukkan bahawa sistem mempunyai kecekapan tenaga dan exergy sebanyak 14.3% dan 4.3%, masing-masing menggunakan kuasa penyejukan 36 W. Manakala CPL, mitigasi $CO_2$, enviro-economic dan exergo-economic didapati sebanyak 0.036 $/L, 2.97 tan $CO_2$, $ 83.21 dan 4.64 kWj/$. Oleh itu, hasil penyelidikan menyerlahkan prestasi unggul menggunakan permukaan kebolehbasahan campuran digabungkan dengan penyejukan termoelektrik untuk aplikasi alat penyulingan solar.

**Kata kunci:** Alat penyulingan solar, Bahan penutup, Penyahgaraman, Permukaan campuran kebolehbasahan, Penyejukan termoelektrik

**ACKNOWLEDGEMENTS**

First of all, I would like to give praise to Allah S.W.T, who has blessed and guided me to complete my PhD thesis. I would like to express my greatest gratitude and appreciation to my supervisors, Assoc. Prof. Dr. Mohd Faizul Mohd Sabri, Dr. Mohd Faiz Mohd Salleh and Assoc. Prof. Dr. Mohd Hanafi Ani for their dedication, time and effort in supervising and assisting me throughout the whole process of research and experimentation. For their guidance and support in every step that I take to assert myself in academia and start my career as a researcher. A million thanks to NanoMicro Engineering lab mates for their advice and support throughout my entire study. My difficulties in research and publishing were eased with the help of my lab mates and for that, I am forever grateful to them.

Thank you to my parents, Dr. Mohd Shatar and Dr. Kamilah Hanum for all their help in supporting me throughout my entire PhD journey. Especially to my mother for taking care of my daughter from birth until the end of my studies. Thank you to my siblings, cousins, and friends for their emotional support throughout my study. Finally, a special thank you to my husband, Muhammad Ainuddin Mohd Azani, for his never-ending support and love from the start of my studies to finally completing my PhD. I love you very much and thank you for all your hard work in raising our two children. Thank you to all involved in the completion of this thesis and may God bless all of you and repay your kindness InsyaAllah.

## TABLE OF CONTENTS

## LIST OF FIGURES

## LIST OF TABLES

## LIST OF SYMBOLS AND ABBREVIATIONS

| | | |
|---|---|---|
| $A_c$ | : | Cover area ($m^2$) |
| AMC | : | Annual maintenance cost |
| ASV | : | Annual salvage cost |
| $A_w$ | : | Basin area ($m^2$) |
| $C_p$ | : | Specific heat capacity (kJ/kg.K) |
| CPL | : | Cost per litre |
| CRF | : | Capital recovery factor |
| CSS | : | Conventional solar still |
| DS | : | Double slope solar still |
| ED | : | Electrodialysis |
| $Ex_{in}$ | : | Exergy output of solar still (W) |
| $Ex_{out}$ | : | Exergy input (W) |
| F | : | Fixed cost |
| FAC | : | First annual cost |
| $h_{c,cw-c}$ | : | Convective heat transfer coefficient ($W/m^2.K$) |
| $h_{ev}$ | : | Evaporative heat transfer coefficient($W/m^2.K$) |
| $h_{fg}$ | : | Latent heat of vaporization (J/g) |
| $h_{t,w-c}$ | : | Total heat transfer coefficient ($W/m^2.K$) |
| Irr | : | Solar radiation ($W/m^2$) |
| $I_{TEC}$ | : | TEC input current (A) |
| $I_{total}$ | : | Total solar irradiance ($W/m^2$) |
| M | : | Annual productivity ($L/m^2$) |
| $m_c$ | : | Mass of cover (kg) |
| MED | : | Multi-effect distillation |

| | | |
|---|---|---|
| $\dot{m}_{ev}$ | : | Freshwater yield (kg/m$^2$) |
| MSF | : | Multi-stage flash |
| PC | : | Polycarbonate |
| PMMA | : | Polymethyl methacrylate (acrylic) |
| $Q_{ev}$ | : | Evaporative heat transfer (W) |
| RO | : | Reverse osmosis |
| S | : | Salvage value |
| SFE | : | Surface free energy |
| SS | : | Single slope solar still |
| SSF | : | Sinking fund factor |
| $T_a$ | : | Ambient temperature (°C) |
| TAC | : | Total annual cost |
| $T_c$ | : | Cover temperature (°C) |
| $T_{c, in}$ | : | Inner cover temperature (°C) |
| $T_{c, out}$ | : | Outer cover temperature (°C) |
| $T_{cw}$ | : | Cooling water temperature (°C) |
| TEC | : | Thermoelectric cooler |
| $T_v$ | : | Vapour temperature (°C) |
| $T_w$ | : | Water temperature (°C) |
| $T_{w-c}$ | : | Temperature difference between water and cover (°C) |
| VC | : | Vapour compression |
| $\dot{W}_{pump}$ | : | Pump power (W) |
| $\dot{W}_{TEC}$ | : | TEC input power (W) |
| $\alpha$ | : | Absorptivity |
| $\eta$ | : | Energy efficiency for conventional solar still (%) |
| $\eta_{ex}$ | : | Exergy efficiency (%) |

| | | |
|---|---|---|
| $\eta_{TEC}$ | : | Energy efficiency for TEC cooled solar still (%) |
| $\eta_{wc}$ | : | Energy efficiency for water cooled solar still (%) |
| $u$ | : | Standard uncertainty |

## LIST OF APPENDICES

# CHAPTER 1: INTRODUCTION

## 1.1 Background of research

Water scarcity is a major concern worldwide, particularly in high water stress regions. Tackling the issue of water security and safety for consumption and sanitation is among the main agenda to be accomplished through the Sustainable Development Goals 2030 (United Nations, 2022a). Water treatment plants employing desalination processes have been growing in numbers due to the lack of freshwater resources and the abundance of seawater supply. The desalination process can be achieved with minimal carbon footprints using renewable energy such as geothermal, biomass, and solar energy as its thermal energy source (Sharon & Reddy, 2015). Large-scale desalination methods include multi-effect distillation, multi-stage flash, and reverse osmosis, and at a smaller-scale level, methods such as solar still are employed (Panchal & Patel, 2017). Solar still produces freshwater through the evaporation and condensation process, whereby the saline water placed in the basin area evaporates after being heated by the solar energy, and the distillate condensates on the cover of the solar still which enables the collection of freshwaters as shown in Figure 1.1.

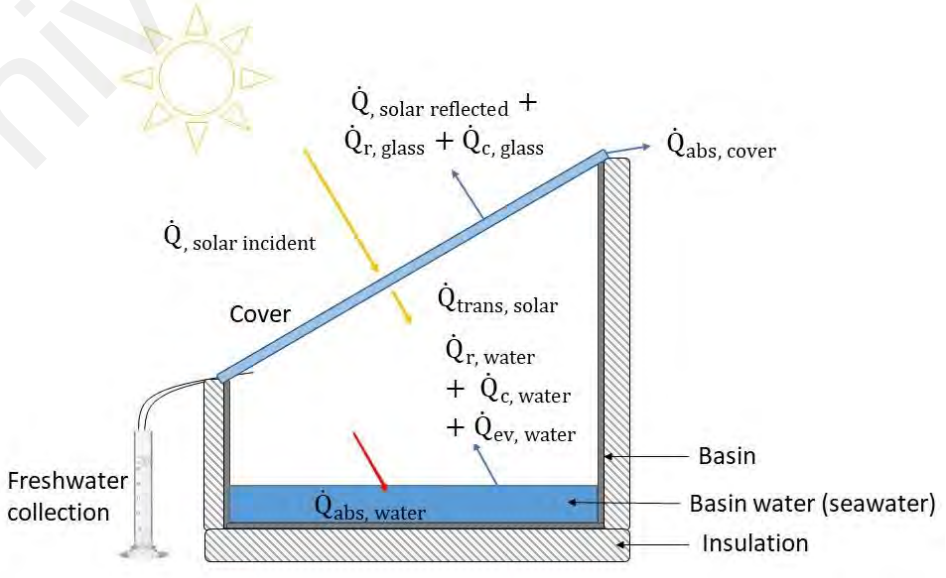


**Figure 1.1: Diagram of the solar still operating principle.**

Solar still is a great desalination method due to its simplicity and versatile design with no moving parts which lowers its setup and maintenance cost. Solar still also requires no operation cost due to the use of free seawater supply and solar thermal energy. However, passive single slope solar still was reported to have low freshwater productivity and efficiency (Mohsenzadeh et al., 2021). Hence, studies on improving solar still freshwater productivity through various modifications have been increasing in recent years.

Solar still productivity is affected by several parameters which include environmental factors such as solar irradiance, wind velocity and ambient temperature as well as the factors relevant to the evaporation and condensation process such as solar still design and operational parameters. While environmental factors are beyond our control, modifications to the design and operations of the solar still allow improvement to the temperature of basin water, basin and cover which results in a high performing solar still (Abu-Arabi et al., 2020). Design of the solar still starts with the selection of the main components which includes the basin, and cover. The most important criterion in the selection of these components is the material. Solar still basin is usually made up of highly conductive materials such as copper and steel to facilitate the heat transfer process between the basin and basin water. The selection of cover material on the other hand is based on the transmissivity of the material to allow sunlight to enter the basin area. Glass has shown superiority over other transparent materials in terms of transmissivity and overall material properties for solar still productivity. However, recent studies have shed some light on the material's wettability property in determining the solar still productivity based on the material's ability to form and collect condensate. The addition of nano-coating on the cover surface to produce a hydrophobic or hydrophilic surface has shown promising results in improving solar still productivity. Hydrophobic surfaces increase the cover heat transfer by allowing the condensate to be easily removed whereas hydrophilic

surfaces are advantageous for condensate formation due to their high surface tension which leads to a higher volume of condensate droplet (Zanganeh et al., 2020a).

In terms of operation mode, conventional solar still is modified from passive to active mode with the inclusion of other components using additional energy from electricity such as a thermal energy collector, reflector, heater, and condenser (Sharshir et al., 2016). Although both methods have shown their ability to increase the freshwater yield as compared to the basic passive solar still, at the fundamental level, the determining factor for the augmentation selection process depends on the temperature of the basin water and cover. The temperature difference between the water and cover drives the desalination process of the solar still due to the condensate formation. Higher temperature difference results in higher condensate formation which increases productivity. This is achieved by either increasing the basin temperature or lowering the cover temperature. There are multiple methods used for increasing the saline water temperature in the basin such as heating using solar thermal collectors, thermal storage materials and nanoparticles (Mu et al., 2021). Whereas cover temperature is lowered through the inclusion of a cooling system to the solar still cover using water or air as the coolant medium (Omara et al., 2017). Utilisation of the thermoelectric cooling module (TEC) has also been adopted as a cover cooling method. The addition of TEC made it possible for a solar still to produce freshwater earlier than the conventional solar still method thus increasing the total freshwater yield (Rahbar & Esfahani, 2012). Furthermore, TEC can be used alongside water and air-cooling systems to provide better cooling distribution on the cover of the solar still (Panchal et al., 2020).

## 1.2 Problem statement

Although cover cooling has been shown to have a positive effect on solar still productivity, there have also been reports of the negative impact of using cover cooling.

Elashmawy (2019) found that an opposite effect was seen when cover cooling was added to the tubular solar still due to the minor difference between the water temperature and cover temperature for a small basin size. The longer duration of the cover cooling flash tactic (15 minutes on 15 minutes off) showed poorer freshwater yield compared to the shorter duration (5 minutes on 5 minutes off) for similar water flow rates (Morad et al., 2015). A laboratory experiment on solar still using TEC cooling revealed that the increase in water yield with a higher TEC power input depended on the basin water temperature whereas a low basin water temperature had a negative outcome using higher TEC power (Al-Madhhachi & Min, 2018). Therefore, this raised an issue regarding the optimum cooling requirement to produce maximum freshwater productivity for the cover cooling method.

Furthermore, solar still covers material characteristics, especially surface wettability, has been shown to play an important role in condensate collection. Despite the improvement shown to the solar still performance through the addition of surface coating on the solar still cover, the results showed varied outcomes with the use of a single wettability surface. The usage of silicon (Si) coating on a glass cover to produce a hydrophobic surface resulted in lower solar still productivity compared to an uncoated glass surface when a low tilt angle of 25° was applied. However, the usage of titanium dioxide ($TiO_2$) coating to produce a hydrophilic surface showed better solar still productivity than uncoated glass cover at the same tilt angle. The results observed using a higher cover tilt angle of 45° contradicts this pattern whereby Si coating enhanced the solar still productivity by more than 20% compared to uncoated glass cover while $TiO_2$ coated cover had a dropped in solar still enhancement from 5.7% to 2.3% (Zanganeh et al., 2020a). Moreover, the application of hydrophobic coating led to an increase in the amount of condensate dripping from the cover at low tilt angle due to the reduced surface tension which decreased the solar still freshwater output (Zanganeh et al., 2019).

Depending on the location of the solar still, usage of a low cover tilt angle is necessary to ensure that the solar still receives a high amount of solar radiation for optimum performance (Khalifa, 2011).

Hence, this research proposes solar still using a cover with mix wettability surface to overcome the negative effect of a hydrophobic coating at a low tilt angle while also making use of the improvement associated with the addition of hydrophobic coating. Besides that, an investigation of the optimal TEC cooling system is also necessary to determine the impact of cover cooling on the solar still performance.

## 1.3 Objectives

The main objective of this research is to investigate the effect of incorporating mixed wettability cover and TEC cover cooling on the solar still performance. To achieve this, the study has the following subsequent objectives:

1. To determine the optimal coated surface area of the mix wettability cover that supports both condensate formations and minimises condensate loss due to low tilt angle.
2. To compare the performance of the mix wettability cover with other cover materials (glass, polycarbonate, and acrylic) under both passive mode and water-cooled solar still conditions.
3. To analyse the effect of different TEC cooling power (ranging from 12 W to 36 W) on the various cover materials.
4. To establish the ideal TEC cooling power application for the mix wettability cover solar still based on factors such as freshwater productivity, energy and exergy output, economic viability, and environmental impact.

## 1.4 Methodology

Figure 1.2 depicts the flowchart illustrating the research activities conducted based on the objectives outlined in the previous section. The initial experimental investigation involved a laboratory experiment to determine the optimal coated surface area of the mix wettability cover for passive solar still applications. Subsequent experiments were conducted outdoors, subject to the weather conditions in Malaysia. The second experiment aimed to compare the performance of passive solar stills using a mix wettability cover and other materials (glass, polycarbonate, and acrylic). The third experiment extended the previous one by incorporating a water-cooling system into the solar stills. The fourth experiment explored the integration of a TEC water cooling system with solar stills using the three cover materials. Finally, the study examined the use of a mix wettability cover in conjunction with solar stills employing TEC cover cooling.

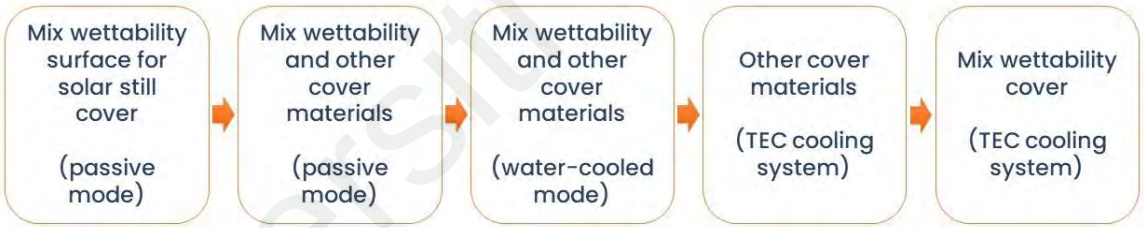


**Figure 1.2: Flowchart of the research activities**

## 1.5 Scope and limitations of research

This research has been conducted by considering the following scopes and limitations:

1. Solar still design

A single slope solar still design was used in this research as it is the most basic design for a solar still. The material selected for the solar still basin was a galvanized iron with a thickness of 1.5 mm for the solar still due to its conductive property which allows a higher rate of heat transfer compared to polymer-based materials (i.e. acrylic basin) to increase the temperature of the basin water. Four solar stills were fabricated with a base

area of 0.25 $m^2$ and one solar still consistently acts as the reference solar still for comparison analysis purposes. The solar still basin was also insulated with a polyethylene foam of 5 cm thickness to minimise the loss of heat to the surroundings. Glass, polycarbonate, and acrylic with a thickness of 3 mm were selected as they are among the commonly used materials for a solar still cover. A cover tilt angle of 25° was selected for this research. This inclination angle was chosen instead of the optimum inclination angle based on the latitude of location (approximately 3°) to reduce the effect of condensate dripping from an almost zero cover inclination angle. Saline water of 3.5% was used as basin water to mimic the salinity of average sea water. The saline water was placed at 1 cm height at the beginning of each experiment as a controlled parameter. A shorter saline water height is preferable to reduce the heating time of the bulk water.

2. Selection of coating used for mix wettability surface and indoor experiment setup

A silicon-based coating was selected due to its ability to produce hydrophobic surfaces based on previous studies. A naturally hydrophilic glass cover was used and modified to become a mixed wettability surface by partially coating the glass surface area with a commercially available water-based polysiloxane sealant to obtain a dropwise condensation mechanism. An indoor lab experiment was conducted at constant ambient temperature, humidity and basin water temperature using a mini acrylic solar still with a base of 0.01 $m^2$.

3. Thermoelectric cooling system design

A laboratory DC power source was employed to apply currents of 2 A, 3 A, and 4 A to the TEC module, resulting in power outputs of 12 W, 27 W, and 36 W, respectively. The deliberate selection of TEC current and power aimed to achieve a minimum cooling water temperature of 20°C, well below the ambient temperature. This decision is crucial

for the efficient cooling of the solar still cover outdoors, ensuring its intended purpose is fulfilled. The TEC setup comprised a single TEC module (40 × 40 mm), with two heatsinks (160 × 100 mm) positioned on the hot and cold sides of the TEC module. Additionally, two heatsinks and two fans were incorporated to dissipate heat by directing air onto the hot side of the heatsink. The parameters of the TEC modules and heatsinks were specifically chosen in accordance with the mentioned cooling water temperature. A single TEC setup was used per solar still and for the experiment conducted on three different solar still covers, three separate TEC setup was designed using the same dimensions. This design was selected to minimise discrepancy in cooling water temperature flowing to the three solar stills which can occur with a bigger setup. All three TECs were connected in series while the fans were connected in parallel. The TEC setup was mounted on an acrylic container filled with water where the heatsink from the cold side was placed inside the container. TEC cooling water flowed down the solar still cover at a flow rate of 2 L/hr which was the optimal cooling water flow rate as established by previous literature.

## 4. Climatic parameters consideration for outdoor experiment

The research was conducted at the Universiti Malaya, Kuala Lumpur, Malaysia (Latitude: 3.118°N/Longitude: 101.656°E). Outdoor experiments were conducted from May to July 2022, leveraging the favourable weather conditions in Malaysia. This timeframe was chosen based on historical weather data, ensuring optimal system performance. The results obtained during this period can also serve as a baseline for future modelling of the solar still's performance throughout the entire year. The experiments were repeated at least twice for a set of solar still design parameters studied. Climatic parameters that include solar radiation, ambient temperature and humidity were

monitored throughout the experiments. Wind velocity is neglected due to the location of the experiment which was not exposed to a high level of wind velocity.

## 1.6 Outline of thesis

This thesis consists of seven chapters. The first two chapters introduce the thesis and provide a comprehensive literature review of the thesis topic. Since this thesis is written in "article style", the subsequent four chapters have been presented as a standalone article with a separate introduction. methodology, results and discussions, and summary. Finally, a conclusion and future work are given to conclude all the summaries presented in the previous chapters based on the objectives of the thesis. Each chapter's information and findings are as elaborated:

1. Chapter two discusses the literature review on the current state of desalination and the application of solar still as a direct desalination method. It highlights past research done on improving the rate of condensation of the solar still through augmentation of the cover which includes variation in cover geometrical design, the addition of cover cooling and cover material properties. This chapter also addresses the limitations of previous studies associated with the augmentation method on solar still performance.
2. Chapter three presents the use of mixed wettability surface on the solar still cover for freshwater productivity enhancement. The introduction and the motivation of the study are given in the first subsection of this chapter. The second subsection elaborates on the methodology of the mix wettability surface fabrication, surface characterisation and the solar still laboratory experiment conducted. The following subsection includes the results and discussion analysis on the effect of mixed wettability with different coated surface areas

on the solar still heat transfer, productivity, and the cost per litre of fresh water. Finally, a summarisation of the chapter is given.

3. Chapter four presents the performance of the solar still using different condensing cover materials and mixed wettability cover with cover cooling technique. This chapter includes an introduction and methodology section for the cover materials used in the study and the cooling system design. The results and discussions subsection are discussed in detail on the use of the different cover materials in passive and water-cooled mode solar still based on the productivity, efficiency and economic. The final subsection summarises the study for this chapter.
4. Chapter five presents the investigation of the performance of solar still with a thermoelectric cooling system for various cover materials. This chapter includes an introduction, the experimental work design and the equations used for the theoretical analysis of the solar still with thermoelectric cooling system design. The next subsection of this chapter discussed the results of the solar still design and the use of different cover materials on freshwater productivity, energy and exergy efficiency, and the cost per litre. The last subsection summarised the significant results of this chapter as presented in the previous subsection on results and discussions.
5. Chapter six presents the energy, exergy, economic and environmental analysis for solar still using mixed wettability cover with thermoelectric cover cooling. This chapter begins with an introduction followed by the methodology of the materials used and the experimental setup and procedures as well as the theoretical considerations for this study. The results and discussions subsection discusses the five main parameters of the solar still performance which include freshwater productivity, energy, exergy, environmental and economic as well

as related parameters such as enviro-economic, exergo-economic and energy matrices. The final subsection summarised the study for this chapter.

6. Chapter seven encompasses the conclusion, novelty and significance of research and recommendations for future works. The research objectives achieved are concluded and the novelty and significance of the work are highlighted. Finally, suggestions for future works are provided in this chapter.

# CHAPTER 2: LITERATURE REVIEW

This chapter focus on the literature review concerning the present state of desalination and the utilisation of solar still as a direct method for desalination. This chapter emphasizes on the prior research conducted to enhance the condensation rate of the solar still by modifying the cover, which involves experimenting with different cover geometrical designs, incorporating cover cooling, and examining cover material properties. Additionally, this chapter discusses the drawbacks observed in earlier studies related to the augmentation approach and its impact on the performance of solar stills.

## 2.1 Overview of the current state of desalination technologies

Clean water availability for both consumption and sanitation are among the theme issues being addressed in the Sustainable Development Goals of the 2030 Agenda. The lack of fresh water in less developed countries is more prominent and it is further aggravated by the growing population, urbanization, and industrialization (United Nations, 2022b). Annual renewable water resources (ARWR) are a well-known water scarcity indicator that gauges the availability of freshwater resources per population in a country. The average annual rate of change in ARWR per capita shows a downward trend with -2.4% in the Sub-Saharan Africa region followed by Oceania at -1.5%, Middle East and North Africa at -1.1%, Asia at -0.8% and Latin America, Caribbean, and North America at -0.5% (Baggio et al., 2021). With the current trend in the change of ARWR, most of the regions are likely to face water scarcity by the year 2050. Therefore, it is critical to take further intervention to achieve the target of ensuring clean water accessibility for all.

Obtaining fresh water through desalination processes has been gaining a lot of interest among researchers. About 70% of the world is made up of water bodies where 97% of it is seawater whereas the other 2.5% is from unavailable freshwater resources such as water

deep underground or highly polluted water (Central California Area Office (CCAO), 2022). Less than 1% of the water supply is usable with renewable water resources amounting to 42,000 $km^3$/year (Food and Agriculture Organization, 2016; Rahbar & Esfahani, 2013). Irrigation activity consumes the highest amount of water, about 69%, whilst industries and municipal sector consume about 19% and 12%, respectively. Table 2.1 shows the amount of water withdrawal by sector for the continents around the world (Food and Agriculture Organization, 2016). With the dwindling renewable freshwater resources, it seems logical to make use of the desalination method to increase the amount of freshwater availability.

**Table 2.1: Amount of water withdrawal by sector around the world in 2016 (Food and Agriculture Organization, 2016).**

| Continent | Municipal (%) | Industrial (%) | Agricultural (%) | Total water withdrawal ($km^3$/yr) |
|---|---|---|---|---|
| Africa | 15 | 4 | 81 | 220 |
| America | 14 | 37 | 48 | 855 |
| Asia | 9 | 10 | 81 | 2421 |
| Europe | 21 | 54 | 25 | 332 |
| Oceania | 20 | 15 | 65 | 25 |
| World | 12 | 19 | 69 | 3853 |

There are two main conventional methods for producing freshwater supply through the desalination process which include thermal distillation such as multi-stage flash (MSF), multi-effect distillation (MED) and vapour compression and membrane technologies such as reverse osmosis (RO) or electrodialysis (ED) (Panchal & Patel, 2017). Currently, there are about 16,000 desalination plants operational, with close to 50% of them located in the Middle East and North Africa region (Jones et al., 2019). The daily total volume of desalinated water production globally is approximately 95.37 million $m^3$. The consumption of fresh water produced from the desalination process by major sectors is as shown in Figure 2.1. In contrast to the renewable freshwater sources withdrawn by sector shown in Table 2.1, the largest consumer of desalinated water is

from the municipal and the industry sector with a total capacity of 88.19 million $m^3$/day. Whereas other sectors, which include power, irrigation, military, and others, consumed a marginal amount of 4.56, 1.69, 0.59 and 0.9 million $m^3$/day, respectively.

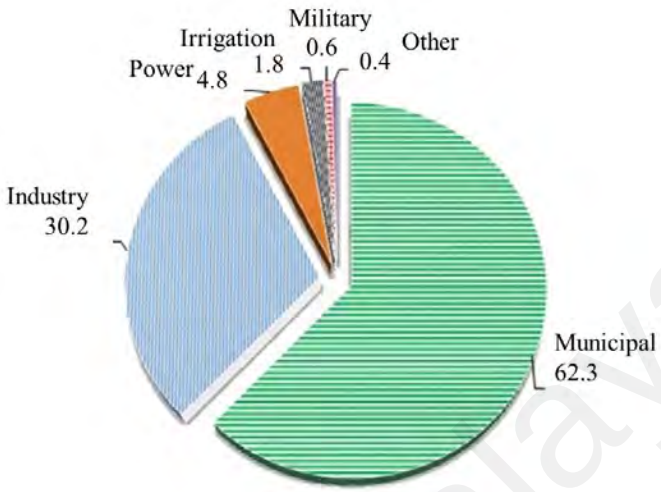


**Figure 2.1: Percentage of desalinated water consumption by sectors.**

Conventional desalination methods are energy intensive. The most common desalination technology applied commercially is the RO technology followed by MSF, MED, Nanofiltration and ED. The energy consumed by RO seawater desalination plants and brackish water desalination plants ranges between 2 kWh/$m^3$ to 7 kWh/$m^3$ and 0.4 kWh/$m^3$ to 3 kWh/$m^3$, respectively (Elsaid et al., 2020). Thermal desalination methods required an even higher energy consumption with MSF desalination plants requiring an even about 3.5 kWh/$m^3$ of electrical energy and 12 kWh/$m^3$ of thermal energy. Whereas MED desalination plants required slightly less electrical and thermal energy of 1.5 kWh/$m^3$ and 6 kWh/$m^3$ compared to the MSF method. Without the usage of renewable energy sources to drive the desalination process, the global warming potential in terms of $CO_2$ can range from 1.78 kg.$CO_2$/$m^3$ to 23.41 kg.$CO_2$/$m^3$ desalted water for MSF, MED, and RO desalination methods (Raluy et al., 2005). Thus, alternative fuel sources from renewable energy were extensively studied for desalination applications to minimise the production of greenhouse gases.

Solar thermal coupled desalination system is one of the extensively researched renewable energies coupled desalination systems (Sharon & Reddy, 2015). Despite the concerns regarding the cost-effectiveness of renewable energy-driven desalination, the cost varies largely depending on the design of the desalination system (Al-Karaghouli & Kazmerski, 2013). Table 2.2 depicts the cost of freshwater produced and the energy required for both renewable and non-renewable driven desalination methods. Among the renewable energy-driven desalination methods, passive solar still has the lowest freshwater cost and requires no electrical energy for freshwater production. Furthermore, conventional solar still mitigates about 20 tons of $CO_2$ in a lifetime (Shoeibi et al., 2021a). Therefore, studies on the improvement of solar still are gaining renewed interest, especially with the possibilities of incorporating new technologies that can further lower its desalinated water cost.

**Table 2.2: Cost of water for various desalination methods using both renewable and non-renewable energy sources (Al-Karaghouli & Kazmerski, 2013).**

| Source of energy | Desalination method | Electrical energy used (kWh/m$^3$) | Cost of water ($/m$^3$) |
|---|---|---|---|
| Non-renewable (Large capacity <10000 m$^3$/day) | MSF (Seawater) | 15.5-27.3* | 0.56-1.75 |
| | MED (Seawater) | 7.5-21.4* | 0.52-1.5 |
| | RO (Seawater) | 2-7 | 0.45-1.62 |
| | RO (Brackish water) | 0.4-3 | 0.26-0.54 |
| | ED (Brackish water) | 2.6-5.5 | 0.6 |
| Renewable (Small capacity >5000 m$^3$/day) | Passive solar still | - | 1.3-6.5 |
| | MED (Solar CSP) | 2-3 | 2.4-2.8 |
| | MED (Geothermal) | 2-3 | 2-2.8 |
| | RO (Solar PV) | 1.5-6 | 6.5-15.6 |
| | RO (Wind) | 1.5-6 | 1.95-9.1 |
| | EDR (Solar PV) | 1.5-4 | 10.4-11.7 |

*Combined with thermal energy converted to equivalent electrical energy

## 2.2 Solar still as a direct solar desalination method

The solar desalination process is divided into direct and indirect methods and the subcategories are as shown in Figure 2.2. The direct method for solar desalination such

as solar still has a few advantages over the indirect method such as having a simple design and low water production cost. A solar still produces freshwater through a distillation process whereby the saline water or brackish water is placed in the basin of a solar still and heated via thermal energy gained from the sun. The evaporation process occurs from the difference in temperature on the condensing surface cover and water and thus, clean water is obtained. The solar still consists of only two main components, the basin and condensing cover as shown in Figure 2.3. Conventional passive solar still cost per litre ranges from 0.0014 $/L to 0.18 $/L while the active solar still cost per litre ranges between 0.006 $/L to 0.29 $/L (Shoeibi et al., 2021b). The "cost per litre" (CPL) acts as an indicator for the cost-effectiveness of the method used for freshwater production, where other economic factors such as the fixed and operating cost are considered. A higher CPL translates to a low-cost effectiveness of the desalination method. Nevertheless, the passive still faced a challenge in its low water productivity compared to other desalination processes despite its low CPL (Kaushal & Varun, 2010). Consequently, improvement to the evaporation and condensation process in the still is required to increase the freshwater productivity of the traditional solar still.

Improvement in freshwater productivity depended on several parameters such as solar irradiance, ambient temperature, wind velocity, basin water temperature and condensing cover temperature. While most of the parameters depended on the environmental factor, the temperature difference between condensing cover and basin water is the determining factor in enhancing freshwater productivity (Manokar et al., 2014). Most of the literature has been more focused on increasing the saline water temperature in the basin while minimizing heat losses in the basin.

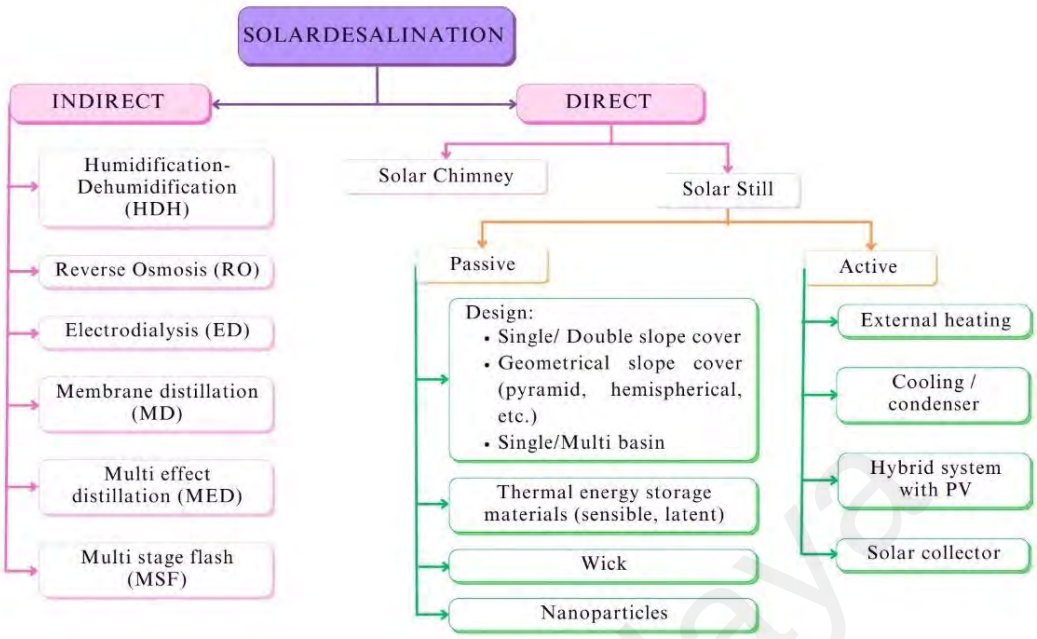


**Figure 2.2: Solar desalination methods.**

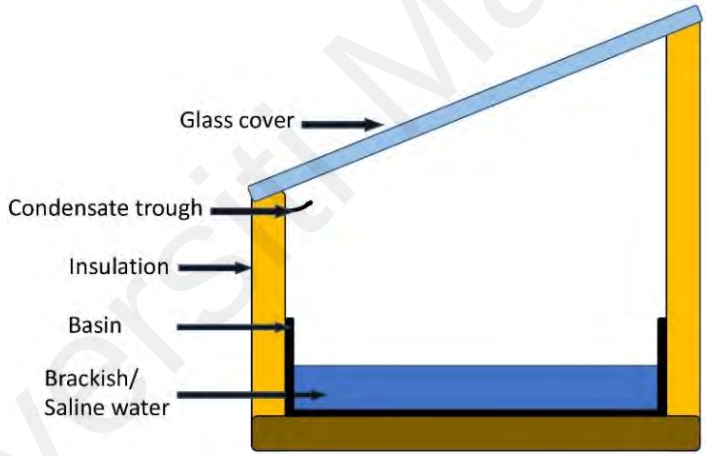


**Figure 2.3: Basic components of passive single slope solar still.**

The usage of sensible and latent thermal storage materials for surface area increment improved the absorptivity of the solar still basin which helped in raising the basin water temperature (Chauhan et al., 2022). Furthermore, the addition of nanomaterials and the use of metal with a high thermal conductivity as the basin material also helps in conducting the heat from the basin to the basin water to raise the water temperature (Alarifi et al., 2021). Besides that, the inclusion of heating elements and solar collectors were also done to promote a higher basin water temperature (Arunkumar et al., 2019a). While these studies were more focused on improving the

evaporation rate, another deciding factor in increasing freshwater productivity is the rate of condensation. The rate of condensation is improved by augmentation of the condensing surface area, in most cases the solar still covers. A review of the cover enhancement methods that includes variation in cover geometrical design for increased condensing surface area, the addition of cover cooling to improve the condensation rate and enhancement of the cover material wettability property must be fully reported to determine the best approach to increasing the solar still productivity through improved condensation rate.

## 2.3 Geometrical design of the solar still covers

Solar still design was manipulated based on changes made to the design of the basin such as by using multi basins in a single still or changing the geometrical design of the condensing cover (Patel & Modi, 2020). Current solar still cover designs include single slope, double slope, pyramid-shaped, tubular-shaped, hemispherical-shaped, and conical-shaped. The single slope is the most basic design for a solar still with the ability to produce a substantial amount of freshwater. Nonetheless, a few weaknesses can be seen in the single slope design such as its inability to capture sunlight from various angles which resulted in shadow formation, thus lowering the water productivity (Sathyamurthy et al., 2014; Tiwari & Tiwari, 2005). In a laboratory experiment, Tiwari and Tiwari (2005) discovered that the freshwater production varies with the solar still inclination with 30° inclination producing the highest yield. Yet, Khalifa (2011) concluded that the optimal tilt angle was similar to the latitude angle of the solar still position. Hence to obtain the best cover inclination angle while minimising shadow formation, Sohani et al. (2021) conducted a study on the usage of reflectors and sun-tracking systems for passive solar still. The addition of both components managed to increase the daily water production by approximately 43% from 1.53 L to 2.19 L. Regardless, the addition of these components increased the CPL of the freshwater produced by 10% compared to the traditional solar

still. Besides that, Fang et al. (2021) investigated the use of a Fresnel lens to concentrate the sun rays on the solar still cover and sides. The addition of this lens improved the yield by 32% more compared to the traditional solar still while maintaining a similar distilled water cost to the conventional solar still.

While these studies were focused on minimising the weakness of a single slope cover by altering the angle of inclination of the cover and optimal solar still positioning for maximising direct sunlight transmitted to the basin, the condensing surface area remained the same for these methods. A past study showed that the condensing cover area had a significant effect on the solar still productivity for equal solar still inclination. Bhardwaj et al. (2015) observed an increase in freshwater production by about 50% when the condensation area was increased by 6.5 times larger from 0.08 $m^2$ to 0.52 $m^2$. Furthermore, comparisons between other cover designs as illustrated in Figure 2.4 showed that the single slope solar still had the highest CPL compared to other designs. Therefore, modification to the condensing cover area has been deemed essential to overcome the limitations that exist from the basic single slope design.

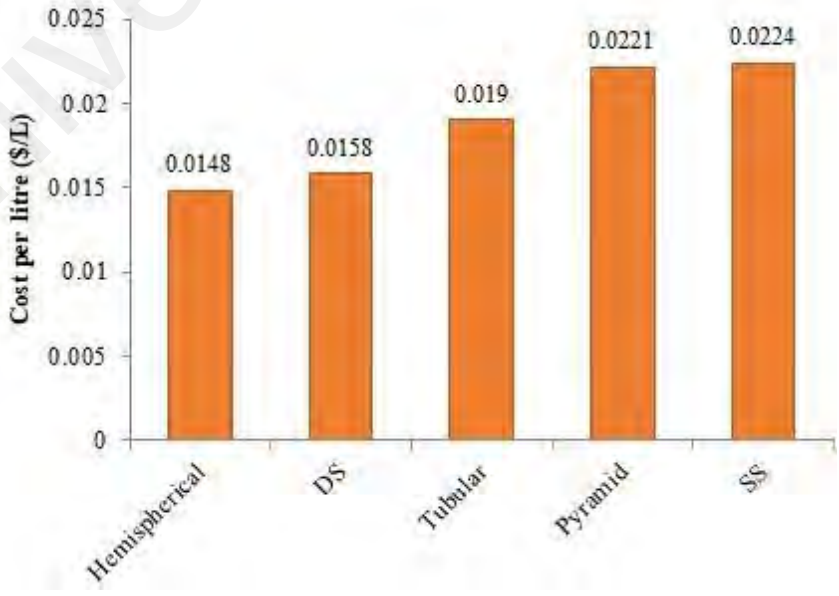


**Figure 2.4: Average cost of distilled water for different cover designs of passive solar still.**

### 2.3.1 Double slope

Double slope solar still is the second most common shape for solar still cover after the single slope. Double slope allowed the solar irradiance to be transmitted into the solar still from two different orientations as compared to one orientation for the single slope as illustrated in Figure 2.5. Double slope solar stills were usually positioned in the east-west orientation for optimal solar irradiance transmission (Elmaadawy et al., 2021; Morad et al., 2015). Despite the ability to increase the solar irradiance transmission via the double slope cover into the solar still basin, Dwivedi and Tiwari (2009) found that the annual freshwater production of double slope solar still was lower than the single slope solar still at 0.01 m water depth with a value of 464.68 $kg/m^2$ and 499.41 $kg/m^2$, respectively. However, Elmaadawy et al. (2021) reported a different pattern where the unmodified double slope solar still obtained a higher yield than the conventional single slope solar still with a value of 3.4 $L/m^2$ and 2.9 $L/m^2$, respectively. Morad et al. (2015) observed an improvement in water productivity for the passive double slope solar still with a brine depth of 0.01 m and glass cover thickness of 3 mm. Other than that, methods involving augmentation of the basin such as the inclusion of thermal energy storage, fins and wick for the double slope solar still showed apparent improvement in water productivity when compared to the unmodified double slope solar still (Tuly et al., 2021).

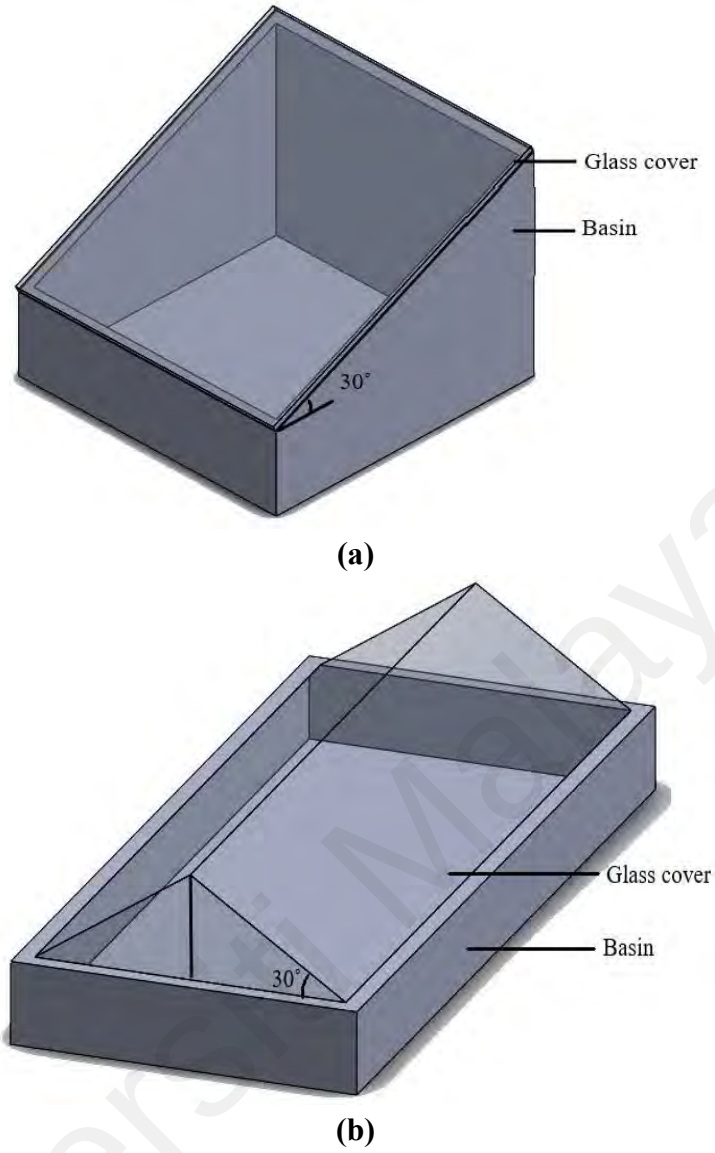


**Figure 2.5: Typical cover design for (a) single slope and (b) double slope solar still.**

### 2.3.2 Tubular-shaped

A growing amount of literature on the tubular-shaped cover solar still was recently seen with a few published review papers specifically on this solar still geometrical design (Ahmed et al., 2021; Kabeel et al., 2020a; Panchal et al., 2019; Sharshir et al., 2019). Tubular solar still can be operated either horizontally or vertically positioned (Ahmed et al., 2021; Hou et al., 2018). Advantages of tubular solar still over other designs include a larger condenser surface area compared to the basin area, portability, and faster freshwater production due to its smaller basin area (Ahmed et al., 2021). The tubular solar still design was found to perform better than the triangular solar still by 20% with a daily

water yield of 1.6 L/m$^2$ and 1.33 L/m$^2$ for tubular and triangular solar still designs, respectively (Rahbar et al., 2018). Other than that, water depth played an important role in determining the maximum basin temperature achievable and the cover temperature (Kabeel et al., 2019; Kabeel et al., 2020b). For the tubular solar still setup as shown in Figure 2.6, Kabeel et al. (2019) found that the freshwater yield dropped with the increase in water depth from 4.2 L/m$^2$ to 3.09 L/m$^2$ for 1 cm and 3 cm depth, respectively. Other techniques used to improve the freshwater productivity of the tubular still include basin modifications using fins, wick materials and vibrated wire mesh, the addition of thermal energy storage materials and nanofluids as well as usage of parabolic concentrator with and without a solar tracking system (Abdelgaied et al., 2021; Elashmawy, 2020; El-Said et al., 2020; Kabeel et al., 2020c; Kabeel et al., 2021).

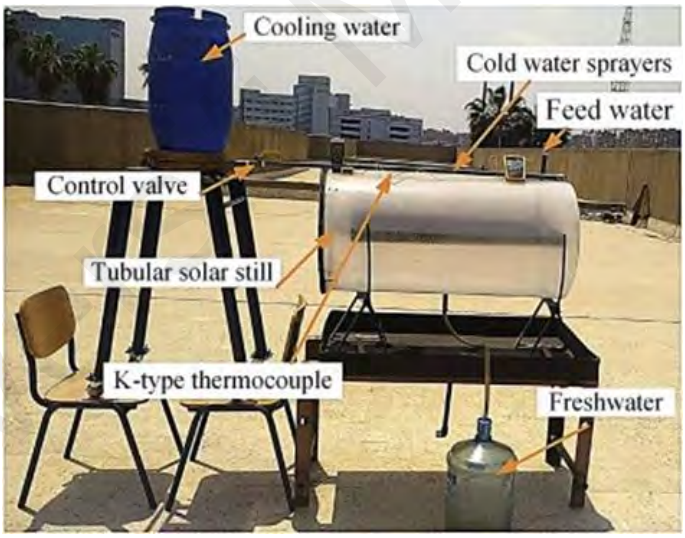


**Figure 2.6: Tubular solar still design (Kabeel et al., 2019).**

### 2.3.3 Pyramid-shaped

Similar to the tubular solar still, the pyramid solar still has garnered much interest among researchers as an alternative cover design for the solar still (Nayi & Modi, 2018). Al-Maddhachi and Smaisim (2021) studied the effect of three different pyramid solar still designs shown in Figure 2.7 which consisted of a triangle, square and pentagon-shaped, on the productivity of the solar still. The authors concluded that a higher number of sides

in a pyramid-styled solar still design increased the overall water production due to the increase in glass cover surface area. A triangle-shaped with a surface area of 1.14 $m^2$ obtained a water output of 1.9 $L/m^2$ whereas a pentagon-shaped with a surface area of 2.16 $m^2$ obtained a water output of 2.4 $L/m^2$. Although a positive effect was seen from the increase in surface area, a larger surface area caused an increase in cost from the amount of material used to build the cover. Similar to single slope solar still, the triangular pyramid solar still freshwater yield was also negatively affected by the increase in basin water depth (Manokar et al., 2020). Sathyamurthy et al. (2014) found that water depth and wind velocity affected the water productivity of triangular pyramid solar still. Water productivity improved with the increase in wind velocity over the cover but reduced with the increase in water depth. Nonetheless, a comparison between the single slope, double slope, and pyramid passive solar still designs showed that the productivity of a single sloped solar still was slightly higher than the double slope and pyramid-shaped one, respectively (Altarawneh et al., 2017; El-Sebaii & Khallaf, 2020). In order to counter the low water production in the passive pyramid solar still, active pyramid solar still had been introduced using methods such as cover cooling and basin water heating (Fallahzadeh et al., 2020; Kabeel & Abdelgaied, 2020; Manokar et al., 2018).

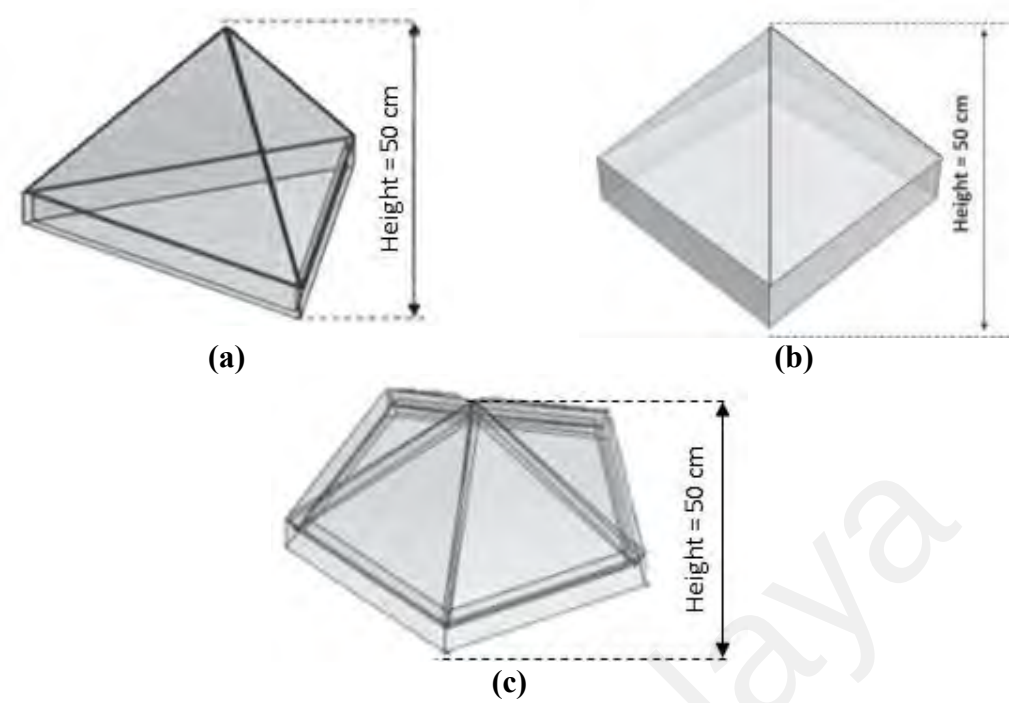


**Figure 2.7: Different number of sides for the pyramidal shape cover designs (a) triangular (b) square (c) pentagon (Al-Maddhachi & Smaisim, 2021).**

### 2.3.4 Hemispherical shaped

Hemispherical-shaped solar still was designed to increase the solar still cover surface area. Attia et al. (2021a) proved that the hemispherical designed cover as illustrated in Figure 2.8 positively affected the freshwater yield as opposed to the single-slope solar still with a daily output of 5.38 kg/m$^2$ for the hemispherical cover and 3.64 kg/m$^2$ for the single slope cover. Besides that, Arunkumar et al. (2012a) found that hemispherical solar still had also shown a higher production value of 3.3 L/m$^2$ compared to pyramid solar still output of 2.73 L/m$^2$ in a day. The efficiency and still conversion ratio of portable hemispherical type solar still with differing saline water depth was studied by Ismail (2009). The author found that both the efficiency and still conversion ratio decreased with an increase in the saline water depth where the daily efficiency reached a peak value of 32.6% and conversion ratio of 49.4% at a saline water depth of 12 mm. Modification on the type of material used for the basin and addition of fins in hemispherical solar still did not affect the temperature of the glass cover, nonetheless, improvement in water productivity existed due to the change in basin temperature (Attia et al., 2021b; Attia et

al., 2021c). Other types of enhancement on the hemispherical solar still included the addition of nanofluid and thermal energy storage material (Attia et al., 2021d; Attia et al., 2022; Bellila et al., 2021; Kabeel et al., 2022).

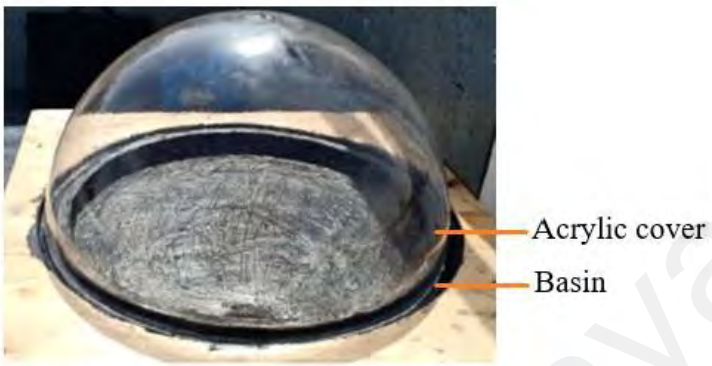


**Figure 2.8: A conventional hemispherical solar still experimental setup (Attia et al., 2021a).**

### 2.3.5 Conical-shaped

Conical-shaped solar still cover as depicted in Figure 2.9, had also been previously investigated. Gad et al. (2015) experimental results showed that the conical solar still design affected the temperature of the acrylic cover where the peak value obtained was 66.5°C around 2 p.m., whereas the cover temperature for the single slope conventional solar still was only 46.5°C. This resulted in a vast difference in accumulated productivity whereby the conical solar still obtained 3.38 L/m$^2$ whilst the conventional solar still only obtained 1.93 L/m$^2$. The effect of inclination angle on the water productivity of conical-shaped solar still cover was investigated by Tiwari et al. (2020). The authors found that an increase in the cover inclination angle for the active conical solar still resulted in an increase in freshwater yield compared to the passive conical solar still. Mishra et al. (2021a) confirmed the results with similar findings where the highest yield obtained by the authors was 6.79 kg/m$^2$.day for the cover inclination of 60°. Also, similarly to other solar still cover designs, an increase in water depth negatively affected the conical solar still productivity whilst improvement to the basin absorptivity resulted in improved productivity (Mishra et al., 2021b).

A summary of the different geometrical cover designs for the passive solar still reviewed in this section is shown in Table 2.3. The highest passive solar still productivity obtained by tubular, double slope, pyramid, hemispherical and conical is 10.2 L/$m^2$.day, 6.38 L/$m^2$.day, 4.43 L/$m^2$.day, 4.08 L/$m^2$.day and 3.67 L/$m^2$.day, respectively. The highest solar still thermal efficiency was from the pyramid cover design at about 60% while other designs' efficiency ranges between 15% to 41%. Although solar still productivity is proportional to thermal efficiency, it does not translate to the still having a high freshwater output. This is seen from the tubular having the larger freshwater output despite the pyramid design's high efficiency. Nonetheless, changing the solar still cover design showed improvement to the solar still productivity in most cases, although a few studies consistently proved that the single slope solar still productivity was comparable to other cover designs.

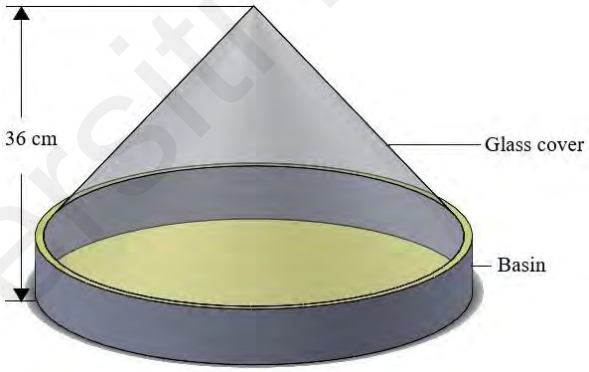


**Figure 2.9: Conventional conical shaped cover solar still.**

**Table 2.3: Summary of different geometrical cover designs for passive solar still.**

| Design | Cover | | | Daily productivity ($L/m^2$) | Reference |
|---|---|---|---|---|---|
| | Inclination (°)/ Area ($m^2$) | Material | Thickness (mm) | | |
| Double slope | 31/- | Glass | 3 | 3.4 | (Elmaadawy et al., 2021) |
| | 25/- | Glass | 3 | 6.38 | (Morad et al., 2015) |
| | 15/- | Plane glass | 4 | 1.11-1.25 | (Dwivedi & Tiwari, 2009) |
| | 35/- | Glass | 4 | 0.7/hr (max) | (Al-Hayeka & Badran, 2004) |
| Tubular | -/0.314 | Plexiglas | 5 | 1.6/hr (average) | (Rahbar et al., 2018) |
| | -/1.57 | Polycarbonate | 15 | 3.09-4.45 | (Kabeel et al., 2019) |
| | -/0.314 | PMMA | 3 | 4.27 | (Elashmawy, 2020) |
| | -/0.212 | Polyethene film, Vinyl chloride sheet | 0.32, 0.05 | 9.18, 10.2 | (Ahsan et al., 2010) |
| | -/0.283 | Glass | 2.5, 5 (airgap) | 5 | (Arunkumar et al., 2013) |
| Pyramid square | 13/- | PMMA | - | 1.59-2.93 (no insulation) | (Manokar et al., 2018, 2020) |
| | 10-60/ 0.063-0.125 | Glass | - | 1.52-4.43 | (El-Sebaii & Khallaf, 2020) |
| | 30.47/- | Glass | 3 | 4.37-4.43 | (Kabeel & Abdelgaied, 2020) |
| | - | PMMA | 3 | 2.73 | (Arunkumar et al., 2012a) |
| Pyramid triangular | 13/- | Glass | - | 0.5-4.3 | (Sathyamurthy et al., 2014) |
| Pyramid triangular/ square/ pentagon | 45/ 1.14-2.16 m | Glass | - | 1.9-2.4 | (Al-Maddhachi & Smaisim, 2021) |

**Table 2.3: Continued.**

| Design | Cover | | | Daily productivity ($L/m^2$) | Reference |
|---|---|---|---|---|---|
| | Inclination (°)/ Area ($m^2$) | Material | Thickness (mm) | | |
| Hemispherical | -/0.377 m | Plastic | 3 | 4.08 | (Attia et al., 2021b; Attia et al., 2021c). |
| | -/1.5 m | Plastic | - | 2.8-5.7 | (Ismail, 2009) |
| | -/2.104 m | PMMA | 3 | 3.66 | (Arunkumar et al., 2012b) |
| Conical | 31/- | PMMA | 5 | 3.38 | (Gad et al., 2015) |
| | 15-75/- | Glass | 3 | 3.67 | (Tiwari et al., 2020) |

## 2.4 Cooling system

Cover cooling is a method that gained the interest of many researchers as a way to aid in the thermal energy removal from the condensing cover. Cover cooling has shown its growing literature body from a few published reviews on this topic (Manokar et al., 2014; Omara et al., 2017; Panchal et al., 2020). Condensing glass cover cooling has been shown to make the most improvement in freshwater productivity of the solar still as opposed to heating the basin water (Sadeghi & Nazari, 2021). Previous literature covered the three main cooling methods which were using air, water and thermoelectric. Air-cooled was done by forced convection through the inclusion of a fan placed near the glass cover (Nazari et al., 2019a). Whereas, water-cooling was done by sprinkling water or allowing a film of water to flow on the glass cover (Morad et al., 2015; Shoeibi et al., 2020). Thermoelectric cooling was achieved using a thermoelectric module that was placed directly on the glass or combined with an air or water-cooling system (Pounraj et al., 2018; Sadeghi & Nazari, 2021; Shoeibi et al., 2020).

### 2.4.1 Water cooling system

#### 2.4.1.1 Film

The commonly used method for solar still cover cooling was by using water films. Abu-Hijleh (1996) highlighted that besides reducing the cover temperature, water cooling acted as a maintenance method by continuously cleaning the cover from dirt and filth. The presence of dirt reduced the amount of solar radiation entering the solar still which negatively affected the solar still productivity. Badran (2007) found that water film cooling further increases the productivity of the passive single slope solar still lined with asphalt by 22% compared to using the asphalt liner alone. Kabeel and Abdelgaied (2020) discovered that glass cooling of pyramid solar still increased the temperature variance between the basin and glass cover by 4°C to 17.5°C compared to without glass cooling. Freshwater production also showed a vast amount of increment with the usage of water cooling and graphite basin ranging from 105.9% to 107.7% for the modified pyramid solar still. Furthermore, Arunkumar et al. (2012b) found that water cooling increased freshwater productivity by about 15% for the hemispherical solar still cover. The daily freshwater yield obtained by the authors ranged from 3.58 $L/m^2$ to 3.68 $L/m^2$ and 4.18 $L/m^2$ to 4.2 $L/m^2$ without cooling and with cooling, respectively. Apart from that, water film between glass covers was also previously investigated by several authors. Mousa and Abu Arabi (2013) found that the addition of water cooling in between glasses improved the total water production for single slope solar still from 1.67 $L/m^2$ to 4 $L/m^2$ in a day. Arunkumar et al. (2013) studied the effect of cooling for a compound parabolic concentrator-concentric tubular solar still. Water cooling with a flow rate of 10 mL/s enhanced the water productivity by 64% compared to the without water cooling. Nonetheless, the addition of water cooling between glass cover can also negatively affect the solar still productivity as observed by Al-Hilphy (2013). The author stated that the drop in productivity was affected by the solar reflection and refraction from the moving

water which diminished the total solar radiation transmitted to the basin water. A similar effect was also seen on tubular solar still with a small basin surface area (Elashmawy, 2019). However, this was due to the minor difference between the water temperature and cover temperature which reduced the rate of evaporation of the solar still.

#### 2.4.1.2 Sprinkler

The water sprinkling method was reported to have a similar effect on the freshwater yield as the water film method. Mamlook and Badran (2007) obtained an improvement of about 21.8% in the solar still productivity using the sprinkler cooling method which was at par with the previous study done by Badran (2007) using the water film method. Water sprinklers for double slope solar still produced a freshwater output of 7.80 L/m$^2$, whereas the production of passive solar still without cooling was 6.38 L/m$^2$ in a day (Morad et al., 2015). A yield of 4.5 L/m$^2$ without cooling to 5.85 L/m$^2$ with cooling was obtained for tubular cover solar still at a cooling flow rate of 2 L/h for 0.5 cm basin water depth (Kabeel et al., 2019). A negative effect on solar still productivity was also seen with the water sprinkler cooling method (Pounraj et al., 2018). However, the effect on freshwater productivity was not as drastic as compared to the water film cooling method.

### 2.4.2 Air cooling

Air cooling was studied for the concentric tubular cover solar still with an airflow of 4.5 m/s (Arunkumar et al., 2013). Freshwater productivity improved by 49% from 2.05 L/day to 3.05 L/day. Air cooling was also studied for a cooling system combined with thermoelectric modules where the addition of cover cooling increased the energy efficiency of the solar still by 20.94% compared to the traditional solar still (Sadeghi & Nazari, 2021). The daily productivity showed a drastic change from 2.75 L/m$^2$ to 4.39 L/m$^2$ with the use of the cover cooling method.

### 2.4.3 Utilisation of thermoelectric cooling modules for cover cooling

The recent trend pointed towards the usage of a thermoelectric cooler as an alternative cover cooling method. A thermoelectric cooler is a solid-state device that operates using the Peltier effect to produce temperature difference between two junctions when connected to a power source. Thermoelectric coolers are commonly used in the automotive, refrigeration and electronics industries due to their versatility and compact sizing (He et al., 2015; Pourkiaei et al., 2019). In solar still application, the thermoelectric cooler is used to cool the solar still cover to improve the freshwater yield. Cover cooling using thermoelectric was achieved either with direct or indirect thermoelectric module contact to the solar still cover. Direct thermoelectric cooling was done by placing the thermoelectric directly on the condensing cover or with the addition of an aluminium plate as the condensing area (Al-Madhhachi & Min, 2017; Pounraj et al., 2018; Rahbar et al., 2016). A cooling medium such as air or water was used for the indirect thermoelectric cooling technique, where the coolant facilitates heat transfer between the thermoelectric cold side and the solar still cover (Nazari et al., 2019b; Shoeibi et al., 2020).

#### 2.4.3.1 Direct thermoelectric cooling

Earlier designs of the solar still using thermoelectric cooling were focused on the direct placement of the thermoelectric cooler as the condensate area, as depicted in Figure 2.10. The performance of the portable single slope solar still with thermoelectric cooling was investigated by Rahbar and Esfahani (2012). The authors reported a large temperature difference between the basin water and thermoelectric cooler of about 28°C occurred at an earlier time, thus making it possible for a solar still to produce freshwater earlier than the conventional solar still method. Besides that, the condensing cover surface with added thermoelectric coolers was seen to have a higher productivity of 3.2 times more than the glass surface without cooling despite having a lower surface area than the glass cover

(Rahbar et al., 2016). Parsa et al. (2020a) reported that cooling using thermoelectric coolers improved the freshwater productivity of the solar still by 5 times higher than using water cooling. However, the usage of heat sinks for the thermoelectric cooler hot side surface increased the overall cost of the solar still system (Parsa et al., 2020a; Rahbar & Esfahani, 2012). Al-Madhhachi and Min (2017) provided a simple solution to the heat sink issue by circulating the basin water over the hot side surface. This method eliminated the usage of heat sinks and allowed basin water to be preheated. Besides that, the addition of water heating combined with thermoelectric cover cooling showed further solar still productivity improvement. Pounraj et al. (2018) found that a total daily yield of 8.77 L was obtained for the solar still with thermoelectric heating and cooling whilst thermoelectric cooling only produced a yield of 3.36 L.

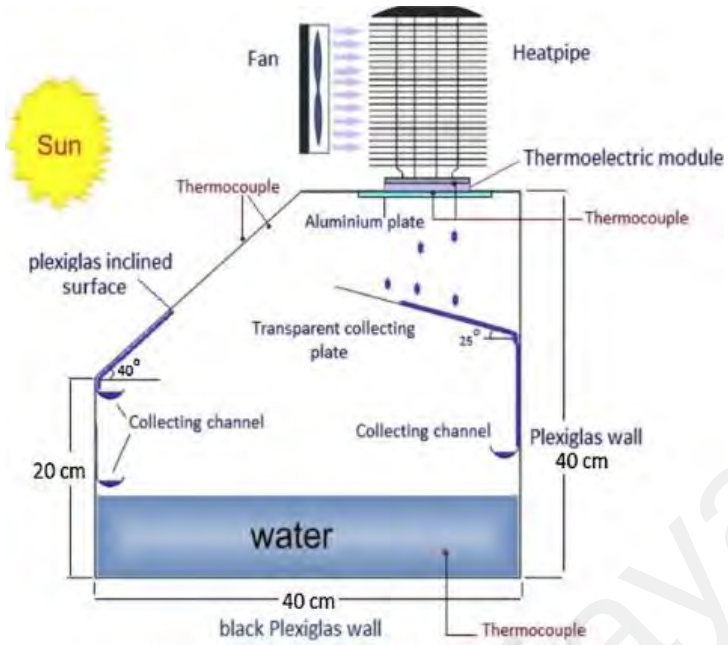


**(a)**

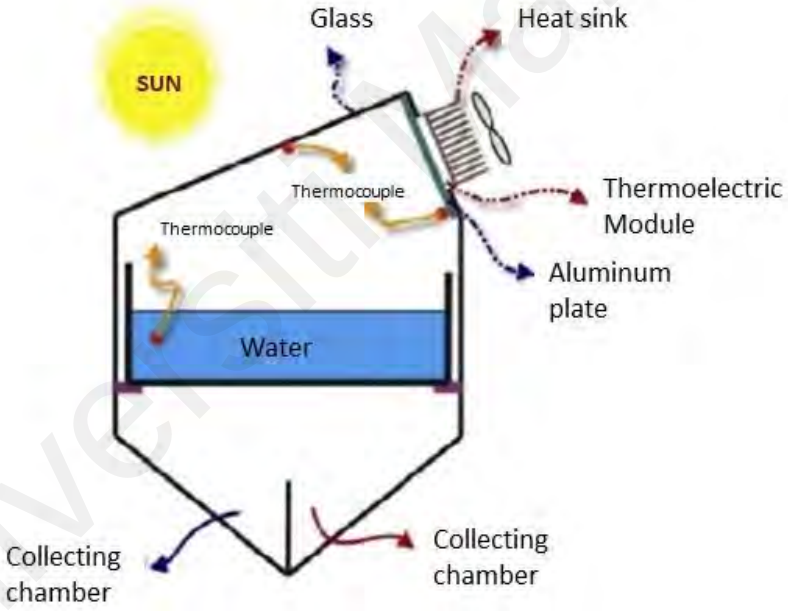


**(b)**

**Figure 2.10: Direct thermoelectric cooling setup for (a) portable solar still design and (b) asymmetrical solar still design (Rahbar et al., 2016).**

#### 2.4.3.2 Indirect thermoelectric cooling using air and water as cooling medium

Newer studies focused more on implementing the indirect thermoelectric cooling technique which allowed versatility in the cover cooling system design as illustrated in Figure 2.11. Simultaneous heating and cooling were also achievable using the indirect thermoelectric cooling method. Shoeibi et al. (2020) studied the effect of thermoelectric

for simultaneous heating and cooling using water coolant on the double slope solar still. The authors found that the productivity and efficiency of the solar still increased by 2.3 times and 76.4%, respectively with the addition of the thermoelectric system. Fan assisted-thermoelectric cooling system was combined with water heating using a concentrating evacuated tube collector (Sadeghi & Nazari, 2021). The addition of the cooling and heating system improved the hourly freshwater production to 6.625 $L/m^2$ compared to 4.390 $L/m^2$ with just thermoelectric cooling. The inclusion of nanofluid and phase change material was also studied for fan-assisted thermoelectric cover cooling systems (Nazari et al., 2019b, 2019a; Remeli et al., 2019). A study on the exergo-economic and enviro-economic of air and water cooling with thermoelectric showed that water cooling is more productive than air cooling whereby the CPL obtained for air and water cooling was 0.277 $/L and 0.243 $/L, respectively (Shoeibi et al., 2021c).

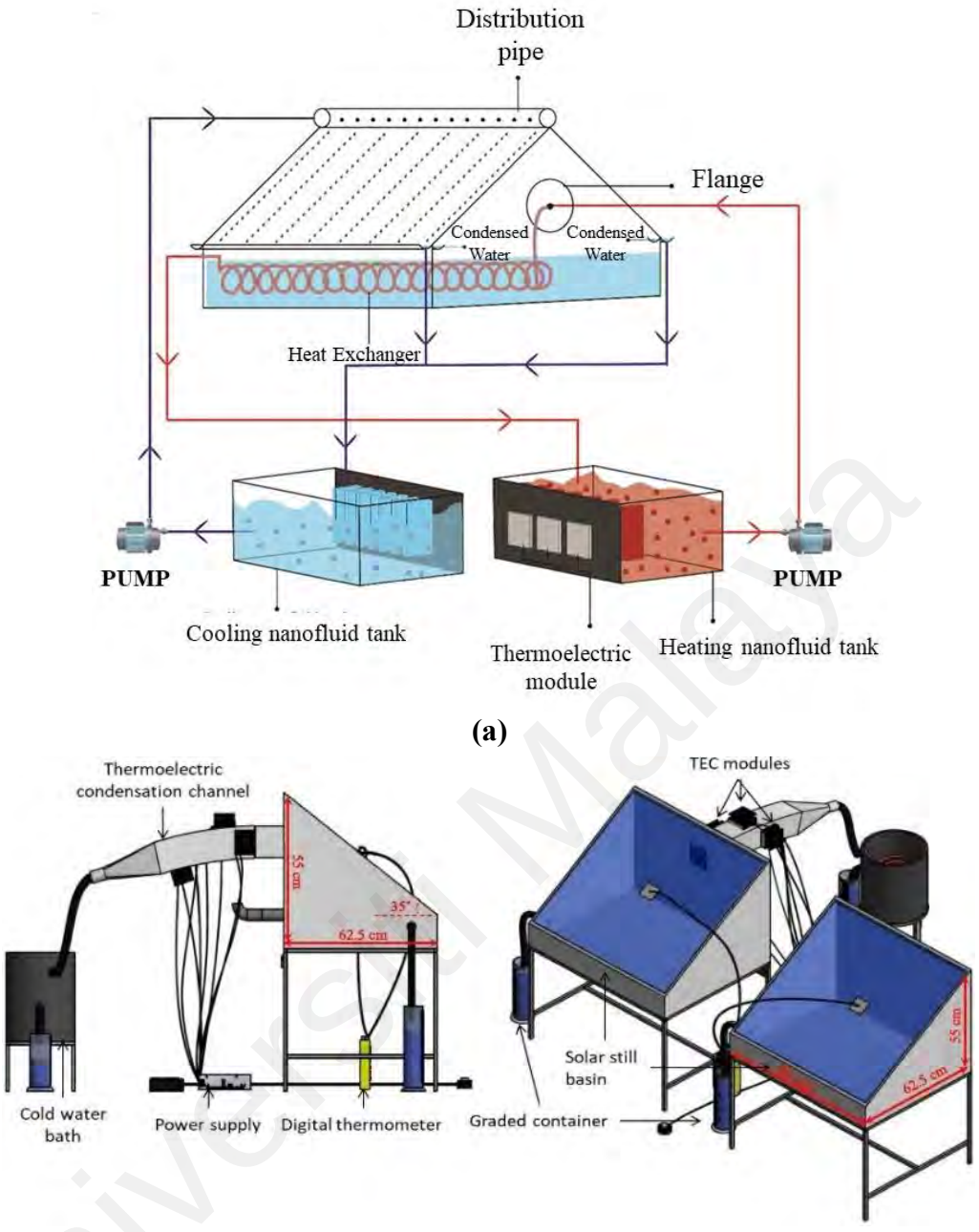


**Figure 2.11: Indirect thermoelectric cooling setup using (a) a water-assisted simultaneous cooling and heating system (Shoeibi et al., 2021d) and (b) a fan-assisted cooling system (Nazari et al., 2019a).**

### 2.4.4 Thermal management for solar still cooling system

The relationship between glass cover temperature and the basin water temperature had mostly shown to be directly proportional to one another in the single slope solar still (Kabeel et al., 2019). This indicates that a lower cover temperature affects the basin water temperature by lowering it to a certain extent. This does not necessarily affect the freshwater productivity of the solar still, particularly if the temperature difference is large

between the cover and basin water (Parsa et al., 2020; Rahbar & Esfahani, 2012; Sharshir et al., 2017). However, controlling the rate of cooling is imperative to avoid inducing a negative effect on freshwater productivity from the lowered cover and basin water temperature difference (Elashmawy, 2019). Several studies have been conducted on the thermal management of the cover cooling for both water cooling and thermoelectric cooling systems through variation of cooling rates as summarised in Table 2.4.

**Table 2.4: Effect of varying cooling rate to the solar still productivity.**

| Cooling method | Cover | | | Daily productivity ($L/m^2$) | Reference |
|---|---|---|---|---|---|
| | Design | Thickness (mm) | ΔTb-g (K) | | |
| Water film (5-15 mL/s) | SS | - | ~2-12 | 4 (10 mL/s) CSS: 1.67 | (Mousa & Arabi, 2013) |
| Water film (time-based: 5, 10, 15 min on/off cooling) | DS | 3 | ~2-13 | 7.8 (5 min on/off cooling) | (Morad et al., 2015) |
| Water sprinkler (1-4 L/hr) | Tubular | 15 | 10-22 | 5.23-5.85 (highest at 2L/hr) | (Kabeel et al., 2019) |
| TEC-12706 Fan aided (vol. flow rate vapor: 60, 120, 180 L/min) | SS | 4 | 0.2-5.3 | No fan: 32.9%, 60 L/min: 36.6%, 120 L/min: 37.2%, 180 L/min: 39.6% (Increased from CSS: 3.2) | (Nazari et al., 2019a) |

Mousa and Abu Arabi (2013) found that the effect of cover cooling with a cooling water flow rate beyond 10 mL/s is minimal to the single slope solar still productivity. This was due to the drop in basin water temperature which reduced the rate of evaporation. Kabeel et al. (2019) found that the cooling water flow rate does not have a linear relationship to the solar still productivity. The authors found the optimal flow rate for the highest freshwater production was 2 L/hr followed by 3 L/hr, 1 L/hr and 4 L/hr. Although both studies focused on varying the cooling water flow rate, there are a few other parameters that affect the productivity and efficiency of solar still such as the cooling water film thickness and glass cover length (Abu-Hiljeh, 1996; El-Samadony &

Kabeel, 2014). Another thermal management technique used was by varying the duration of cooling water flow on the solar still cover. Morad et al. (2015) studied the effect of the flash cooling tactic by adjusting the on and off time for the cooling water to 5 minutes, 10 minutes, and 15 minutes. The authors found that the shortest time of 5 minutes on/off for the cooling flash tactic resulted in the highest productivity. For the thermoelectric cooling system, fans were incorporated with the cooling system to facilitate the heat transfer to the cover (Nazari & Daghigh, 2022). The solar still performed the best in terms of water production, efficiency, economy and environment using the highest volume flow rate of vapor (300 L/min) applied to the thermoelectric condensation channel.

Table 2.5 summarises the effect of the various cover cooling methods on solar still productivity. Typically, the cover cooling method using air and water improved the freshwater productivity while maintaining a low water CPL averaging about 0.015 $/L (Arunkumar et al., 2012a; Arunkumar et al., 2012b; Elmaadawy et al., 2021; Kabeel & Abdelgaied, 2020). Whereas the thermoelectric cooling method had a higher CPL compared to air and water-cooling systems with an average of about 0.17 $/L with recent studies showing a downward trend for the water production cost (Esfahani et al., 2011; Nazari & Daghigh, 2022; Pounraj et al., 2018; Rahbar & Esfahani, 2012; Shoeibi et al., 2020). Solar still productivity improvement was much higher using the thermoelectric cooling method although the highest freshwater output obtained was using the water film method with 9.19 $L/m^2$.day for the pyramid cover design. Furthermore, the indirect thermoelectric cooling system enhanced the solar still efficiency to more than 60% compared to other cooling methods' solar still efficiency of about 20%. Hence, the freshwater output and solar still efficiency improvement justifies the usage of thermoelectric cooling systems despite their high CPL.

**Table 2.5: Summary of cover cooling methods applied for solar still.**

| Cooling rate/TEC type | Cover | | | Daily productivity ($L/m^2$) | Reference |
|---|---|---|---|---|---|
| | Design | Inclination (°) | Thickness (mm) | | |
| Water film | | | | | |
| 10 mL/min | Hemispherical | - | 3 | 4.2 | (Arunkumar et al., 2012b) |
| 10 mL/min (5mm air gap) | Tubular | - | 2.5 | 5 | (Arunkumar et al., 2013) |
| 0.03 kg/s | Single slope | 30 | 3.5 | +graphite: 56.15%, +graphite&PCM: 73.8% (Increased from CSS:2.116) | (Sharshir et al., 2017) |
| 40 mL/min (2mm air gap) | Tubular | - | 3 | 2.4 | (Elashmawy, 2019) |
| 3.5 L/min | Pyramid square | 30.47 | 3 | 9.19 | (Kabeel & Abdelgaied, 2020) |
| 10 L/hr | Double slope | 31 | 3 | +TES: 4.2 | (Elmaadawy et al., 2021) |
| Water sprinkler | | | | | |
| - | Single slope | 32 | 4 | +asphalt: 0.9 (max hourly) | (Badran, 2007) |
| 10 mL/min | Tubular | - | 3 | 3.84 | (Elashmawy, 2019) |
| Air-cooled | | | | | |
| 4.5 m/s | Tubular | - | 2.5 | 3.05 | (Arunkumar et al., 2013) |
| Thermoelectric | | | | | |
| TEC-12706 | Portable still | - | 10 | 1.2 | (Esfahani et al., 2011) |
| TEC-12708 | Portable still | 40 | 6 | 0.493 | (Rahbar & Esfahani, 2012) |
| TEC-12708 | Asymmetrical double slope | - | - | 2.9 | (Rahbar et al., 2016) |

**Table 2.5: Continued.**

| Cooling rate/TEC type | Cover | | | Daily productivity ($L/m^2$) | Reference |
|---|---|---|---|---|---|
| | Design | Inclination (°) | Thickness (mm) | | |
| Thermoelectric | | | | | |
| Water & TEC-12704 TEC-12706 | Single slope | 35 | 4 | 3.82, +nanofluid: 4.85, +nanofluid & condenser: 7.66 | (Parsa et al., 2020a) |
| Water assist 3.4 L/h +heating at 4.2 L/h | Double slope | 30 | 3 | +heating: 2.83 | (Shoeibi et al., 2020) |

## 2.5 Cover material properties

Solar radiation is the main thermal energy source for heating basin water in solar still. The productivity of a solar still is highly dependent on the amount of solar radiation transmitted to the basin. The majority of the literature used glass as the solar still cover due to its low absorptivity coefficient which is necessary to prevent the cover from gaining high thermal energy from the solar irradiance (Khanmohammadi & Khanjani, 2021). This ensures that the cover maintains a lower temperature than the basin for the water evaporation process to occur. Furthermore, glass has a high transmissivity coefficient which allows all solar radiation wavelengths, particularly the longer wavelengths, near-infrared (NIR) and visible light (VIS) to pass through (Al-Nimr & Qananba, 2018). The NIR and VIS spectrum which ranges between 0.4 μm to 3 μm radiates the highest amount of heat energy, thus encouraging a higher thermal energy absorption in the basin water. To maximise the amount of solar radiation received by the basin water, studies on the cover material properties, nano-coating and material layering have been done and are further discussed in these subsections.

### 2.5.1 Optical properties

The optical properties of the solar still cover is considered one of the important properties due to its correlation with solar irradiance transmission. Comparisons of the solar still productivity between glass and other transparent plastic materials at a thickness value of 2 mm demonstrated the superiority of glass in producing the highest freshwater output (Bhardwaj et al., 2013; Zanganeh et al., 2020a). One of the reasons for this is due to the transmissivity and transparency of glass in comparison to other clear plastics as shown in Table 2.6.

**Table 2.6: VIS and NIR transmission in glass and plastics (Nazari et al., 2019a; Serrano & Moreno, 2020).**

| Material | Transmission percentage (%) |
|---|---|
| Methacrylate | 95 |
| Smoked glass | 80 |
| Commercial Glass | 90 |
| Polycarbonate | 45 |
| Fibreglass | 69 |

Different cover materials were studied by Ahsan et al. (2010) where a vinyl chloride sheet and polythene film were used as the cover material for tubular solar still. The authors noticed a difference in water productivity for the two materials, however, it was not correlated to the crucial cover thickness parameter. Besides the usage of glass, plastics and metal, a novel study done by Saini et al. (2019) used a semi-transparent PV on the solar still cover with varying ratios of solar cells area to the area of PV module also known as the "packing factor". The authors found that the packing factor had an adverse effect on the solar still productivity whereby an increase in packing factor caused a reduction in the solar still productivity from the small surface area for solar radiation transmission. However, the overall thermal energy efficiency of the system was improved by 57.5% with a packing factor of 0.85 due to the high electricity energy efficiency from the semi-transparent PV.

### 2.5.2 Thermal property

Several different materials have previously been studied to observe the effect of different cover materials on freshwater production. Based on Dimri et al. (2008) model, a condensing cover made of copper produced the highest daily freshwater yield followed by glass and plastic, respectively. This showed that the thermal conductivity value of a condensing cover played a role in productivity. However, recent studies highlighted the insignificance of this parameter due to the small thickness of the solar still cover (de Paula & Ismail, 2021; Zanganeh et al., 2020a). Considering that the thickness correlates with the degree of thermal resistance, a small thickness leads to negligible resistance as compared to other heat transfer resistance. A similar conclusion was drawn by Zanganeh et al. (2019) with regard to the effect of thermal conductivity on the solar still freshwater productivity. The authors found that the solar still productivity was highly affected by the wettability property instead of the material thermal conductivity property where the usage of aluminium and glass cover material resulted in an increase of the volume of condensate compared to other metals with higher thermal conductivity value, such as copper and brass.

### 2.5.3 Wettability property

Besides the optical and thermal properties of the cover material, the wettability property of the material also played a crucial role in condensate collection. Previous studies have highlighted that the material natural water contact angle is a major factor in enabling higher condensate collection. Figure 2.12 illustrates the water contact angle for common materials used as solar still covers. Materials with low contact angles, such as glass and aluminium, were observed to accumulate higher freshwater output than materials with naturally high-water contact angles (Zanganeh et al., 2019; Zanganeh et al., 2020a).

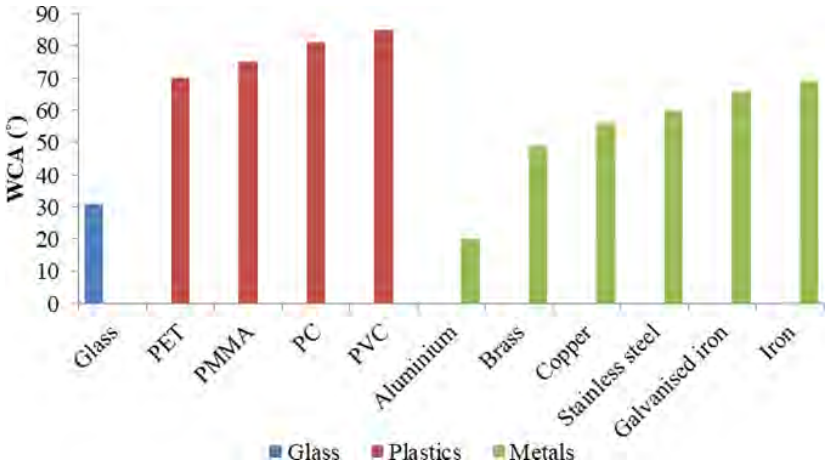


**Figure 2.12: Water contact angle for several materials used as solar still cover (Bhardwaj et al., 2013; Dimri et al., 2008; Zanganeh et al., 2019; Zanganeh et al., 2020a)**.

Nonetheless, altering the material wettability has been shown to have a positive effect on solar still productivity. Zanganeh et al. (2019) found that the addition of nanocoating changed the glass surface topography as illustrated in Figure 2.13. The silica nanocoated surface increased the contact angle of condensate which turned the condensation mode from filmwise to dropwise. The authors observed a considerable amount of improvement in productivity for different cover materials as opposed to without the addition of nanocoating. Coating both the absorber (reduced graphene oxide, rGO) and glass cover (nano-silicon, Si) resulted in a synergetic effect on the conventional solar still. The efficiency increased from 36.3% to 44.2% using only rGO and 49.7% using both rGO and Si coating (Thakur et al., 2022).

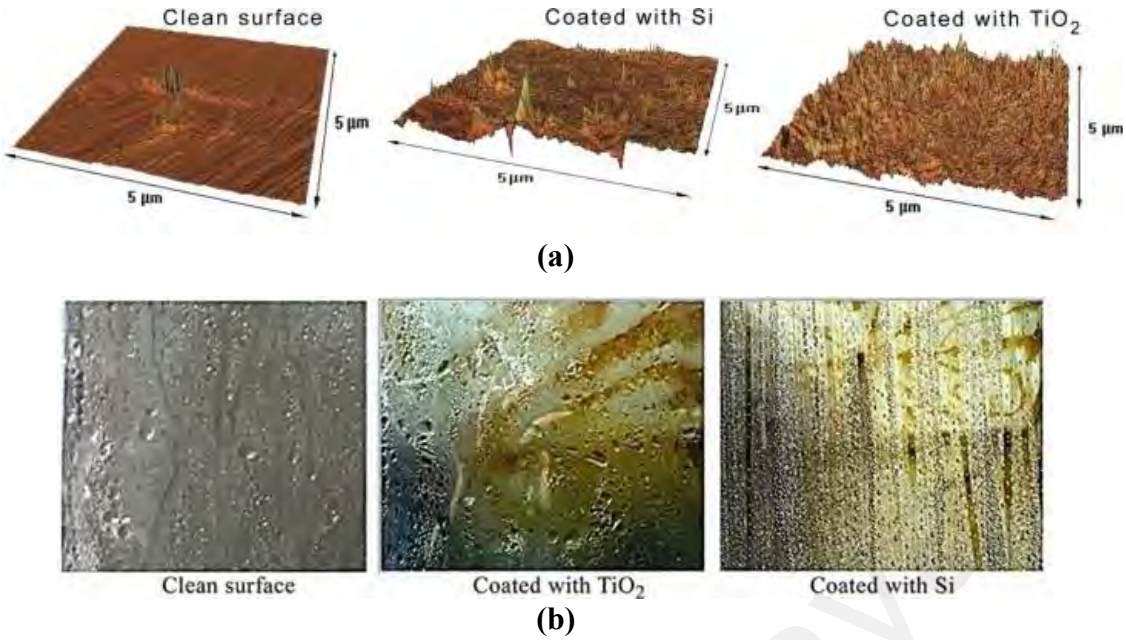


**Figure 2.13: Effects of nano-coating on glass cover (a) topographic images of glass surface before coating and after Si and $TiO_2$ coating; (b) condensate formation on the glass surface before coating and after Si and $TiO_2$ coating (Zanganeh et al., 2020b).**

Furthermore, the addition of nanocoating was attractive economically by the lowered cost per litre from 0.0190 $/L for the clean cover surface to 0.0152 $/L coating (Zanganeh et al., 2020a). However, for inclination below 25°, the filmwise mode was preferable since the dripping effect was enhanced with a smaller inclination angle. Khanmohammadi and Khanjani (2021) agreed that the contact angle played an important role in the condensation collection. The contact angle was manipulated through modification of the hydrophobicity of the surface. Thus, by altering the cover surface into hydrophobic, the freshwater daily productivity was increased to 610 mL as opposed to 480 mL without modification due to the increase in contact angle. However, Bhardwaj et al. (2015) mentioned that a hydrophilic surface might produce a better freshwater output due to its cover clarity which allows higher solar radiation transmission. This was proven by the result obtained by Zanganeh et al., (2020b) where an improvement in productivity was seen from the addition of titanium dioxide coating ($TiO_2$) which reduced the water contact angle, thus producing a hydrophilic surface. Nonetheless, the results showed limitations

in the solar still freshwater productivity as compared to the productivity obtained from the usage of hydrophobic surface as illustrated in Table 2.7.

**Table 2.7: Coating material used for solar still cover (Zanganeh et al., 2019; Zanganeh et al., 2020b).**

| Coating material | Cover material | Inclination angle (°) | Range of productivity ($L/m^2$) |
|---|---|---|---|
| Si | Glass | 10 - 50 | 0.773 - 7.048 |
| | PET | 25/35/45 | 3.380 - 5.154 |
| | PC | | 2.895 - 4.910 |
| | PVC | | 2.810 - 4.876 |
| | Brass | 10/30/50 | 3.612 - 6.500 |
| | Aluminium | | 3.936 - 7.500 |
| | Copper | | 3.612 - 6.580 |
| | Stainless steel | | 3.348 - 5.676 |
| | Galvanised iron | | 3.360 - 5.976 |
| | Iron | | 3.484 - 6.056 |
| | PMMA | | 2.06 - 5.636 |
| $TiO_2$ | Glass | 25/35/45 | 4.876 - 4.940 |
| | PET | | 4.088 - 4.216 |
| | PC | | 3.715 - 3.873 |
| | PVC | | 3.653 - 3.854 |

### 2.5.4 Material layering

A few studies were conducted on the double-layered design of the solar still glass cover as illustrated in Figure 2.14 (Abu-Arabi et al., 2002; Al-Hilphy, 2013; Boutriaa & Rahmani, 2017; Mousa & Arabi, 2013).

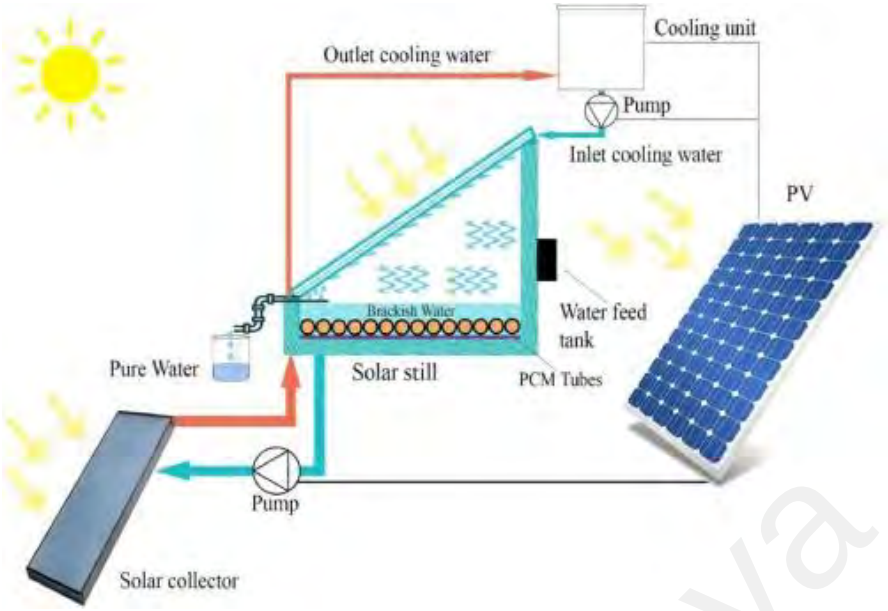


**Figure 2.14: Cooling between double glass with the addition of phase change material and solar collector (Abu-Arabi et al., 2020).**

The double glass design provided an insulation layer which allowed an increase in basin water temperature. Khechekhouche et al. (2019) found that double glass reduced the yield of freshwater by 60% as compared to the single glass cover. This was due to the addition of insulation which blocks the dissipation of heat for the inner glass to ambient, the inner glass temperature increased considerably which lowered the temperature difference between the glass cover and basin water. Nonetheless, the addition of cooling in between the glass cover was able to counteract the negative effect of double layering the cover material during daytime (Abu-Arabi et al., 2002). Freshwater production was almost doubled when double glass was used during nighttime. The added insulation ensured that the basin water temperature remained high even without the availability of solar radiation (Mousa & Arabi, 2013). Figure 2.15 summarises the average productivity of passive single slope solar still with various cover materials. The most promising material to produce a high freshwater output was using material with a low water contact angle such as glass and aluminium. However, material transparency must be considered when choosing a solar still cover since this desalination method utilises the energy from solar radiation. Besides that, addition of coating to increase the material water contact

angle and double glazing for insulation showed favourable outcomes to the improvement of solar still productivity.

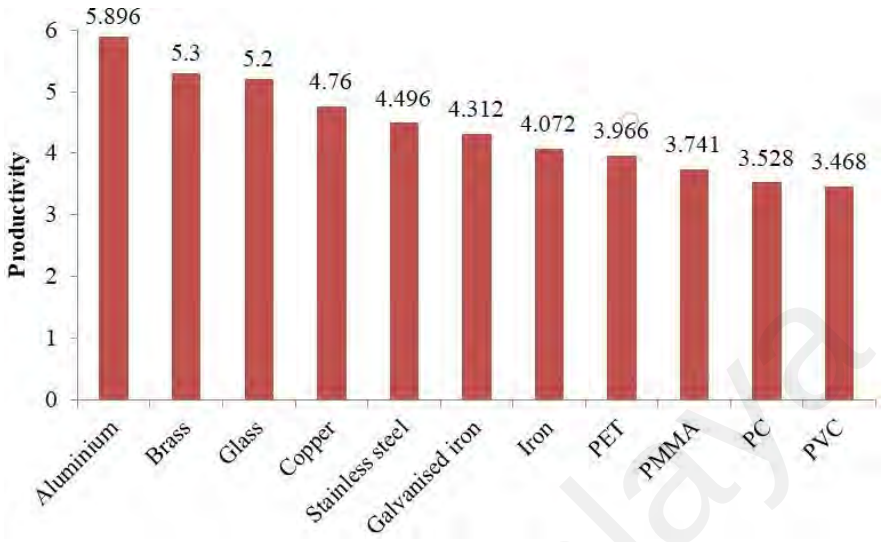


**Figure 2.15: Average freshwater productivity of passive single slope solar still with various cover materials (L/m$^2$) (Zanganeh et al., 2019; Zanganeh et al., 2020b).**

## 2.6 Limitations of previous studies

Solar still proved to be an efficient and cost-effective desalination method which is preferable for a small-scale application. Focus on solar still cover enhancement has been gaining traction among researchers, particularly with the advancement of nanotechnology. Recent findings on the improvement of solar still productivity by cover enhancement showed promising prospects for solar still as a desalination method. Nonetheless, there exist limitations to the solar still cover enhancement discussed in previous sections.

### 2.6.1 Cover surface area

The variation of solar still geometrical design exists to increase the condensation area of the solar still. A large surface area of the condensing cover allows higher heat dissipation and therefore increases freshwater productivity. Furthermore, a larger cover surface area compared to the basin surface area has shown to be advantageous for increasing the heating rate of saline water. An increase in the surface area showed benefits

in terms of reducing the cost per litre as compared to the traditional single slope solar still. Although the construction of the cover complicates the setup of solar still, the availability of accurate theoretical models simplified the decision-making process of developing the design on a larger scale basis (Al-Maddhachi & Smaisim, 2021; Mishra et al., 2021b). Future optimization of the existing model to incorporate other cover parameters such as the material properties, condensate contact angle and cover inclination angle is necessary to further improve the accuracy of the existing model. However, it is important to highlight that while is it cost-effective, the productivity for other cover designs passive solar still maintains in the lower region compared to the single slope solar still (Altarawneh et al., 2017; El-Sebaii & Khallaf, 2020). Other notable factors continue to influence solar still productivity regardless of the cover geometrical design such as the basin water depth and cover thickness. Generally, the basin water depth negatively affects the solar still productivity. Whereas minimising the cover thickness is crucial to diminish the effect of conductive thermal resistance. Besides that, increasing the surface area by variation of geometrical design also risks reducing the amount of direct solar radiation entering the basin. Increasing the number of edges and points also increases the probability of larger shadow formation which has not yet been accounted for in previous studies.

### 2.6.2 Thermal management

Cover cooling allows the temperature of the cover to remain at a much lower level compared to the basin water, however, it also contributes to a slightly lowered basin water temperature. Nonetheless, the tremendous improvement in solar still freshwater productivity is achievable with cover cooling due to its higher temperature between the cover and basin water. While there are advantages between the current cooling method such as the high efficiency of thermoelectric cooling and the dual purpose of the water-cooling method for both cover maintenance and cooling, thermal management has shown

to be an important aspect of the cover cooling system. Currently, thermal management is done by varying the coolant flow rate or duration of flow. However, experimental investigation shows that the cooling flow rate and solar still productivity have a non-linear relationship despite the linearity shown in the solar still model (Abu-Hiljeh, 1996; Kabeel et al., 2019). Besides the variation of coolant flow rate, the time-based thermal management technique should be further investigated due to its limited amount of study. A shorter water sprinkler duration improves solar still productivity due to the minimal solar irradiation refraction time. Besides that, simultaneous heating of basin water and cover cooling shows a favourable outcome which can be further explored with the inclusion of the thermal management technique. Future studies on thermal management for thermoelectric coolers based on other controls such as varying the thermoelectric power output and cooling capacity can also be considered.

### 2.6.3 Material selection

Selection of cover material with good optical and wettability properties is crucial, particularly for designs that make use of solar still cover as its condensing area. Most of the previous studies neglect this aspect while designing the solar still despite the cover material properties having a significant effect on the freshwater outcome. At present, glass is a more commonly used material in solar still due to its superior material properties compared to other transparent plastics at small thickness value because of its high wettability. The addition of coating to the inner glass cover has shown that this method can improve the water productivity of the solar still. The hydrophobic coating produces higher water productivity compared to hydrophilic coating (Zanganeh et al., 2020b). Nonetheless, this improvement was only found for a cover tilt angle of above 30°. For a cover tilt angle of below 30°, it was found that hydrophilic coating contributed to an increase in the solar still performance. The varied results of using a coating to improve the solar still performance highlight the disadvantage of using a single wettability surface

on a solar still cover. Moreover, the fragility of glass compared to other materials also made it necessary for further studies on more durable material to be used as a solar still cover. Concerns about the coating durability and toxicity from coating degradation have not been raised despite it being a major issue in the safety of the water for consumption. These issues need to be addressed in future research on the current and new coating material applied for solar still. Furthermore, there are inadequate fundamental studies on the few parameters of the condensing cover such as the material thermal and optical characteristics and its effects on condensate collection for solar still applications. A fundamental study of the material properties can be the key to determining the importance of this aspect of solar still efficiency and productivity.

## 2.7 Summary of literature review

Several enhancement methods of the solar still condensing cover to improve the solar still productivity have been covered and reviewed. The effect of geometrical cover design which included double slope, tubular-shaped, pyramid-shaped, hemispherical-shaped and conical-shaped on the solar still productivity and efficiency have been discussed. Tubular-shaped produced the highest freshwater output, whereas pyramid-shaped had the best thermal efficiency for passive solar still. The effect of cover cooling on solar still productivity using both conventional and thermoelectric methods was examined. The conventional cooling system showed better cost-effectiveness in freshwater production, however, the thermoelectric cooling system produced a larger freshwater output than its counterpart. Studies on the solar still cover material were also discussed including research on cover coating and material layering. Glass has been established as the most suitable cover material based on its thermal, optical and wettability properties. The cover of a solar still is an essential component of the solar distillation system, hence it is crucial to further explore other cover enhancement techniques to improve the system's productivity, efficiency, and cost-effectiveness.

# CHAPTER 3: MIX WETTABILITY SURFACE ON SOLAR STILL COVER FOR FRESHWATER PRODUCTIVITY ENHANCEMENT

The utilisation of a mixed wettability surface on the cover of a solar still is introduced as a means to enhance freshwater productivity. The first subsection of this chapter provides an introduction and the motivation for the study. The second subsection details the methodology employed for fabricating the mixed wettability surface, conducting surface characterisation, and performing laboratory experiments on the solar still. Subsequently the analysis of results and discussions regarding the impact of varying coated surface areas with mixed wettability on heat transfer, productivity, and the cost per litre of freshwater in the solar still are presented. Finally, a conclusion is provided to summarise the key findings of the chapter.

## 3.1 Introduction

Solar still operates by evaporation and condensation processes to produce fresh water. The evaporation process is driven by the amount of heat gained by the saline water in the basin whereas the condensation process depends on the condensing cover material properties. Previous studies focused on enhancing the solar still productivity via enhancement of either condensation, evaporation or both processes simultaneously (Shoeibi et al., 2021a; Shoeibi et al., 2021d; Shoeibi et al., 2022a). An important component that affects the rate of condensation and evaporation of the solar still is the cover material. The selection of cover material properties is of utmost importance in determining the amount of heat energy received by the still as well as the amount of condensate obtainable by the solar still. A study done by Bhardwaj et al. (2013) found that materials with low contact angles supported a higher water production than hydrophobic surfaces. However, a few studies were inclined towards hydrophobic surfaces to increase the freshwater production of the solar still. The rapid development of

micro and nano materials has paved the way for more efficient solar stills with the incorporation of these materials to further enhance the still's rate of evaporation and condensation (Ding et al., 2017; Peng et al., 2021a; Shoeibi et al., 2022b; Shoeibi et al., 2021e). However, there are some concerns raised regarding the usage of the solar still method combined with the use of coating materials on the environment (Arunkumar et al., 2019b; Som et al., 2011). The consensus dictates that the use of silicone-based coating and solar still for water production showed a low impact on the environment. Fabrication of hydrophobic surfaces was made possible with the development of silicon-based nano-coating (Nguyen-Tri et al., 2019; Sharma et al., 2022). Zanganeh et al. studied the effect of nano-coating on various transparent materials to convert the condensation mechanism of the solar still cover materials. The materials were coated with titanium dioxide to create a filmwise condensation and silicon nanoparticles to create a dropwise condensation. Filmwise condensation showed higher productivity than dropwise condensation for a surface inclination of 25°, however, the opposite was observed for the surface inclination of 35° and 45° where hydrophobic surfaces showed up to 34% increase in freshwater production compared to hydrophilic surfaces (Zanganeh et al., 2020a).

Solar still productivity in terms of condensate collection showed mixed results between the two condensation methods. A hydrophilic surface showed better results for a lower cover inclination angle (less than 30°) whereas a hydrophobic surface is preferred for a higher cover inclination due to a higher rate of surface renewal (above 30°). In order to understand the fundamentals of droplet detachment and condensate formation on surfaces, the effect of surface contact angle towards condensate must first be considered. The wettability of a surface is based on the water contact angle whereby a hydrophilic surface has a contact angle of below 90° while the water contact angle for hydrophobic surfaces is above 90°. Surfaces with water contact angles approaching 0° or 150° are considered super hydrophilic or superhydrophobic, respectively. Superhydrophilic

surfaces possess complete wetting whereas super-hydrophobic show non-wetting characteristics (Song & Fan, 2021). Condensate formation relies on high surface energy that is present on hydrophilic surfaces. A high surface energy promotes a high droplet nucleation rate and thus forms a larger volume of condensate (Jin et al., 2017). Despite that, a hydrophilic surface has a lower threshold in condensate production due to the formation of filmwise condensation that reduces the condensate heat transfer. Furthermore, the hydrophilic surface has low droplet detachment due to its high surface tension thus leading to pooling on the surface's edge (Lee et al., 2012; Lee et al., 2020). Hydrophobic surface forms dropwise condensation which allows good droplet detachment for condensate collection. Moreover, a high condensate removal rate from dropwise condensation increases the rate of surface renewal thus encouraging new condensate to form (Abbasiasl et al., 2021). Therefore, mixed surface wettability has been studied in numerous energy systems applications where condensate drainage is of utmost importance (Edalatpour et al., 2018). Studies on mixed wettability surfaces include investigation on the patterned design of biphilic surfaces as well as wettability gradients of the surface (Deng et al., 2022; Feng & Bhushan, 2020; Han et al., 2021; Tokunaga & Tsuruta, 2020). A combination of both hydrophilic and hydrophobic regions on a surface is termed a biphilic or hybrid surface (Xie et al., 2020). Whereas a gradient or mixed wettability surface refers to a single surface having a combination of areas with different degrees of wettability (Tang et al., 2021). Biphilic and gradient wettability surfaces are achieved via chemical or topographical modification of the surface (Edalatpour et al., 2018). Shen et al. (2020) performed a lattice Boltzmann simulation to study the effect of droplet condensation on gradient wettability surface. The hydrophilic region showed a higher condensation rate and faster condensate formation due to its high surface tension as opposed to the hydrophobic surface. The condensation heat transfer was enhanced by the condensate droplet self-motion from hydrophobic to hydrophilic surface. Water

collection via dewing on various surface wettability was investigated by Lee et al. (2012). The authors observed a similar condensation rate between a moderately hydrophobic surface and a biphilic surface, however, the drainage of the biphilic surface was considerably lower than the hydrophobic surface due to the strong surface tension of hydrophilic covered areas. A study was conducted on the effect of simple repetitive biphilic patterns on an aluminium substrate for condensate recovery. The authors found that the super-hydrophilic surface area ratio (SAR) of 75% to 85% generates maximum condensate recovery by up to 15% greater than the fully super-hydrophilic surface. The poorest condensate recovery was seen for a fully super-hydrophobic surface while a complete super-hydrophilic surface fared better compared to a SAR of 50% (Lee et al., 2020).

More focus has been given to improving the solar still productivity by increasing the evaporation rate of the basin water (Arunkumar et al., 2019b; Faegh & Shafii, 2017; Nazari et al., 2019b). However, condensate formation and recovery are also important aspects in determining the amount of freshwater output achievable. Though the previous study had covered the effect of surface modifications on solar still productivity, the results showed variable outcomes with the use of a single wettability surface. Dripping effects were also prominent on modified surfaces with dropwise condensation particularly at low cover inclination (Wu et al., 2018; Zanganeh et al., 2019). Therefore, this study addresses the need to improve the solar still condensate formation and recovery using a combination of two areas with different degrees of wettability in a single surface also known as mix wettability surface on the condensing cover of a solar still. A low wettability surface promotes droplet nucleation that increases the volume of condensate, whereas a high wettability surface aids in droplet removal for a higher surface renewal rate. By increasing both the volume of condensate and the rate of surface renewal, the rate of condensation is improved thus enhancing the solar still freshwater productivity. This study aims to find

the optimal balance between filmwise and dropwise condensation on a single surface for improved solar still productivity. Analysis of the solar still heat transfer is done through comparative analysis between various coated surface areas on the condensing cover. A cost comparison of the usage of mix wettability and single wettability surface modifications is conducted to examine the cost-effectiveness of using coating for enhancing the solar still freshwater yield.

## 3.2 Methodology

### 3.2.1 Surface fabrication

The material selected for coating was glass due to its performance in producing high freshwater productivity for a solar still compared to other plastic materials (Bhardwaj et al., 2013; Dimri et al., 2008; Zanganeh et al., 2019). Modification to the surface was made by partially coating the glass cover using a commercially available water-based polysiloxane sealant to obtain the dropwise condensation mechanism. This complements the glass surface which is naturally hydrophilic and therefore produces a mix wettability surface on the solar still cover. The silicon-based coating Ecocoat Premier is manufactured by IGL Coatings. The coating was applied to the collection side of the solar still cover to aid in droplet detachment and minimise the pooling effect at the glass cover's edge. The surface area of the solar still cover was 100 $cm^2$ and the coated surface areas were investigated in increments on the same condensing cover as depicted in Figure 3.1 and given in Table 3.1.

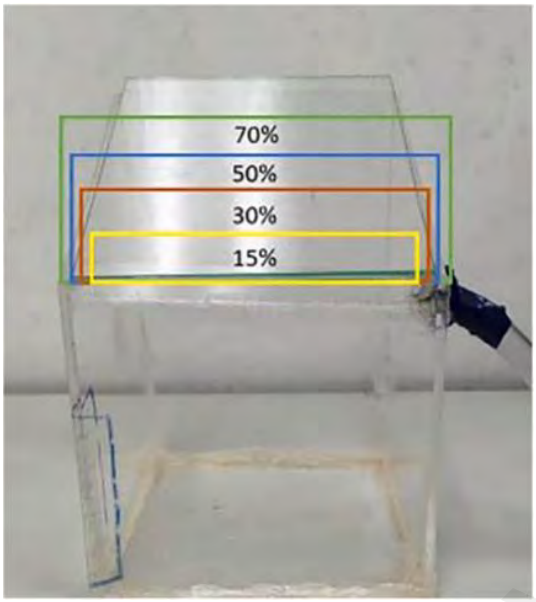


**Figure 3.1: The four different coated areas on the solar still cover.**

**Table 3.1: Coated surface area of condensing cover.**

| Coated surface | Area (cm) |
|---|---|
| 15% | 1.5 × 10 |
| 30% | 3 × 10 |
| 50% | 5 × 10 |
| 70% | 7 × 10 |

Application of this coating was done in two steps, firstly the glass surface was cleaned using IGL Coatings ecoclean precoat. The precoat contains a cleaning agent to remove contaminants from the glass surface to permit sufficient adhesion of Ecocoat Premier coating to the substrate. The cleaning and coating process was done as described in the technical data sheet given by the manufacturer. The following includes the details of the cleaning process:

1. The temperature during application ranged between 20°C and 26°C.
2. The surface was first cleaned using soap and water to remove any visible contaminants on the substrate.
3. Once cleaned, the surface was thoroughly dried before applying the ecocoat precoat.

4. Degreasing was done by polishing the applied precoat using a microfiber cloth to degrease the substrate.

The cleaning process ensures that the surface is cleaned completely to allow a reactive paint surface. The coating's long-term stability and abrasion resistance depend on the quality of the chemical bond created by the coating material with the surface. Hence, Ecocoat Premier was immediately applied to the surface after the cleaning process was completed to ensure zero contaminants on the surface. The coating treatment was done as follows:

1. Ecocoat Premier was properly mixed before being sprayed on a clean microfiber cloth.
2. The product was lightly applied on the surface in a vertical, and then horizontal motion.
3. The areas coated were overlapped to ensure the coating covered the entire coated surface.
4. The coated surface was then polished until the haze disappeared.
5. The coated surface was allowed to cure for 30 min (at room temperature) before a second layer was applied and polished until the haze disappeared.

Surface treatment was done in a controlled environment without direct exposure to sunlight before and during treatment. The substrate was ensured to remain at room temperature during application and precautions were taken to ensure that the surface treatment was successful.

### 3.2.2 Surface characterisation

The contact angle of the coated surface was measured using Attension Theta optical tensiometer. The static contact angle of water for the coated surface was measured at

different points for each coating surface area. The contact angle measurement was repeated at least 3 times in each area. A water droplet of 1 μL was produced on the glass surface. The droplet was triggered, and the contact angle of the water droplet was captured by the camera for a duration of 10 s. A mean contact angle value was obtained from the measured left and right sides of the droplet. The surface free energy (SFE) was also calculated using the equation of state. The surface profile was measured using an atomic force microscope (AFM) from Park Systems. The scanned surface area for both coated and uncoated surfaces was 5 μm × 5 μm. The AFM scan was done by using True Non-Contact mode at a height and frequency of 13 μm and 0.3 Hz.

### 3.2.3 Experimental procedure

A steady-state study was conducted in a controlled environment to gain insights into the effect of coating coverage on the heat transfer process in the solar still without the disturbances of external environmental factors. Figure 3.2 illustrates the laboratory experimental setup. A small solar still prototype was designed and built for an indoor laboratory experiment as given in Figure 3.3 and Table 3.2. The front cover distance was selected based on designs from previous literature (Zanganeh et al., 2019). A data logger and laptop were used to record the temperatures of basin water, vapour, inner cover, and outer cover of the solar still prototype. The experiment was conducted for a period of 110 min with saline water of salinity 3.5% used as the basin water in the solar still. The saline water was first heated to a temperature of 60°C before it was placed in the solar still basin. The temperatures of the solar still parameters were measured using a K-type thermocouple and a NI-USB 9211 data logger. The ambient temperature and humidity level in the laboratory were monitored using a humidity and temperature sensor Benetech GM1361.

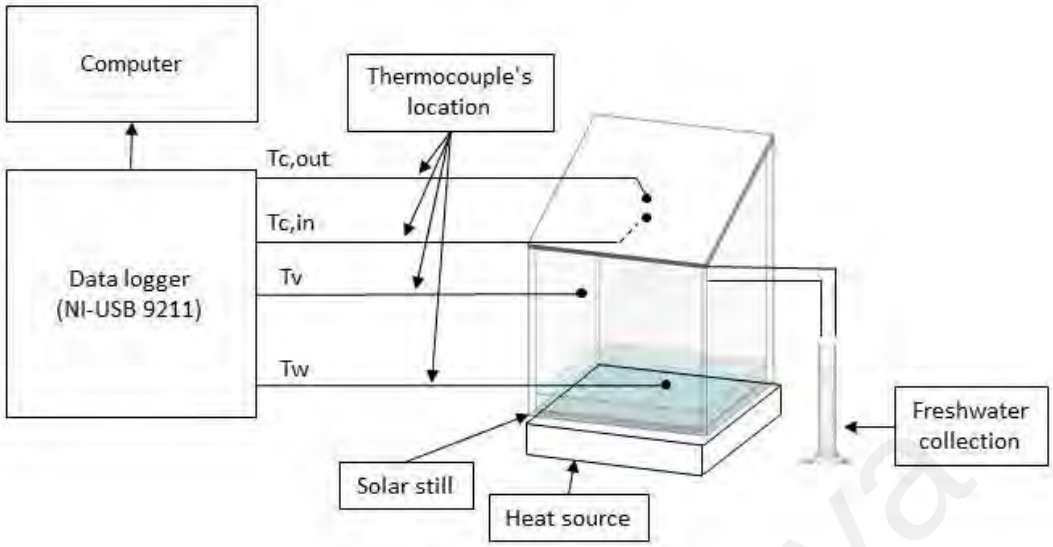


**(a)**

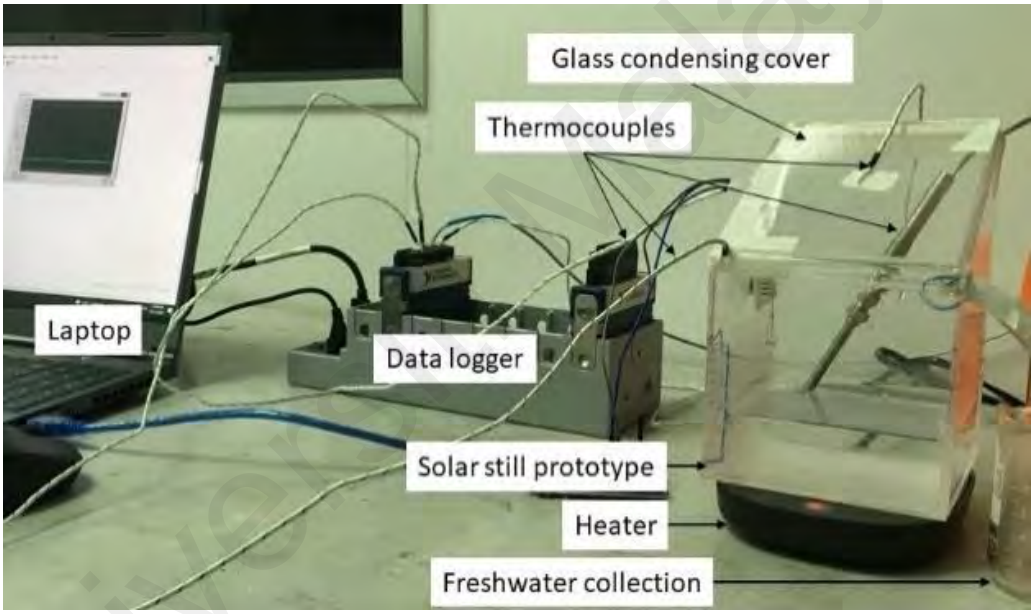


**(b)**

**Figure 3.2: Laboratory experimental setup (a) sketch (b) actual.**

**Table 3.2: Solar still basin parameters.**

| Parameters | Values |
|---|---|
| Water height (m) | 0.01 |
| Area of basin bottom ($m^2$) | 0.01 |
| Wall height low/high (m) | 0.1/0.15 |
| Thickness of basin (mm) | 3 |
| Thickness of cover (mm) | 3 |
| Inclination of cover (°) | 25 |

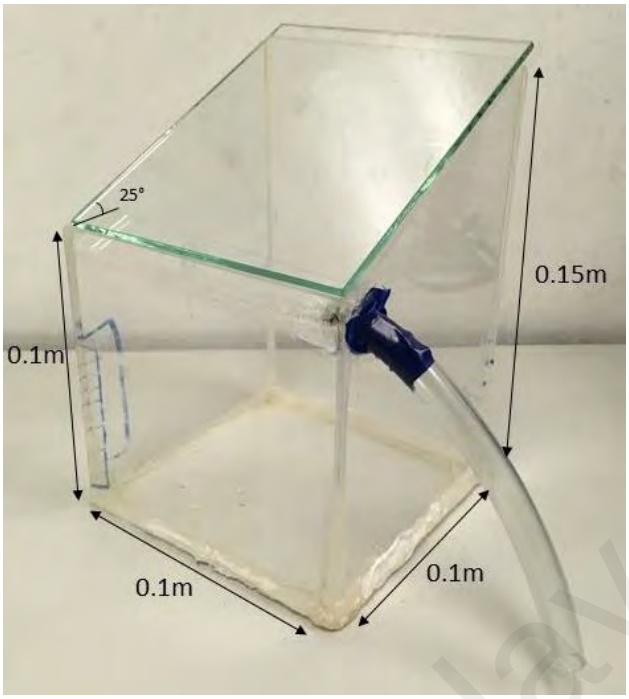


**Figure 3.3: Dimensions of the solar still used in this study.**

The following procedures were employed to ensure the reliability of the experiments and the accuracy of the results.

1. The saline water was brought to a set temperature of 60°C before the measurement was carried out and the temperature was regulated using a heating element to ensure that this parameter remained within the range of 61±1.5°C constant throughout the experiment.
2. Once the set temperature was reached, the cover material was then sealed to ensure no leakage of vapour was present.
3. Laboratory doors and windows were closed to ensure minimum air movement inside the lab during the experiments. The ambient temperature of the laboratory was maintained at 25±1.5°C, and the humidity ranged around 57±5%.
4. The inner cover temperature, outer cover temperature, vapour temperature and water temperature in the still were measured every 10 minutes once the water temperature reached 60 °C and condensate collection began.

5. Total condensate collection was measured after 110 minutes and the experiment was repeated for different coating surface areas with the same inclination angle of 25°.

Accuracies, ranges and standard uncertainty of the components and instruments are listed in Table 3.3.

**Table 3.3: Measuring instruments range and accuracy.**

| Variables | Instrument | Range | Accuracy |
|---|---|---|---|
| Temperature | Type-K thermocouple | 0 - 105°C | ±0.1°C |
| Contact angle | Optical tensiometer | 0 -180° | ±0.1° |
| Fresh water output | Graduated cylinder | 0 - 25 mL | ±0.25 mL |
| Humidity level | Humidity sensor | 0 - 99.9 % | ±0.1%0.62 |

## 3.3 Results and discussion

### 3.3.1 Effect of coated area to the heat transfer of solar still at steady state

The temperature profiles for uncoated cover and different coated surface areas were observed at a constant water temperature, $T_w$, of 61±1.5°C are depicted in Figure 3.4. The vapour temperature, $T_v$, of the solar still for the various coating areas ranged between 45°C and 50°C. At the commencement of the experiment, instances of elevated $T_{c,out}$ arise due to the initial heating phase of the inner cover which was sealed once the water achieved the set temperature of 60°C. The outer cover temperature, $T_{c,out}$, generally maintained a similar temperature for all coating areas between 41°C and 43°C. It was observed that $T_{c,out}$ was sensitive to the change in $T_a$ for the coated surfaces. Despite the increase in $T_{c,in}$, $T_{c,out}$ maintains a temperature range between 41.9°C and 43.9°C whereby the slight temperature change followed the pattern of $T_a$ as shown in Table 3.4.

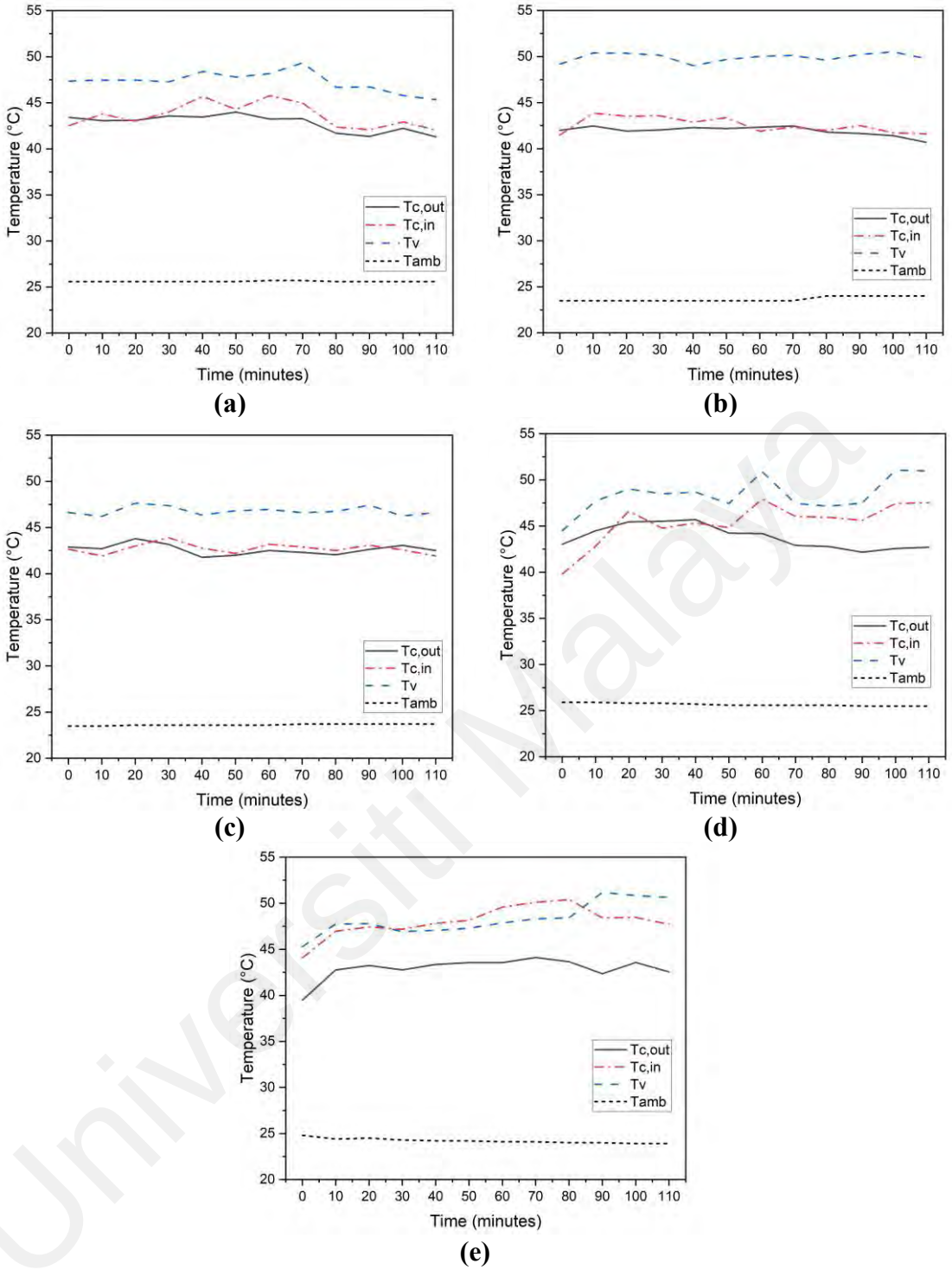


**Figure 3.4: Temperature profile for coated surface areas of (a) uncoated (b) 15% (c) 30% (d) 50% (e) 70%.**

**Table 3.4: Average temperature value for outer cover, inner cover and vapour (water temperature maintained around 60°C).**

| Coated area | $T_a$ (°C) | $T_{c,\,out}$ (°C) | $T_{c,\,in}$ (°C) | $T_v$ (°C) |
|---|---|---|---|---|
| No coat | 25.6 | 42.8 | 43.6 | 47.3 |
| 15% | 23.5 | 41.9 | 42.6 | 49.9 |
| 30% | 23.7 | 42.6 | 42.8 | 46.8 |
| 50% | 25.7 | 43.9 | 45.2 | 48.2 |
| 70% | 24.2 | 42.9 | 48.1 | 48.1 |

The inner cover temperature, $T_{c,in}$, showed changes for different coated surface areas. The AFM scanned surface profile showed an increase in the thickness of the surface with the added layer of coating as illustrated in Figure 3.5.

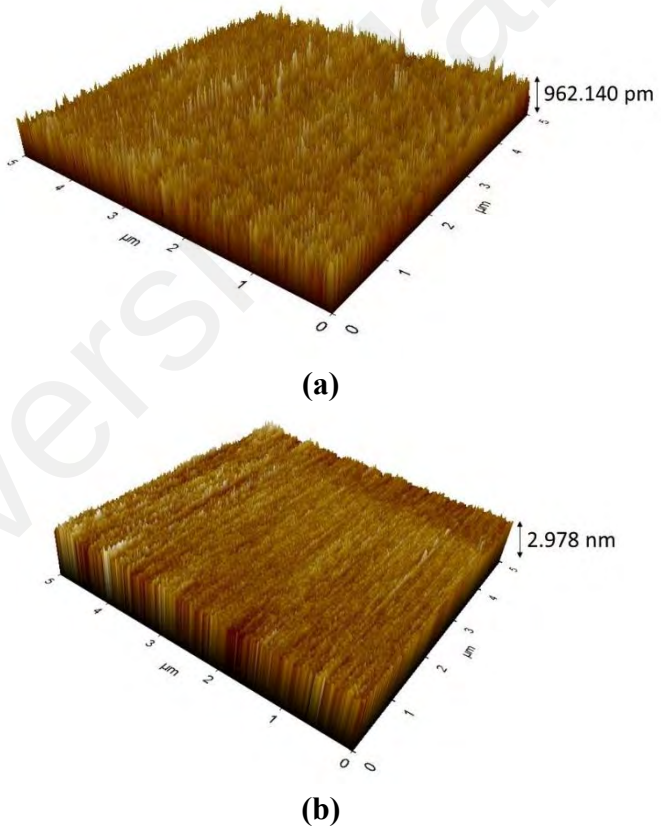


**(a)**

**(b)**

**Figure 3.5: AFM Surface profile for (a) uncoated (b) coated glass cover.**

Surprisingly, adding a 15% coating lowered the $T_{c,in}$ by about 1°C from no coating. However, the temperature gradually increased with an increase in coated surface area as shown in Table 3.4. The coating thickness influenced the thermal resistance of the cover.

When the coating surface area increased, the thermal resistance also increased which was seen by the rise in cover temperature. The increase in $T_{c,in}$ lowered the temperature difference between the water and the inner cover, $dT_{w\text{-}c,in}$. Despite fluctuations in $dT_{w\text{-}c,in}$ observed in Figure 3.6 due to variations from the heat source, 15% and 30% coating showed similar trends for $dT_{w\text{-}c,in}$, whereas the temperature difference dropped starting from 50% and further decreased for 70% as illustrated in Figure 3.6. The drop in $dT_{w\text{-}c,in}$ showed that coating affected the rate of heat transfer by the reduction in heat dissipation from the inner cover to the outer cover with a larger coating surface area.

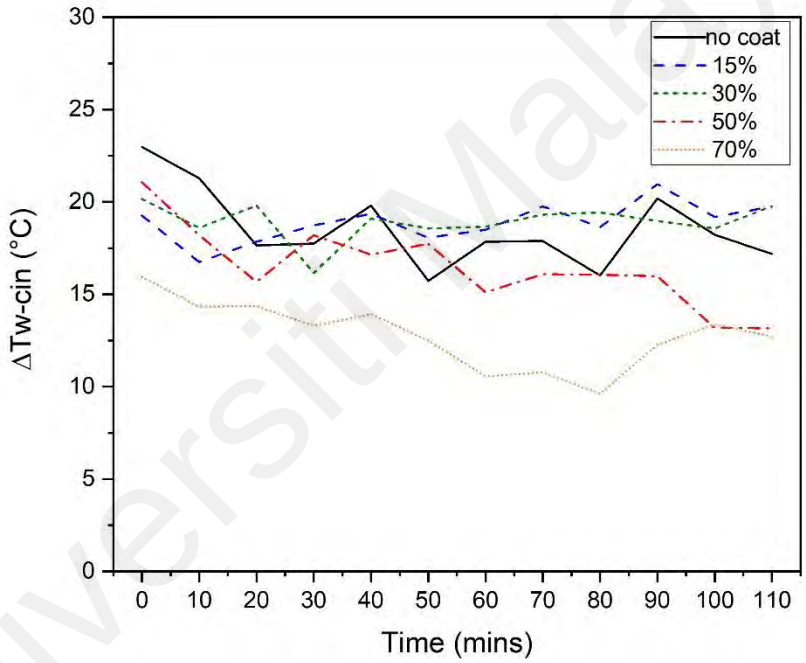


**Figure 3.6: Temperature difference between water and inner cover.**

### 3.3.2 Effect of mixed wettability surface on solar still productivity

The water contact angle and SFE for both uncoated surface and coated are shown in Figure 3.7 and summarised in Table 3.5. Regardless of the small difference in contact angle between the uncoated surface and coated surface, the effect of coating on the glass surface was noticeable as depicted in Figure 3.8.

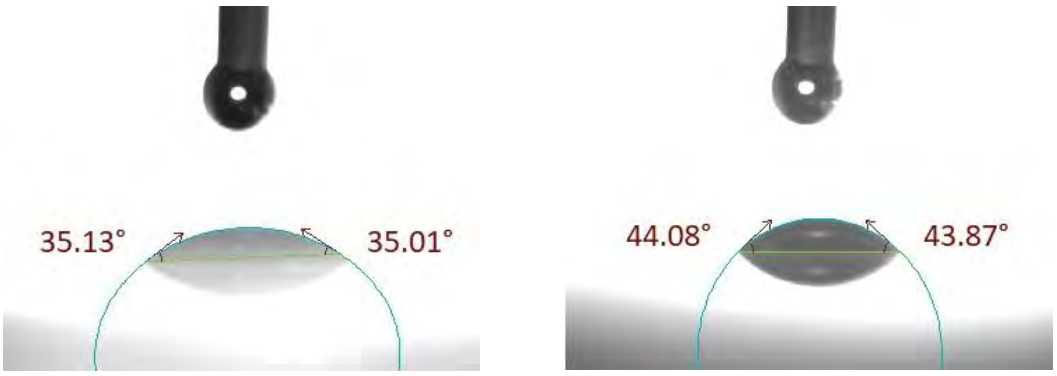


**(a)** **(b)**

**Figure 3.7: Measured water contact angle of droplet for (a) no coating (b) with coating.**

**Table 3.5: Water contact angle and SFE for coated glass.**

| Coating area | Mean contact angle (°) | SFE (mN/m) |
|---|---|---|
| Coated | 42.0 | 58.3 |
| No coat | 35.1 | 62.0 |

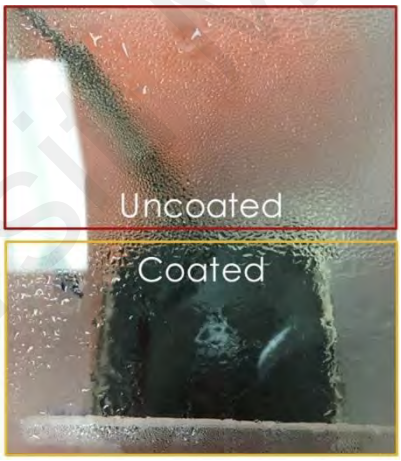


**Figure 3.8: Photograph image of coated and uncoated surface for mix wettability surface of 50% during condensate formation.**

The coated surface exhibited better droplet coalescence due to its lower surface energy. Furthermore, the increase in surface roughness as shown in Table 3.6 also correlates to the droplet detachment on the coated surface. A rougher surface allowed the water droplet to easily roll off the inclined surface thus facilitating the condensate removal process. The effect of mixed wettability on the solar still freshwater yield is shown in Figure 3.9.

**Table 3.6: Surface roughness and surface height.**

| Parameters | Uncoated | With coating |
|---|---|---|
| Surface roughness (pm) | 95 | 114 |
| Surface height (nm) | 0.962 | 2.978 |

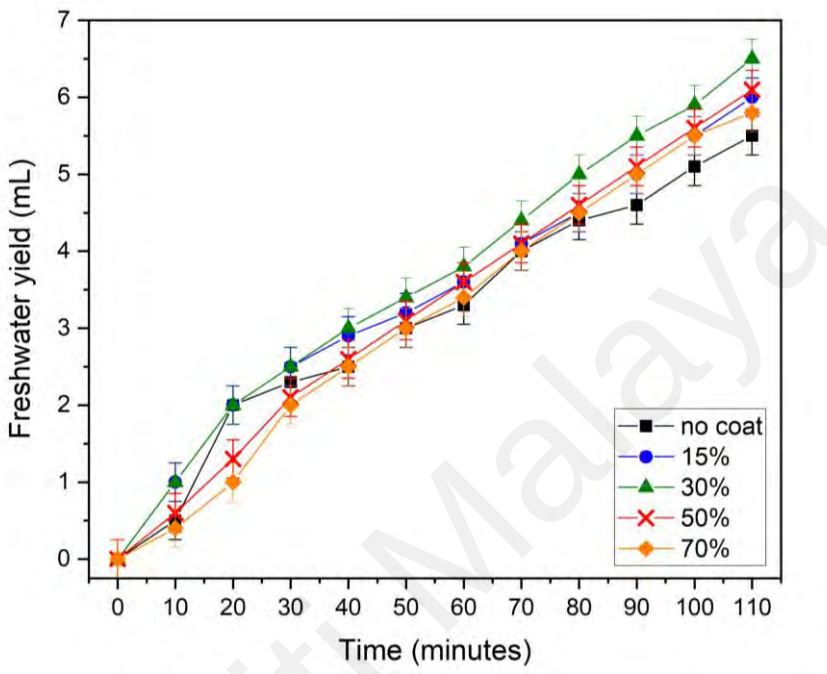


**Figure 3.9: Freshwater yield for uncoated and coated surface areas.**

The graph showed that the relationship between freshwater yield and coated surface with dropwise condensation did not have a linear relationship whereby 30% coating produced a higher output than 50% and 70% coating. To better understand the correlation between freshwater yield and coated surface area, it is essential to consider the effect of temperature difference between water and inner cover. $T_{c,in}$ and freshwater productivity showed to have an inverse relationship as depicted in Figure 3.10 (a) Hence freshwater production improved drastically by 18.2% higher for the 30% coated surface area compared to non-coated surface due to its low $T_{c,in}$. The opposite was true for freshwater productivity and $dT_{w\text{-}c,in}$ whereby a higher $dT_{w\text{-}c,in}$ resulted in high productivity as shown in Figure 3.10.

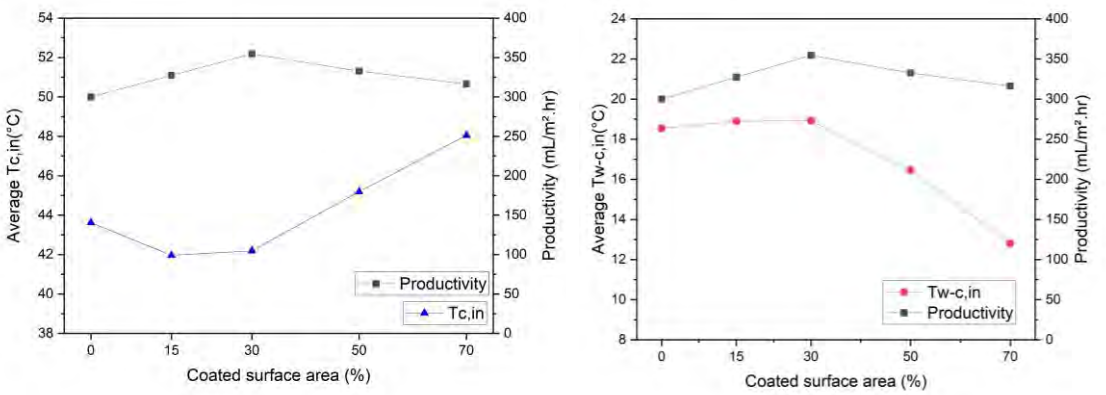


**(a)** **(b)**

**Figure 3.10: (a) Productivity and (b) $dT_{w\text{-}c,in}$ as a function of coated surface area.**

Nevertheless, the surface area of dropwise condensation remained an important factor in determining freshwater productivity. Despite having similar $T_{c,in}$ and $dT_{w\text{-}c,in}$ with 30% coating, the 15% coated surface area showed only a slight improvement in the freshwater yield as shown in Table 3.7. For a passive solar still, the energy efficiency is given by the Equation 3.1 (Shoeibi et al., 2020; Tiwari et al., 2009):

$$\eta = \frac{\Sigma \dot{m}_{ev} h_{fg}}{I_{total} A_w} \tag{3.1}$$

**Table 3.7: Solar still productivity and efficiency for different coated surface areas.**

| Coating area | Rate of productivity ($mL/m^2.hr$) | Improvement (%) | Efficiency (%) |
|---|---|---|---|
| No coat | 300.0 | – | 10.9 |
| 15% | 327.3 | 9.1 | 11.9 |
| 30% | 354.6 | 18.2 | 12.9 |
| 50% | 332.7 | 10.9 | 12.1 |
| 70% | 316.4 | 5.5 | 11.5 |

The difference in freshwater yield was due to the small coated surface area (15%) which lowered the glass condensate collection as compared to when the coating was doubled in surface area (30%). Moreover, low temperature difference for $dT_{w\text{-}c,in}$ and high cover temperature resulted in poor condensate collection for the coated area of 50% and 70% as compared to 30% coating. The productivity of the solar still drops from

354.6 mL/m$^2$.hr to 332.7 mL/m$^2$.hr for 50% coating and even further to 316.4 mL/m$^2$.hr for 70% coated surface area. Nonetheless, the productivity of solar still showed improvement even with 70% coating as opposed to without coating. Although the applied commercial coating resulted in just a slight increase of water contact angle, the results showed favourable outcomes to the improvement of the solar still productivity. Combining both types of wettability showed improved freshwater production due to the material's ability to maintain its high surface tension while also allowing droplet detachment to occur at the coated section. Increasing the water contact angle also allowed better droplet detachment despite the poor performance of the cover material in terms of heat dissipation for 50% and 70% coating as compared to without coating surface. The addition of coating also allowed a steady rate of condensate collection to occur at 0.05 mL/min. The steady condensate collection rate occurred due to the stable heat transfer between the cover and water as well as the lowered surface energy at the coated edge of the cover.

### 3.3.3 Cost analysis of using coating at different coverage

A simple cost analysis was done to find the difference between the cost of freshwater on various coated surface areas. According to the manufacturer datasheet for the commercial coating, the consumption of sealant to cover a surface area ranges between 5 mL/m$^2$ to 10 mL/m$^2$. The commercial coating cost approximately 0.313 $/mL and the overall experimental setup for the solar still prototype was $ 16. Assuming a mean range was used to cover per square meter of surface and a solar still operation of 9 hours daily, Equation 3.2 is used to calculate the CPL based on the daily solar still output:

$$\mathbf{CPL} = \frac{\mathbf{cost\ of\ setup+coating}}{\mathbf{daily\ freshwater\ output}} \tag{3.2}$$

The cost of coating and CPL are shown in Table 3.8. The lowest CPL obtained was using 30% coating followed by 15%, 50%, no coat and 70%. The pattern reflects the

freshwater yield obtained by the different coating whereby 30% achieved the highest yield followed by 15% and 50%. However, despite having a higher freshwater yield for 70% coating compared to no coating, the CPL for no coating was lower than 70% coating. Therefore, the coated surface area must be limited to below 50% in order to achieve both cost-savings while maintaining a high solar still productivity.

**Table 3.8: Cost per litre of freshwater for various coated surface areas.**

| Coating area | Cost of coating ($) | CPL ($/L) |
|---|---|---|
| 15% | 0.3512 | 0.0555 |
| 30% | 0.7036 | 0.0524 |
| 50% | 1.1727 | 0.0574 |
| 70% | 1.6417 | 0.0620 |
| No coat | - | 0.0593 |

Table 3.9 compares the performance of several solar still enhancement methods (Shoeibi et al., 2021b). In general, the active solar still performed better than a passive solar still as shown by the low CPL with a higher $CO_2$ mitigation than the passive solar still. Nonetheless, the current solar still method has shown to be quite competitive when compared to other passive solar still designs. The CPL obtained ranged between 0.0524 $/L to 0.0620 $/L with the lowest CPL obtained from 30% coating coverage. This method also showed a reasonable amount of $CO_2$ mitigation for an average lifetime of 10 years. The highest amount of $CO_2$ mitigation was 16.92 tonnes/lifetime for 30% coating coverage.

**Table 3.9: Comparisons between different types of solar stills.**

| Type of solar still | Enhancement method | CPL ($/L) | $CO_2$ mitigation (tonnes/lifetime) | Reference |
|---|---|---|---|---|
| Active | PCM | 0.0072 | 28.83 | (Yousef & Hassan, 2020) |
| | Sand in basin | 0.021 | 20.84 | (Hassan et al., 2020) |
| | Aluminium heat sink | 0.023 | 19.45 | (Hassan & Yousef, 2021) |
| | Thermoelectric heating and reflectors | 0.0372 | 19.05 | (Parsa et al., 2020b) |
| Passive | Pin fin absorber | 0.0416 | 14.4 | (Yousef et al., 2019) |
| | External aluminium condenser | 0.0232 | 13.68-17.15 | (Abo-Elfadl et al., 2021) |
| | Gravel sensible heat storage | 0.0618 | 5.75-8.27 | (Dhivagar et al., 2021) |
| | Current solar still | 0.0524 -0.0620 | 14.31-16.92 | - |

## 3.4 Summary

In summary, an investigation on a mixed-wettability surface application for the condensing cover of passive solar still has been carried out. A commercially available water-based polysiloxane sealant was used as a coat to modify the glass surface for several different coated surface areas. The experimental results showed that coating improved the overall productivity of the solar still. The results are summarised as follows:

i. A surface area coating of below 30% improved the inner cover temperature than the uncoated surface. The degree of improvement for the solar still productivity relied on the coated surface area, whereby 30% coating surface area showed the most improvement in freshwater output followed by 15%, 50% and 70% coated surface area.

ii. Cost comparison between different coating surface areas demonstrates the cost-effectiveness of using coating compared to bare glass cover with a limit of not more than 50% coated surface area coverage.

iii. This method also showed comparable CPL and $CO_2$ mitigation compared to other types of passive solar still. Therefore, this study highlights the advantage of using a mixed-wettability surface to improve the condensate formation and collection in passive solar still that uses a glass condensing cover.

# CHAPTER 4: TECHNO-ECONOMIC ANALYSIS OF SOLAR STILL USING VARIOUS CONDENSING COVER MATERIAL AND SURFACE COATING WITH COVER COOLING

In this chapter, the performance of the solar still is examined by employing various condensing cover materials and incorporating a mixed wettability cover with a cover cooling technique. This chapter encompasses an introduction and a methodology section that outlines the selection and usage of cover materials in the study, as well as the design of the cooling system. The results and discussions section provides a comprehensive analysis of the productivity, efficiency, and economic aspects associated with using different cover materials in both passive and water-cooled mode solar stills. Finally, the chapter concludes with a summary of the study's findings.

## 4.1 Introduction

Single slope solar still is one of the most used thermal desalination methods particularly in rural communities (Das et al., 2020). However, passive solar still has low freshwater productivity ranging below 2000 L/m$^2$ per year compared to an average of 3000 L/m$^2$ per year for active solar still (Shoeibi et al., 2021b). Therefore, design modifications were made to the passive solar still to improve heat absorption and vapour condensation (Mohsenzadeh et al., 2021). Active solar still refers to solar still that includes an additional component to assist in increasing the heat of saline water or lowering the condensing cover surface (Chauhan et al., 2020). Heating of saline water was achieved through the addition of solar collectors, reflectors and external heating (Fang et al., 2021; Rahbar et al., 2017; Singh et al., 2021). Condensing cover cooling is achieved using water cooling, air cooling or thermoelectric cooling system (Fu et al., 2021). Numerous works of literature on water-cooled glass covers point toward the positive impact of cover cooling on freshwater productivity. The water-cooling method

showed a higher heat transfer rate that allowed the productivity of the solar still to improve significantly as compared to air cooling (Arunkumar et al., 2013).

Cover material properties such as its surface wettability, optical and thermal properties have also been shown to play an important role in the condensate collection that determines the solar still productivity. Several different materials have previously been studied to observe the effect of cover materials on freshwater production (Dimri et al., 2008). Based on Tiwari et al. (2009) thermal model, a condensing cover made of copper produced the highest daily freshwater yield followed by glass and plastic. The authors concluded that the thermal conductivity value of a condensing cover played a role in productivity. Zanganeh et al. (2019) found that solar still productivity was highly affected by the wettability where the usage of aluminium and glass cover material with high wettability resulted in an increase in the volume of condensate compared to other metals with higher thermal conductivity value, such as copper and brass. Dropwise condensation mode occurs on material with low wettability or hydrophobic while filmwise mode occurs on material with high wettability or hydrophilic surfaces. The previous study showed that both condensation modes resulted in improvements to the solar still productivity (Zanganeh et al., 2020b). However, low wettability surfaces of plastic materials exhibited lower solar still productivity compared to using glass as the solar still cover (Maheswari et al., 2022; Zanganeh et al., 2020a). Different cover material was applied in separate studies to determine the effect of solar still cover water cooling on freshwater productivity. A double slope glass cover obtained a daily freshwater yield of 7.80 $L/m^2$ at 1 cm brine depth and 3 mm glass cover thickness (Morad et al., 2015). An acrylic sheet hemispherical cover of 3 mm thickness produced a yield of 4.2 $L/m^2$ a day with cover cooling (Arunkumar et al., 2012b). Polycarbonate material was used as a cover for tubular solar still improving the productivity of solar still by 7.93% with a total daily yield of

about 6 L/m$^2$ for a 2 L/h water cooling flow rate with a basin water depth of 1 cm (Kabeel et al., 2019).

Previous literature found that the material selection for a solar still cover is an important criterion that must be considered in the design of the solar still. A particular focus on the cover material's wettability was put into perspective based on recent findings. In general, the consensus agrees that water-cooled solar still has higher productivity compared to passive solar still. Despite the improvement shown in the cover cooling technique for different cover materials, a consolidated study on the magnitude of the cover cooling effects encompassing various cover materials with similar solar still designs and setups has yet to be established. Different solar still designs result in varying outcomes which leads to inconsistent findings on the actual solar still performance among the common cover materials used. Therefore, this study aims to compare the performance of passive and active solar stills that use various condensing cover materials with varying degrees of wettability as well as glass cover with mixed wettability using the surface coating. The water-cooled and passive solar still freshwater yield and efficiency are measured and calculated to show the performance of the solar still using different cover materials. Finally, an economic analysis is done to determine the effect of cover material on the cost of freshwater produced for passive and water-cooled solar stills.

## 4.2 Methodology

### 4.2.1 Materials and methods

Four different cover materials were tested in this study, glass, polycarbonate (PC), acrylic (PMMA), and mix wettability cover. A glass cover was used as a reference for the water-cooling experiment. The cover materials were 3 mm thick with a dimension of 0.5 m x 0.61 m. The mix wettability cover was prepared by applying a silicon-based coating on 30% surface area of the glass and the coated surface was positioned on the

front end of the solar still. The coating was done to improve the solar still condensate removal for a glass surface. The characterisation and selection of the coated surface area have already been given in our previous work-.

### 4.2.2 Outdoor experimental setup and procedure

Four solar stills setup with a base area of 0.25 $m^2$ was constructed using galvanized iron (GI) sheets with a thickness of 1.5 mm. The dimensions of the solar still front and back walls were 0.1 m and 0.33 m, respectively to give a cover tilt angle of 25°. The outer surfaces of the solar still were covered with polyethylene foam (PE foam) of a thickness of 5 cm to minimise heat loss from these surfaces. Water cooling was used for the solar stills with a flow rate of 2 L/hr and was maintained by circulating the cooling water through a water reservoir using a pump before dispensing it into separate cooling water containers for each solar still. The experiment was conducted in May and June 2022 and located at the Universiti of Malaya, Kuala Lumpur, Malaysia (Latitude: 3.118°N/ Longitude: 101.656°E). The solar still was first tested without any cooling and with water cooling on separate days. The results were compared to a glass cover solar still reference (without cooling) to provide better comparisons between the data regardless of the variable weather conditions. The experiments were conducted from 9 a.m. to 5 p.m. and for water-cooled solar still, cover cooling started at 10 a.m. The solar stills were positioned facing south to receive maximum solar radiation. Saline water of 3.5% salinity was used in the experiment and placed in the basin with a depth of 1 cm before commencing the experiment. The temperatures of the basin water, inner cover, and cooling water were measured and recorded using K-type thermocouples. The outdoor ambient temperature and humidity were measured using a temperature and humidity sensor (Benetech1361). The solar irradiance was measured using a solar power meter (TES-132). The accuracies and ranges of the instruments and sensors are listed in

Table 4.1. A photograph and a schematic diagram of the outdoor experimental setup are shown in Figure 4.1.

**Table 4.1: Measuring instruments range and accuracy.**

| Instruments/Sensors | Range | Accuracy |
|---|---|---|
| Type-K thermocouple | 0 – 105 °C | ±0.1 °C |
| Temperature data logger | 0 – 200 °C | ±0.9 °C |
| Solar power meter | 0 – 2000 W/m$^2$ | ±1 W/m$^2$ |
| Graduated cylinder | 0 – 25 mL | ±0.25 mL |
| Humidity sensor | 0 – 99.9 % | ±0.1 % |


**(a)**

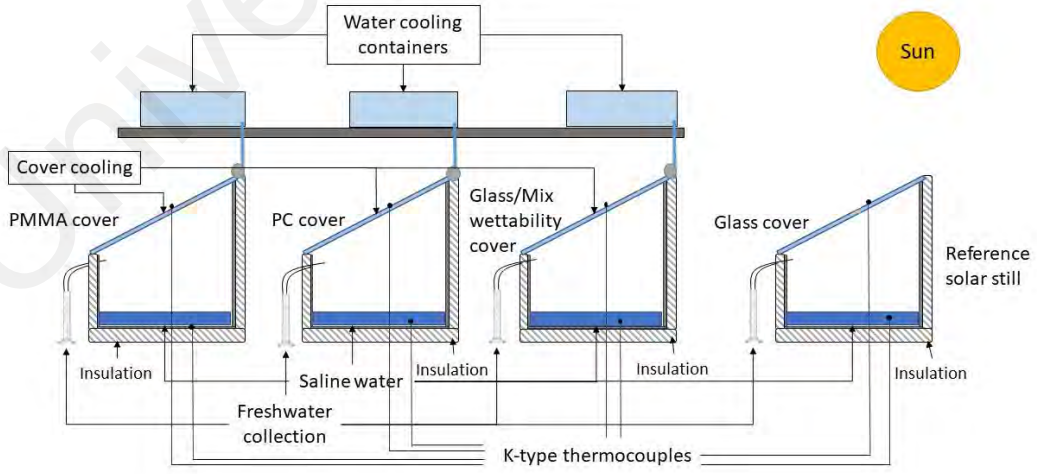


**(b)**

**Figure 4.1: Solar still outdoor experimental setup (a) photograph and (b) schematic diagram.**

## 4.3 Results and discussions

### 4.3.1 The effect of water cooling on glass cover solar still

The solar still design was first experimented with using a glass cover to determine the improvement of the glass cover with the addition of water cooling using the same setup. The experiment was conducted on a separate day on 26 May 2022. The experiment followed the same methodology as given in the previous subsection with saline water used as the basin water and the initial height of the basin water added was 1 cm. The solar radiation, $T_a$, $T_w$ and $T_c$ for both reference and water-cooled solar still measured on the day of the experiment are shown in Figure 4.2.

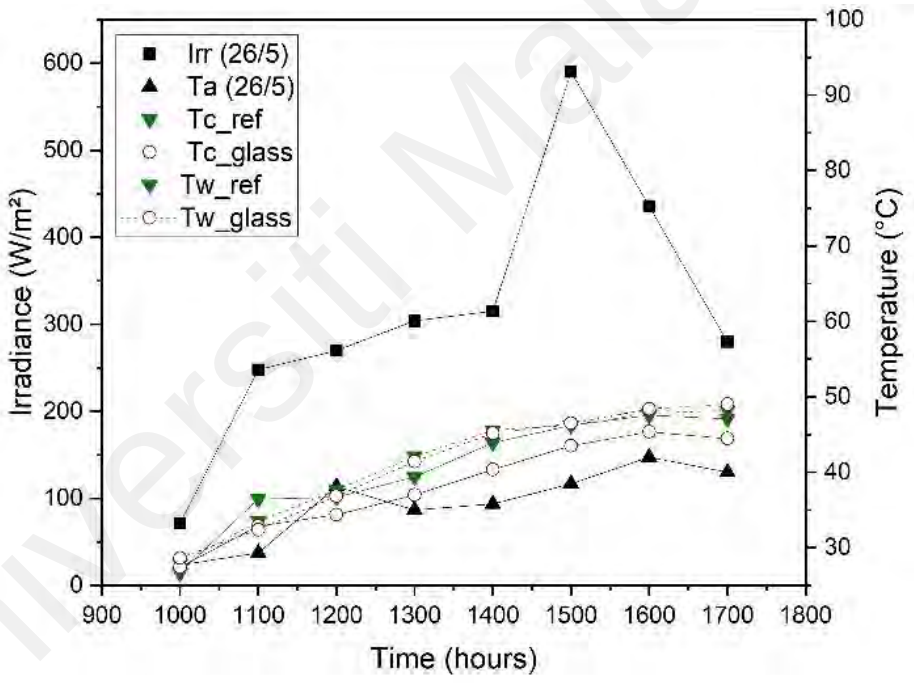


**Figure 4.2: Solar irradiation, Irr, ambient temperature, $T_a$, cover temperature, $T_c$ and water temperature, $T_w$ for the glass cover cooling experiment on 26 May.**

The $T_c$ was lower for the water-cooled solar still compared to the reference solar still due to higher heat dissipation from water cooling the solar still cover. However, the addition of water cooling lowered the $T_w$ slightly compared to the reference before 3 p.m. The low $T_w$ for water-cooled solar still was because of the low irradiance that ranges around 300 W/m$^2$ before 2 p.m. which delayed the basin water heating with the addition of water cooling. Nonetheless, water cooling allowed a higher temperature difference

between cover and basin water which increased solar still productivity as shown in Figure 4.3. The daily freshwater yield produced for water-cooled glass cover was 158.7 mL whereas reference solar obtained a yield of 144.2 mL.

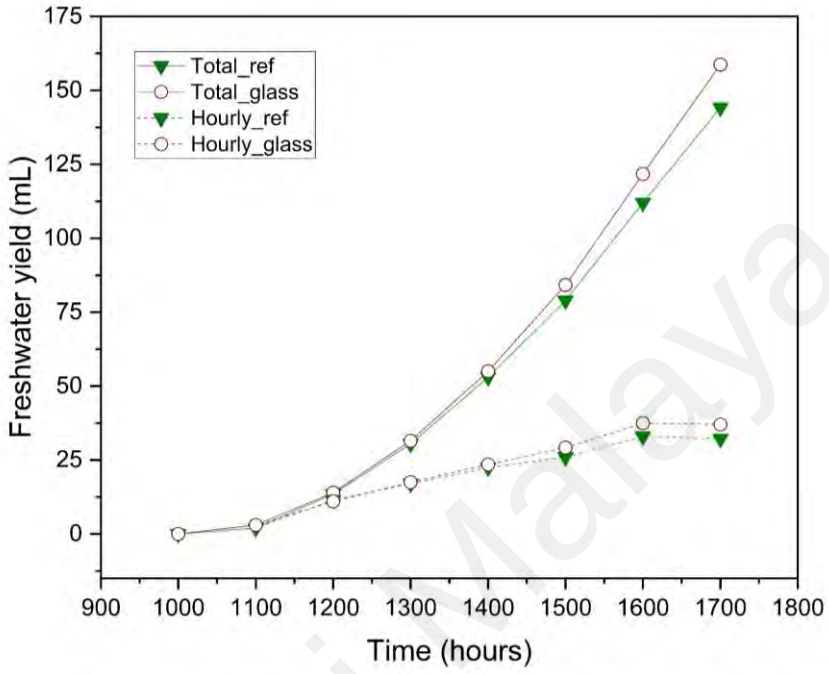


**Figure 4.3: Hourly and total freshwater yield of the water-cooled and reference solar still.**

### 4.3.2 Mix wettabillity cover comparison between passive and water-cooled solar stills

Figure 4.4 showed that the measured peak irradiance for both experiment days was obtained at 1 p.m. while $T_a$ ranged between 27°C to 40°C.

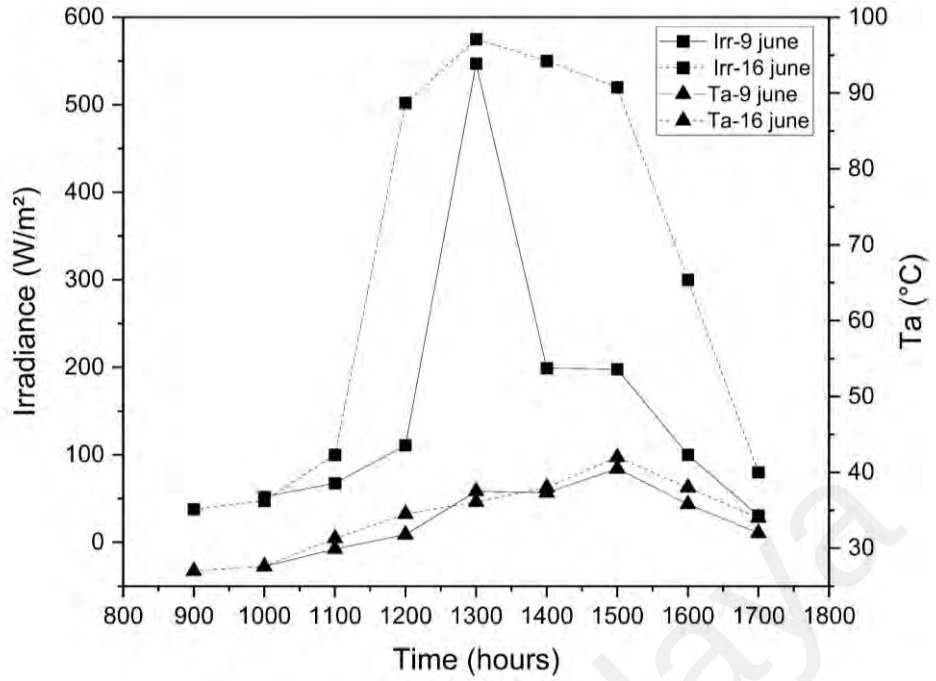


**Figure 4.4: Weather conditions during the conducted experiment days on 9 June (no cool) and 16 June (with cooling).**

For the mix wettability cover, $T_w$ and $T_c$ were higher than the uncoated glass cover as shown in Figure 4.5 (a). This was attributed to the rise in thermal resistance due to the addition of coating. During heating from 9 a.m. to 2 p.m., $T_c$ was slightly higher than $T_w$ for mix wettability cover solar still, but $T_c$ remained consistently lower than $T_w$ for glass cover solar still. The addition of water cooling showed improvement in $T_c$ for mix wettability cover solar still where the temperature was lower than $T_w$ throughout the day and was also lower than $T_w$ reference before 3 p.m. as shown in Figure 4.5 (b). After 3 p.m., $T_c$ was slightly higher than the $T_c$ reference due to the increase in temperature of the cooling water. A slight decrease in $T_w$ occurred once water cooling started at 10 a.m. However, a higher $T_w$ was achieved from 12 p.m. and continued to remain higher than $T_w$ reference as opposed to a similar $T_w$ with reference for the passive solar still. The lowered $T_c$ and high $T_w$ with the use of water cooling showed to have a positive effect on the freshwater yield of the mix wettability cover solar still.

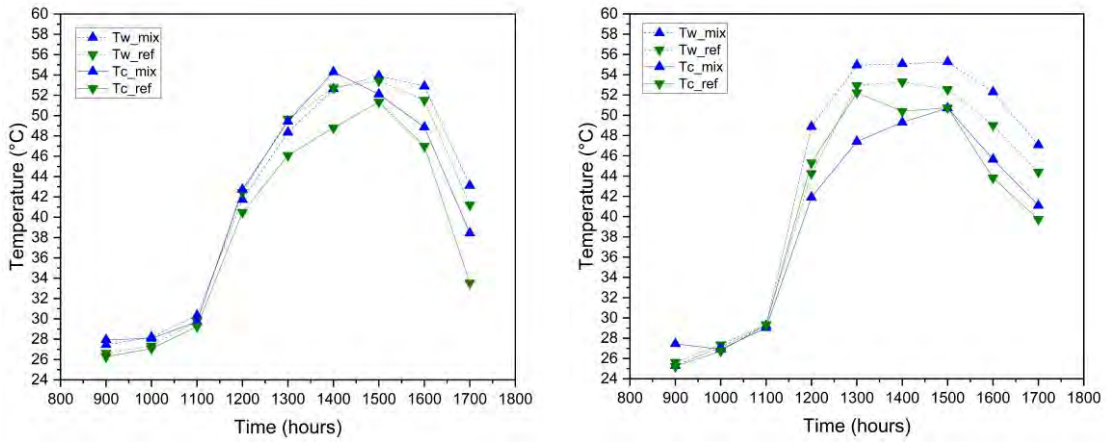


**Figure 4.5: Temperature of basin water and cover for mix wettability and reference solar still under (a) passive and (b) water cooling.**

Figure 4.6 depicts the cumulative freshwater yield for the passive and water-cooled solar still using mix wettability surface. The yield for the passive solar stills was 128 mL and 154.2 mL whereas water-cooled solar stills were 200.5 mL and 252.2 mL for reference and mix wettability cover, respectively.

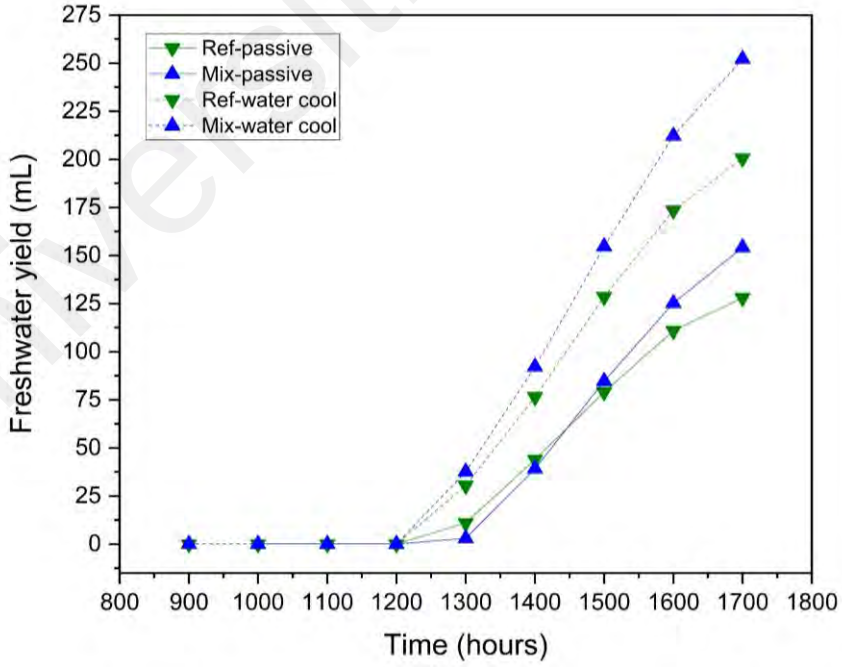


**Figure 4.6: Cumulative freshwater yield of passive and water-cooled solar still for reference and mix wettability.**

### 4.3.3 PC and PMMA cover comparison between passive and water-cooled solar stills

For PC and PMMA cover, the experiments were repeated twice for water cooling under different weather conditions as shown in Figure 4.7 (a) and 4.7 (b). For passive solar still shown in Figure 4.7 (c), $T_w$ and $T_c$ for PMMA obtained the highest temperature whereas $T_w$ and $T_c$ for PC had a slightly higher temperature compared to reference solar still. When water cooling was applied to the PC and PMMA cover, $T_w$ was only slightly higher than the $T_w$ reference on 26 May. Whereas $T_w$ on 16 June dropped lower than $T_w$ reference from 11 a.m. to 2 p.m. before it reached a higher temperature from 2 p.m. until 5 p.m. $T_c$ were similar to $T_w$ for PC and PMMA from 11 a.m. to 2 p.m. on 16 June compared to 26 May. The low $T_w$ was caused by the added thermal resistance from the water cooling on the PC and PMMA cover. Both PC and PMMA have a higher specific heat capacity compared to glass, hence, the addition of water cooling made it difficult for heat transfer to occur which caused the low $T_w$ from 11 a.m. to 1 p.m. Nonetheless, water cooling raised the $T_w$ for PC cover solar still higher than $T_w$ reference compared to passive solar still. $T_c$ also were significantly lower for water-cooled solar still, particularly for PMMA cover.

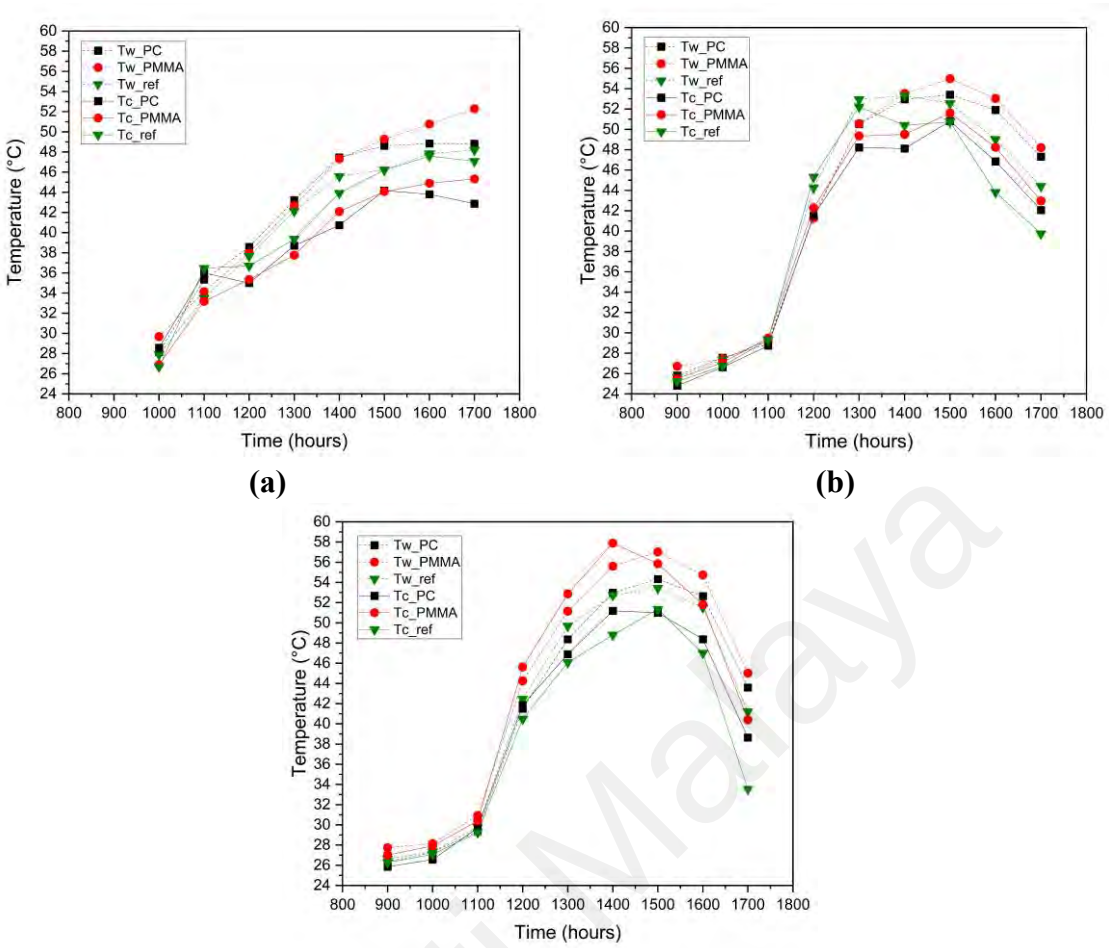


**Figure 4.7: Temperature of basin water and cover for PC and PMMA cover, and reference solar still (a) water cooling 26 May (b) water cooling 16 June (c) passive 9 June.**

For both passive and water-cooled solar stills, PC cover solar stills had a lower freshwater yield compared to PMMA cover solar stills as shown in Figure 4.8. The freshwater yields obtained for passive solar still were 32.1 mL and 72.5 mL for PC and PMMA cover, respectively. For water-cooled solar still, PC and PMMA freshwater yields were 5.4 mL and 49.6 mL on 26 May and 49.5 mL and 114.9 mL on 16 June.

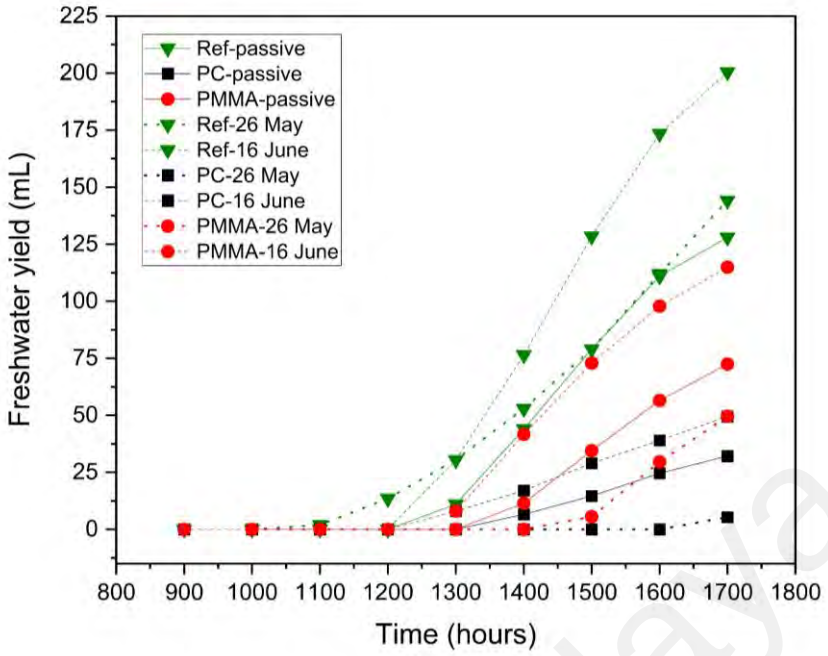


**Figure 4.8: Cumulative freshwater yield of passive and water-cooled solar still using different cover materials.**

### 4.3.4 Solar still productivity between passive and water-cooled for various cover materials

The freshwater yield produced for water-cooled glass cover solar still was 725.5 mL/m$^2$ per day whereas reference solar still obtained a yield of 659.2 mL/m$^2$. Water cooling for normal glass cover improved by 10% compared to passive glass cover solar still. The freshwater yield for solar still using mix wettability cover showed the highest output for both passive and water-cooled with daily productivity of 759.14 mL/m$^2$ and 1008.8 mL/m$^2$, respectively as shown in Figure 4.9 (a). For both passive and water-cooled solar still, the trend was the same where the highest solar still productivity was using mix wettability cover, followed by PMMA, and PC cover. Glass cover and mix wettability cover showed an improvement using water cooling with an increase in productivity by 10% and 6% compared to passive solar still as shown in Figure 4.9 (b). However, PMMA and PC cover showed a reduction of 22% and 21% in productivity when subjected to water cooling on 26 May, but there was only a slight difference on 16 June.

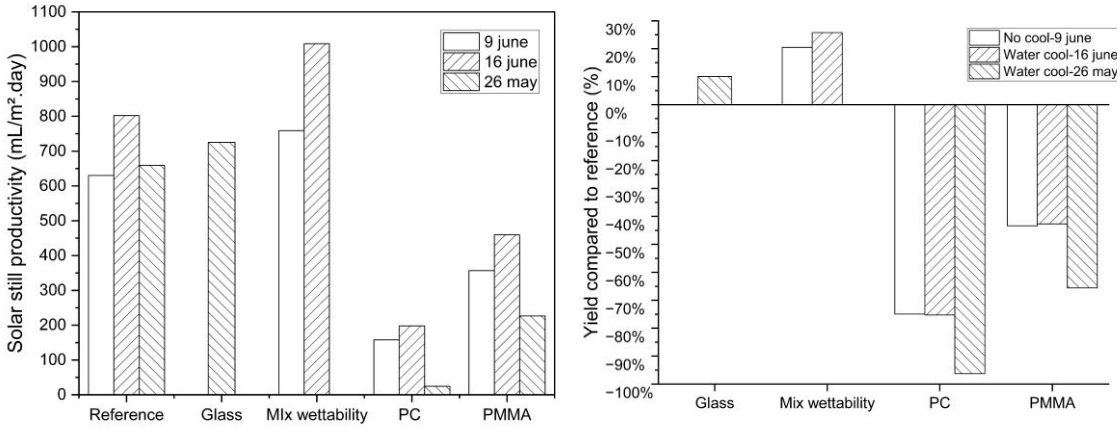


**(a)** **(b)**

**Figure 4.9: (a) Daily productivity and (b) difference in freshwater yield between different cover materials with reference solar still (using glass cover).**

Although Figure 4.10 showed that the cooling water temperature, $T_{wcool}$, had a similar measurement during the two days, water cooling had an adverse effect on the solar still productivity for PC and PMMA cover during poor weather conditions with low irradiance and $T_a$.

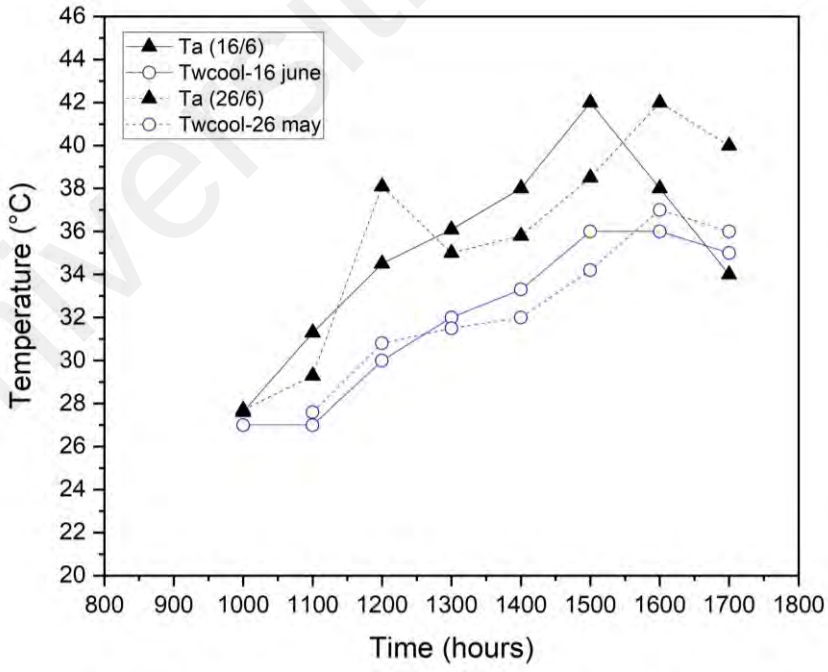


**Figure 4.10: Difference between $T_a$ and $T_{wcool}$ for two different days.**

Using the same water-cooling speed and setup, solar still using cover material PMMA and PC showed poorer performance for water-cooled solar still compared to passive solar

still. This is attributed to the material's characteristics with low wettability, low thermal conductivity, and high specific heat capacity. The combination of these characteristics hinders the material's ability to dissipate heat even with water cooling and reduces the freshwater yield due to the low rate of condensate formation from its low wettability. The glass cover solar still showed improvement with water cooling rather than passive solar still due to its low specific heat capacity. A low specific heat capacity allows the glass cover to dissipate heat better than the plastic covers. The addition of coating for mix wettability cover improved the condensate collection while also allowing condensate formation on the uncoated surface. Both high and low wettability areas on a surface contribute to the high productivity of solar still by producing a favourable surface for condensate formation and collection. However, the mix wettability cover did not perform as well as the glass cover with water cooling partly due to the addition of a coated layer that reduced the material's ability to remove heat effectively using water cooling. Nonetheless, the mix wettability cover performs the best compared to other materials for both passive and water-cooled solar still due to its combined wettability surface that allows both condensate formation on the uncoated area and promotes condensate collection on the coated area.

### 4.3.5 Daily energy efficiency

For a passive solar still, the energy efficiency is the ratio of energy produced by the solar still to energy input which is the total solar radiation times with the solar still basin area as given in Equation 3.1 in the previous chapter.

For a water-cooled solar still, the energy input includes the power consumption from the water pump, $\dot{W}_{pump}$ used as shown in Equation 4.1:

$$\eta_{wc} = \frac{\Sigma \dot{m}_{ev} h_{fg}}{I_{total} A_w + \dot{W}_{pump}} \quad (4.1)$$

The latent heat of vaporization, $h_{fg}$ (J/kg) is calculated based on the following Equation 4.2 (Fernández & Chargoy, 1990):

$$\mathbf{h_{fg} = 3161500 - 2407.41 \times T_w} \quad (4.2)$$

The efficiency of reference solar still on 26 May, 9 June, and 16 June were 15.3%, 26%, and 19.7%. The variation in thermal efficiency was due to the difference in solar radiation and freshwater yield between the three experimental days. The highest overall thermal efficiency for the studied cover materials with water cooling was obtained by mix wettability glass cover followed by PMMA and PC cover with an efficiency of 24.5%, 11.2% and 4.8% as given in Table 4.2. The efficiency for PC and PMMA showed almost no difference between passive and water-cooled solar still. Water-cooled solar still with mix wettability cover showed a considerable amount of improvement from the passive solar still by 5.5%. Comparison between passive solar still and water-cooled solar still for glass also showed an increase in thermal efficiency from 15.3% with passive to 18.7% with water-cooled solar still. Water cooling positive effect on the efficiency of the solar still using different cover materials had a similar trend with the productivity. Plastic materials had the poorest efficiency, and the efficiency was not improved using water cooling while the opposite is true for glass and mix wettability cover.

**Table 4.2: Comparison between thermal efficiency for different cover materials and surface coating.**

| Solar still type | Cover material | Average solar radiation ($W/m^2$) | Average $T_a$ (°C) | Thermal efficiency (%) | Efficiency improvement to reference (%) |
|---|---|---|---|---|---|
| Passive | Glass | 314.3 | 35.8 | 15.3 | - |
| | Ref | 163.1 | 34.1 | 26 | - |
| | Mix wettability | 163.1 | 34.1 | 31.3 | 20.4 |
| | PC | 163.1 | 34.1 | 6.5 | -75 |
| | PMMA | 163.1 | 34.1 | 14.7 | -43.5 |
| Water-cooled | Glass | 314.3 | 35.8 | 18.5 | 21.4 |
| | Ref | 334.4 | 34.3 | 19.7 | - |
| | Mix wettability | 334.4 | 34.3 | 24.5 | 25.5 |
| | PC | 334.4 | 34.3 | 4.8 | -75.3 |
| | PMMA | 334.4 | 34.3 | 11.2 | -42.8 |

### 4.3.6 Economic analysis

The cost per litre, CPL, based on the annual productivity of the solar still, M (solar still is considered to be operating for 365 days) is calculated by Equation 4.3 (Shoeibi et al., 2020):

$$\mathbf{CPL} = \frac{\mathbf{TAC}}{\mathbf{M}} \tag{4.3}$$

Where the total annual cost of the solar still, TAC, is calculated using Equation 4.4:

$$\mathbf{TAC} = \mathbf{FAC} + \mathbf{AMC} - \mathbf{ASV} \tag{4.4}$$

The first annual cost of solar still, FAC in Equation 4.5 is a product of initial fixed cost, F and the capital recovery factor as shown in the equation below:

$$\mathbf{FAC} = \mathbf{F} \times \mathbf{CRF} \tag{4.5}$$

The capital recovery factor, CRF shown in Equation 4.6 depended on the interest rate for commercial loans in Malaysia, i = 3.5% and the lifespan of the solar still, n = 10 years.

$$\mathbf{CRF} = \frac{\mathbf{i(1+i)^n}}{\mathbf{(1+i)^n - 1}} \quad (4.6)$$

The annual maintenance cost of the solar still, AMC is considered as 15% of the first annual cost of the solar still as shown in Equation 4.7:

$$\mathbf{AMC} = \mathbf{0.15} \times \mathbf{FAC} \quad (4.7)$$

20% of the fixed cost is commonly calculated as the salvage value of the solar still (S = 0.2F). Hence the first annual salvage value (ASV) of solar still is calculated using the following Equation 4.8:

$$\mathbf{ASV} = \mathbf{S} \times \mathbf{SSF} \quad (4.8)$$

where the sinking fund factor, SSF is given by Equation 4.9 and can be calculated:

$$\mathbf{SSF} = \frac{\mathbf{i}}{\mathbf{(1+i)^n - 1}} \quad (4.9)$$

**Table 4.3: Economic analysis parameters for different cover materials.**

| Cover material | Glass | Mix wettability | PC | PMMA |
|---|---|---|---|---|
| Fixed cost, F ($) | 145.84 | 146.28 | 130.44 | 128.24 |
| First annual cost, FAC ($) | 17.54 | 17.59 | 15.68 | 15.42 |
| Annual maintenance cost, AMC ($) | 2.63 | 2.64 | 2.35 | 2.31 |
| Annual salvage value, ASV ($) | 2.49 | 2.49 | 2.22 | 2.19 |
| Total annual cost, TAC ($) | 17.68 | 17.73 | 15.81 | 15.55 |
| Annual productivity, M (L/m$^2$) | 264.80 | 368.21 | 72.27 | 167.75 |
| CPL ($/L/m$^2$) – water-cooled | 0.067 | 0.048 | 0.219 | 0.093 |
| CPL ($/L/m$^2$) – reference | 0.072 | 0.059 | 0.059 | 0.059 |

Table 4.3 illustrates the economic analysis parameters calculated for the present study. The results showed that mix wettability cover had a CPL of $ 0.048 which was lower than the CPL for reference solar still which was $ 0.059. The CPL for PC doubled the price compared to PMMA with the value of $ 0.219 and $ 0.093. Water-cooled glass cover solar still had a lower CPL than reference solar still at $ 0.067 and $ 0.072. Although the

initial cost for PC and PMMA was lower than using a glass cover, the reduced freshwater yield caused an increase in CPL. Hence, despite PC and PMMA being the cheaper alternative to glass covers, the performance was inferior compared to the glass cover. Table 4.4 illustrates the comparison between other types of solar still designs with water cooling systems. For single slope solar still, the thermal efficiency is much lower in contrast with different solar still designs. The CPL for this study is also much higher as opposed to other studies due to the low freshwater yield.

**Table 4.4: Comparison between the present study with other designs and cover materials for water-cooled solar still.**

| Solar still design | Cover material | Average solar radiation ($W/m^2$) | Daily yield ($mL/m^2$) | Yield enhanced to reference (%) | Thermal efficiency (%) | CPL ($/L/m^2) |
|---|---|---|---|---|---|---|
| Single slope (present study) | Glass | 314.3 | 725.5 | 10 | 18.5 | 0.067 |
| | Mix wettability | 334.4 | 1008.8 | 26 | 24.5 | 0.048 |
| | PC | 334.4 | 198 | -75 | 4.8 | 0.219 |
| | PMMA | 334.4 | 459.6 | -43 | 11.2 | 0.093 |
| Double slope (+gravel immersed in nanofluid) (Elmaadawy et al., 2021) | Glass | 437.5 | 4200 | 46 | 46.9 | 0.015 |
| Tubular (+parabolic concentrator) (Elashmawy, 2019) | PMMA | 636 | 3843 | -10 | 29.8 | 0.02 |
| Tubular (Kabeel et al., 2019) | PC | 782 | 5850 | 32 | 54.9 | 0.019 |

## 4.4 Summary

An experimental investigation was conducted to study the performance of passive and water-cooled solar still using different condensing cover materials. The cover materials selected for this study were glass, polycarbonate (PC), and acrylic (PMMA) as well as a

silicon-coated glass cover to produce a mixed wettability surface. Based on the analysis conducted, glass cover was proven to be superior to plastic cover materials in terms of productivity, efficiency, and CPL. Under similar operating conditions and design, the addition of water cooling for PC and PMMA cover solar still was not beneficial and did not improve the performance of the solar still compared to passive solar still using the same cover materials. Nonetheless, mix wettability had the best performance among other cover materials when used with passive solar still and water-cooled solar still. The following findings are summarised below:

i. The addition of water cooling improved the productivity of solar still for glass cover and mix wettability cover whereby the freshwater yield obtained was 725.5 mL/$m^2$ and 1008.8 mL/$m^2$, respectively. Glass cover solar still improved by 10% compared to reference solar still while mix wettability cover improved by 26% compared to reference solar still.

ii. The productivity of water-cooled solar still using PC and PMMA cover differs depending on the amount of solar radiation received by the solar still. During low solar radiation, the performance of water-cooled solar still using PC and PMMA cover dropped by 21% and 22%, respectively as compared to passive solar still using PC and PMMA cover.

iii. The thermal efficiency obtained for water-cooled solar still using glass, mix wettability, PC and PMMA cover was 18.5 %, 24.5%, 4.8%, and 11.2%. The efficiency for glass and mixed wettability cover improved with water cooling, whereas the thermal efficiency difference was insignificant for solar still using plastic cover materials.

iv. Economic analysis showed that mix wettability had the lowest CPL followed by reference solar still, PMMA and PC with a cost of $ 0.048, $ 0.059, $ 0.093, and

$ 0.219, respectively. Glass cover solar still also had a lower CPL than reference solar still without water cooling.

v. The results of this study showed that the use of water cooling improved the passive mix wettability covered solar still performance whereby an improvement of 26% was found using the water-cooling method compared to 18.2% for the passive mix wettability solar still shown in the previous study. The water-cooling method also enhanced the thermal efficiency and lowered the CPL of passive mix wettability covered solar still.

# CHAPTER 5: INVESTIGATION ON THE PERFORMANCE OF SOLAR STILL WITH THERMOELECTRIC COOLING SYSTEM FOR VARIOUS COVER MATERIAL

This chapter is focus on examining the performance of a solar still equipped with a thermoelectric cooling system using various cover materials. This chapter comprises an introduction, the design of the experimental work, and the equations utilised for the theoretical analysis of the solar still with the thermoelectric cooling system. The subsequent subsection delves into the outcomes of the solar still design and explores the impact of different cover materials on freshwater productivity, energy, and exergy efficiency, as well as the cost per litre. The final subsection provides a summary of the significant results discussed in the preceding subsection on results and discussions.

## 5.1 Introduction

The selection of basin and the cover material is essential when designing a solar still due to the effect of material on the rate of evaporation and condensation process. Basin material is often chosen based on the ability of the material to absorb and retain heat energy which increases the temperature of basin water and enhances the rate of evaporation (Arunkumar et al., 2019b). Whereas for cover material, the selection is based on the ability of the material to transmit solar energy into the solar still (Sharshir et al., 2016). Hence, solar still are often designed using glass as the cover material as it has good transmissivity value (Serrano & Moreno, 2020). However, recent studies have revealed that the wettability of the cover is a crucial factor in determining the productivity of the solar still. Solar still is usually designed with the cover working as the condenser to collect the freshwater condensate, although several designs were built with an external or internal condenser (Mohaisen et al., 2021; Tuly et al., 2021). Therefore, the effect of wettability for the solar still cover plays a role in the formation and collection of the condensate

which influences the productivity of the solar still. Several studies have shown that using a material with low wettability, such as plastic, negatively affected the solar still freshwater output as compared to using a material with high wettability (Bhardwaj et al., 2013; Dimri et al., 2008; Zanganeh et al., 2019). To study the effect of wettability on the productivity of solar still, Zanganeh et al. (2020b) produced a nano-coated surface using titanium dioxide and silicon for different cover materials. The results showed that titanium dioxide coating which produced a high wettability surface increased the productivity of the solar still at a 25° tilt angle but reduced the productivity as the cover tilt angle increased while the opposite effect was seen for silicon cover which produced a low wettability surface.

Another factor that affects condensate formation is the temperature of the cover. Multiple studies have concluded that cover cooling had a positive effect on the productivity of the solar still (Fu et al., 2021). Cover cooling is achieved using different methods which include air cooling, water cooling, thermoelectric cooling, and a combination of these cooling methods (Omara et al., 2017). There have been several studies on the cover cooling system that considered the effect of cooling parameters on solar still productivity. Cooling water flow rates have been shown to affect solar still productivity where the highest freshwater output obtained was 5.85 L/m$^2$ with a 2 L/hr flow rate followed by 5.53 L/m$^2$, 5.42 L/m$^2$, and 5.23 L/m$^2$ at 3 L/hr, 1 L/hr, and 4 L/hr flow rate (Kabeel et al., 2019). Another study focused on the effect of cooling time where a longer duration of cover cooling flash tactic (15 min on 15 min off) showed poorer freshwater yield compared to a shorter duration (5 min on 5 min off) for a similar water flow rate (Morad et al., 2015). A laboratory experiment was conducted by Al-Maddhachi and Min (2018) to study the effect of design parameters which includes water temperature, vapor temperature, thermoelectric input power and Peltier current on the solar distillation. The authors found that the water production rate increased dramatically

using a Peltier current of 6 A, but decreased when a higher Peltier current was used. This study also revealed that water production increased with higher thermoelectric input power however, this factor depended on the water temperature where lower water temperature showed the opposite outcome using higher thermoelectric power.

Previous studies have revealed that cover cooling improved the solar still outcome. The utilisation of TEC has also been shown to raise freshwater production higher than cover cooling using water. Although a laboratory experiment has been done to study the effect of TEC power input on the productivity of the solar still, this study was done at a small scale and used an internal condenser rather than the cover as a condenser (Al-Madhhachi & Min, 2018). Besides, other outdoor experimental investigations using the TEC system have yet to correlate the effect of TEC power input on the productivity of solar still (Parsa et al., 2020a; Rahbar et al., 2016; Rahbar & Esfahani, 2012). Cover material selection has been deemed as an essential parameter in determining the performance of the solar still yet to the best of the authors' knowledge, no study has been done regarding the effect of TEC cooling on different cover materials. Therefore, this study focused on investigating the performance of single slope solar still using various cover materials combined with a TEC cooling system operating under different power inputs. The performance of the solar still is analysed based on freshwater production, energy, exergy, and economy.

## 5.2 Methodology

### 5.2.1 Solar still setup

Three types of cover materials were tested in this study, glass, polycarbonate (PC), and acrylic (PMMA). A glass cover was used as the cover for reference solar still in the TEC cover cooling experiment. The schematic of the solar still setup is shown in Figure 5.1 (a). The cover materials were 3 mm thick with a dimension of 0.5 m × 0.61 m. Four solar

stills were fabricated using galvanized iron sheets with a thickness of 1.5 mm and each solar still had a base area of 0.25 $m^2$. The height of the solar still front and back walls were 0.1 m and 0.33 m, respectively to produce a cover tilt angle of 25°. The solar stills were insulated using polyethylene foam (PE foam) with a thickness of 5 cm to minimise heat loss from the wall surfaces. The experiments were conducted from May to June 2022, located at the Universiti Malaya, Kuala Lumpur, Malaysia (Latitude: 3.118°N/Longitude: 101.656°E).

### 5.2.2 TEC cover cooling setup

The TEC cover cooling system consisted of three separate TEC setups for each solar still. A single TEC unit setup comprises a single TEC module, two heatsinks on the cold and hot side, and two fans to remove heat by blowing air onto the heat sink's hot side surface as illustrated in Figure 5.1 (b). The details of the TEC setup are given in Table 5.1.

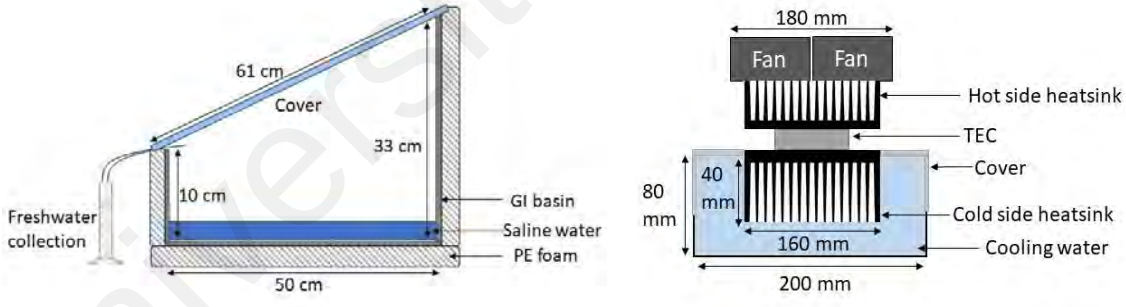


**Figure 5.1: Schematic of (a) solar still and (b) TEC setup (single unit).**

**Table 5.1: Specifications for items used in TEC setup.**

| Item | Manufacturer | Model | Dimension | Specifications |
|---|---|---|---|---|
| TEC | Wakefield-Vette | TEC 40-33-127 | 40 × 40 mm | $Qmax$ = 72 W |
| Heatsink | Fischer electronics | SK 85 | 160 × 100 mm | $Rth$ = 0.9 K/W DC |
| Fan | CJY | - | 90 × 90 mm | 12 V/0.2 A |
| DC source | Keithley | 2230G-30–6 | 3 channels | $Vout$ = 30 V $Iout$ = 6 A |

All three TECs were connected in series while the fans were connected in parallel. The TEC setup was mounted on a container filled with water where the heatsink from the cold side was placed inside the container as shown in Figure 5.1 (b). TEC cooling water flowed down the solar still cover at a flow rate of 2 L/hr. The TEC cover cooling experiment was conducted for three days using an input power, $W_{TEC}$ of 12 W (30/5), 27 W (1/6), and 36 W (2/6) which was achieved by adjusting the applied current, $I_{TEC}$ from 2 A (12 W) to 4 A (36 W). The data was compared to a solar still reference (without cooling) to help make better comparisons between the results regardless of the changes in weather conditions during the experiments. The experiments were conducted from 9 a.m. to 5 p.m. and cover cooling started at 10 a.m. Since the solar stills were single slopes, the stills were south oriented for maximum solar radiation absorption. Saltwater with 3.5% salinity was used and placed in the basin at a depth of 1 cm before commencing the experiment. After completion of each experiment, the basins were cleaned, and new saline water was added for the subsequent experiments. The temperatures were measured using K-type thermocouples for the basin water, inner cover, and cooling. The outdoor ambient temperature and humidity were measured using a temperature and humidity sensor (Benetech1361). A solar power meter (TES-132) was used to measure and record the solar radiation and the sensor was placed on the solar still cover to measure the direct solar radiation obtained by the solar still. Photographs of the solar stills, TEC setup, and a schematic diagram of the overall experimental setup are illustrated in Figure 5.2. The accuracy and ranges of the measuring instruments are listed in Table 5.2.

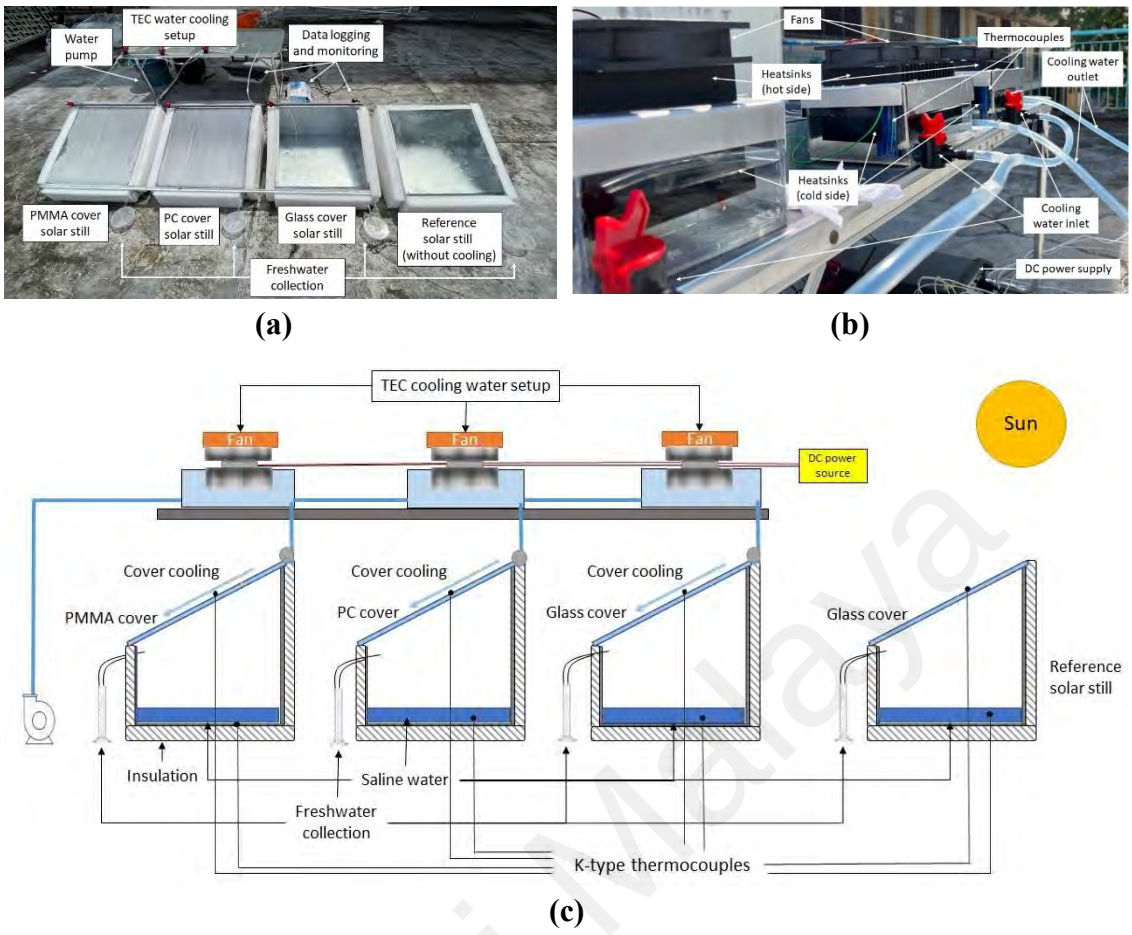


**Figure 5.2: Solar still outdoor experimental setup (a) photograph of the setup and (b) TEC setup (c) schematic diagram of the setup.**

**Table 5.2: Measuring instruments range, accuracy, and standard uncertainty.**

| Instruments | Range | Accuracy | Standard uncertainty |
|---|---|---|---|
| Type-K thermocouple | 0–105°C | ±0.1°C | 0.0577°C |
| Data logger (NI-9211) | 0–200°C | ±0.9°C | 0.5°C |
| Solar power meter | 0–2000 W/m$^2$ | ±10 W/m$^2$ | 5.7 W/m$^2$ |
| Graduated cylinder | 0–25 mL | ±0.25 mL | 0.14 mL |
| Humidity sensor | 0–99.9% | ±0.1% | 0.057% |

## 5.3 Theoretical analysis

### 5.3.1 Uncertainty analysis

The standard uncertainty of the measured data and the accuracy of the instruments used in measurements are reported in Table 5.2.

The uncertainty analysis is tabulated as follows in Equation 5.1 (Sardarabadi et al., 2014):

$$\mathbf{u} = \frac{\mathbf{a}}{\sqrt{\mathbf{3}}} \tag{5.1}$$

where $a$ corresponds to the accuracy limits of measuring instruments and $u$ is the standard uncertainty.

The combined uncertainty of experimental data is obtained using Equation 5.2 (Bell, 1999):

$$\mathbf{u(y)} = [\left(\frac{\delta \mathbf{y}}{\mathbf{x_1}}\delta \mathbf{x_1}\right)^{\mathbf{2}} + \left(\frac{\delta \mathbf{y}}{\mathbf{x_2}}\delta \mathbf{x_2}\right)^{\mathbf{2}} + \cdots]^{\mathbf{0.5}} \tag{5.2}$$

where $y$ indicates the function value of the input $x_1$, and $\delta x_1$ shows the measured input values of $x_1$. Substituting the measured parameters into Equation 5.2, the maximum combined uncertainty for the energy and exergy efficiency of solar still using the TEC cooling system was estimated to be 0.045.

### 5.3.2 Energy efficiency

For conventional solar still, the energy efficiency, $\eta$ is the ratio of energy output (evaporative heat transfer energy) to energy input (sum of solar radiation times with the solar still basin area) given by Equation 3.1 in **3.3.2 Effect of mixed wettability surface on solar still productivity**. For solar still using the TEC cooling system, the energy efficiency includes the energy input from the power consumption of the TEC module, $\dot{W}_{TEC}$, water pump, $\dot{W}_{pump}$ and fans, $\dot{W}_{fan}$ used for the system. The equation is as given below in Equation 5.3 (Shoeibi et al., 2020):

$$\boldsymbol{\eta_{TEC}} = \frac{\boldsymbol{\Sigma \dot{m}_{ev} h_{fg}}}{\mathbf{I_{total} A_w + \dot{W}_{pump} + \dot{W}_{TEC} + \dot{W}_{fan}}} \tag{5.3}$$

### 5.3.3 Exergy efficiency

The exergy efficiency of the solar still, $\eta_{ex}$ is given by the following Equation 5.4 (Shoeibi et al., 2020):

$$\boldsymbol{\eta_{ex} = \frac{Ex_{out}}{Ex_{in}}} \tag{5.4}$$

where the exergy produced by the solar still, $Ex_{out}$ is given by Equation 5.5:

$$\boldsymbol{Ex_{out} = m_{ev} h_{fg} \left(1 - \frac{T_a}{T_w}\right)} \tag{5.5}$$

whereas exergy input, $Ex_{in}$ is calculated using the following Equation 5.6 and 5.7 for solar still using TEC cooling system and reference solar still respectively:

$$\boldsymbol{Ex_{in} = I_{total} A_w \left[1 - \frac{4T_a}{3T_s} + \frac{1}{3}\left(\frac{T_a}{T_s}\right)^4\right] + \dot{W}_{TEC} + \dot{W}_{pump} + \dot{W}_{fan}} \tag{5.6}$$

$$\boldsymbol{Ex_{in} = I_{total} A_w \left[1 - \frac{4T_a}{3T_s} + \frac{1}{3}\left(\frac{T_a}{T_s}\right)^4\right]} \tag{5.7}$$

where $T_s$ is the temperature of the sun which is approximately 6000 K (Kabeel et al., 2019).

### 5.3.4 Cost analysis

The cost per litre, CPL of annual freshwater productivity of the solar still, M is calculated based on Equation 4.3 to 4.9 given in **4.3.6 Economic Analysis**.

## 5.4 Results and discussion

### 5.4.1 Temperature profile of solar still basin and cover

Weather conditions on the days of the experiments are depicted in Figure 5.3. The highest solar radiation was obtained around 1 p.m. whereas $T_a$ continues to rise until 5 p.m. The average solar radiation and $T_a$ obtained for experimental day 30/5, 1/6 and 2/6 were 373.4 W/m$^2$, 339 W/m$^2$ and 328.9 W/m$^2$ and 37.1°C, 37.7°C, 36.5°C, respectively.

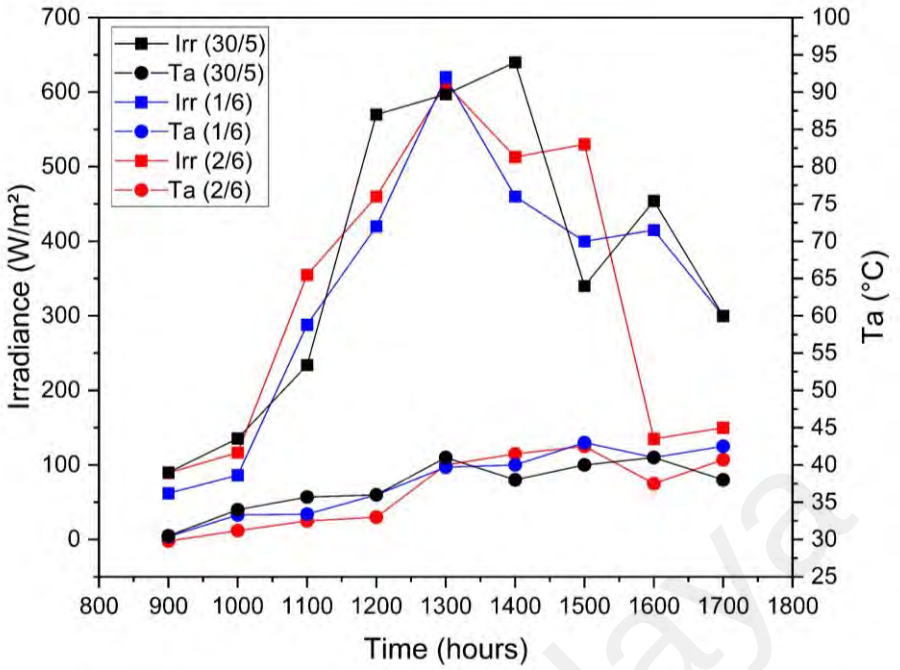


**Figure 5.3: Solar irradiance, Irr and ambient temperature, $T_a$ measured on experimental days 30/5 (2 A), 1/6 (3 A), and 2/6 (4 A).**

#### 5.4.1.1 Effect of $I_{TEC}$ on different cover material

Figure 5.4 illustrates the $T_w$ and $T_c$ for glass, PC, and PMMA cover with TEC cooling and reference solar still. Based on Figure 5.4 (d), the highest temperature obtained for reference solar still was on 30/5 (2 A) with $T_w$ and $T_c$ of 60.6°C and 61.7°C, respectively. On 1/6 (3 A) and 2/6 (4 A), the temperatures for reference solar still were similar except for a faster drop in temperature on 2/6 starting from 3 p.m. The $T_w$ trend for all the solar stills with TEC cooling corresponded with the amount of cooling obtained whereby a higher $I_{TEC}$ caused a lower $T_w$ and vice versa. However, a similar $T_w$ was recorded for PMMA cover solar still for $I_{TEC}$ of 3 A and 4 A. $T_c$ for glass cover solar still did not show much difference for all $I_{TEC}$ applied where the temperature of $T_c$ ranged between 28°C to 51°C. In contrast to $T_c$ for glass cover, the $T_c$ for PC cover solar still followed the trend of $T_w$ whereby a high $I_{TEC}$ resulted in a low $T_c$. For PMMA, the highest $T_c$ was also seen for $I_{TEC}$ of 2 A, but $T_c$ was higher when $I_{TEC}$ of 4 A was applied compared to 3 A.

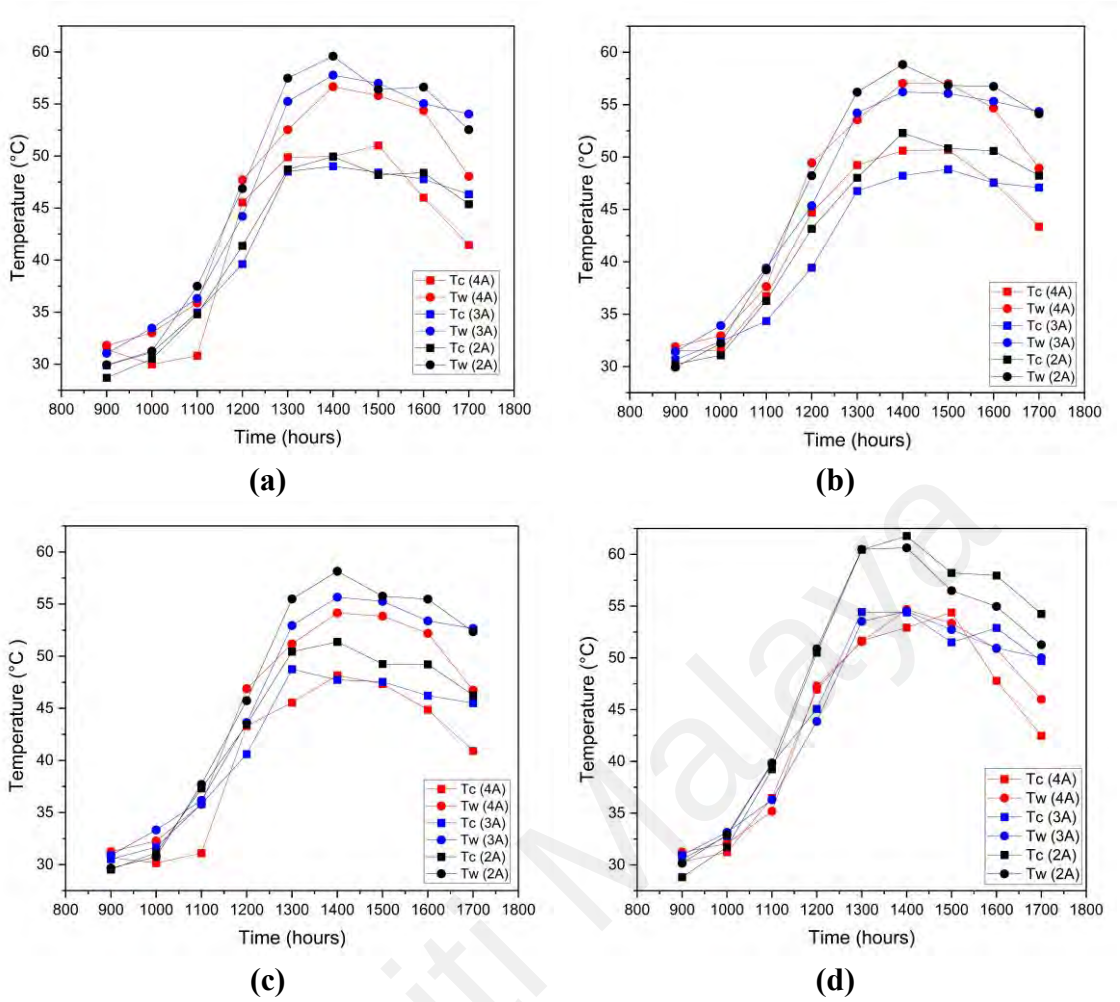


**Figure 5.4: Temperature of cover, $T_c$ and basin water, $T_w$ for (a) glass, (b) PMMA, (c) PC subjected to various $I_{TEC}$, and (d) temperature for reference solar still (without cooling).**

### 5.4.1.2 Comparison of $T_w$, $T_c$ and $T_{w-c}$ for different cover materials

In comparison with reference solar still illustrated in Figure 5.5, $T_w$ was lower for all cover materials with TEC cooling using $I_{TEC}$ of 2 A. However, $T_w$ using TEC cooling of 3 A and 4 A was higher compared to the reference. This increase in temperature was caused by the improvement in the heat transfer rate between the cover and water. The lowest $T_w$ was observed for PC cover solar still compared to glass and PMMA with TEC cooling. $T_c$ for glass cover was the lowest using $I_{TEC}$ of 2 A compared to PC and PMMA but PC had the lowest $T_c$ with 4 A $I_{TEC}$. The addition of TEC cover cooling was shown to reduce $T_c$ for solar still with glass cover compared to the reference solar still that also used glass cover. The TEC cooling system used water as the coolant medium to remove

heat from the solar still covers. TEC cooling water temperature was affected by applied $I_{TEC}$ and subsequently $W_{TEC}$.

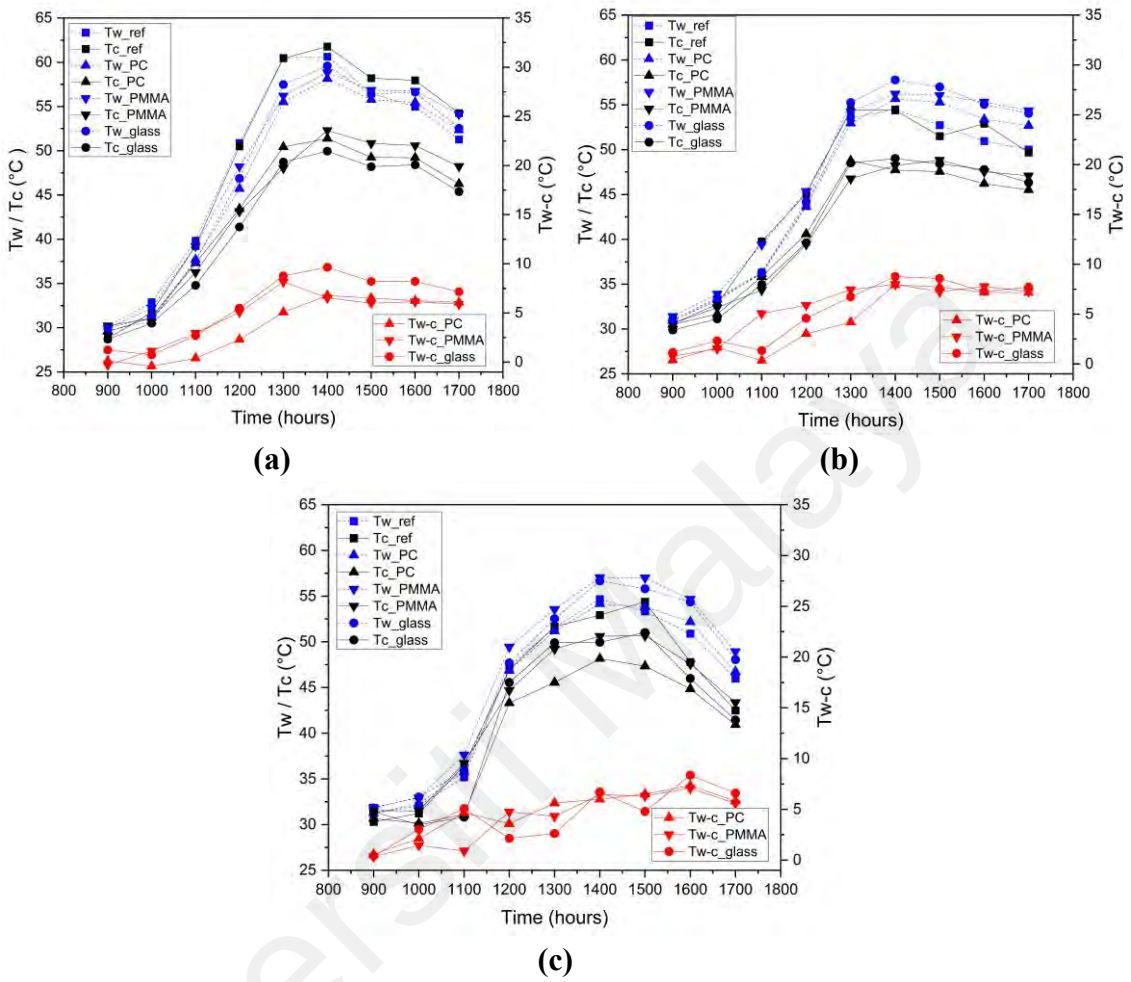


**Figure 5.5: Temperature of $T_c$, $T_w$ and $T_{w-c}$ for various cover materials with $I_{TEC}$ of (a) 2 A, (b) 3 A and (c) 4 A.**

Based on Figure 5.6, the average cooling water temperature, $T_{cw}$ for $I_{TEC}$ 2 A (12 W), 3 A (27 W) and 4 A (36 W) were 31.9°C, 31.6°C and 31.4°C, respectively. Although $T_{cw}$ variation exists depending on weather conditions, a slight change is noticeable between all three $I_{TEC}$. A high $I_{TEC}$ produced an increase in TEC cooling power, $W_{TEC}$ and thus caused a lower $T_{cw}$. Therefore, $T_{cw}$ affected $T_w$ and $T_c$ for all cover material as compared to reference solar still. Besides that, the temperature pattern for $T_w$ and $T_c$ varied based on the cover material used despite being subjected to the same cooling power. Properties such as the specific heat capacity and density of the cover material affected the rate of

heat dissipation from the solar still. The difference between $T_w$ and $T_c$, $T_{w-c}$ was much higher for glass cover solar still after 1 p.m., followed by PMMA and PC cover.

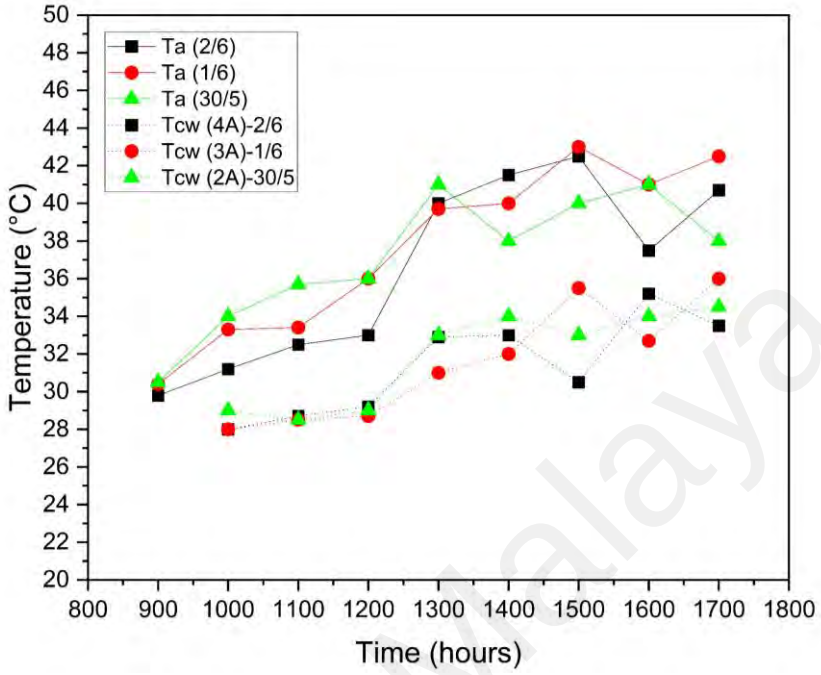


**Figure 5.6: $T_a$ on different experiment days and $T_{cw}$ for different $I_{TEC}$.**

Among the reasons for this difference was that glass dissipates heat better and thus promotes higher heat transfer than plastic materials, resulting in a low $T_c$ and high $T_w$ for glass cover solar still. According to Equation 5.8, the thermodynamic equation for cover with water cooling shows that the energy released from the cover includes both the heat energy of the cover and heat energy removed via forced convection from cooling water (Nazari et al., 2019a; Shoeibi et al., 2021d). Since all three cover materials had similar convective heat transfer coefficients due to a similar cooling system design, the difference that affected the heat energy removal was the density and specific heat of the material. As given in Table 5.3, glass had a higher density than plastic cover which leads to a higher product of mass and specific heat (given all materials had the same volume) compared to PC and PMMA. Therefore, glass had a better heat energy removal than other cover materials which was shown by the low $T_c$ and high $T_{w-c}$.

$$\mathbf{m_c C_p \frac{dT_c}{dT} + h_{c,cw-c} A_c (T_c - T_{cw}) = \alpha I_{total} A_c + h_{t,w-c} A_w (T_{w-c})} \quad (5.8)$$

**Table 5.3: Material properties used in the present study (Zanganeh et al., 2020a).**

| Properties | Glass | PMMA | PC |
|---|---|---|---|
| Transmissivity (VIS range) | 0.87 | 0.92 | 0.92 |
| Absorptivity (VIS range) | 0.056 | 0.03 | 0.04 |
| Emissivity | 0.96 | 0.95 | 0.95 |
| Water contact angle (°) | 31 | 75 | 81 |
| Density (kg/m$^3$) | 2490 | 1180 | 1200 |
| Specific heat capacity (kJ/kg.K) | 0.84 | 1.27 | 1.2 |

### 5.4.2 Freshwater productivity of solar still with various cover material using different TEC cooling power

#### 5.4.2.1 Cumulative freshwater yield

Figure 5.7 depicts the cumulative freshwater yield of various cover materials with an applied $I_{TEC}$ of 2 A, 3 A, and 4 A. There is a difference in the start time of freshwater production for the solar still depending on the cover materials and applied $I_{TEC}$. Reference solar still freshwater production started at 12 p.m. but glass cover solar still with TEC cooling started producing freshwater yield at an earlier time. The glass covered solar still production started around 11 a.m. for applied $I_{TEC}$ of 2 A and 3 A and began earlier by one hour at 10 a.m. for $I_{TEC}$ of 4 A. For PMMA covered solar still, freshwater production began at 1 p.m. for applied $I_{TEC}$ of 2 A and 3 A and at 12 p.m. for $I_{TEC}$ of 4 A. Whereas PC cover had the latest freshwater production around 2 p.m. to 3 p.m. The difference in freshwater production time between the $I_{TEC}$ was due to the reduced $T_c$ from the addition of cover cooling with high $I_{TEC}$ which enables the freshwater to be produced earlier for applied $I_{TEC}$ of 4 A. The starting time of freshwater production for solar still with cover cooling also differs for each cover material depending on the wettability of the material. Glass has the lowest water contact angle followed by PMMA and PC as shown in Table 5.3. A low water contact angle translates to a high wettability of the material's

surface which allowed condensate to form faster than a surface with a higher water contact angle, and thus low wettability. Therefore, the freshwater collection time correlates with the wettability of the surface where the earliest yield was obtained by glass cover followed by PMMA and finally PC.

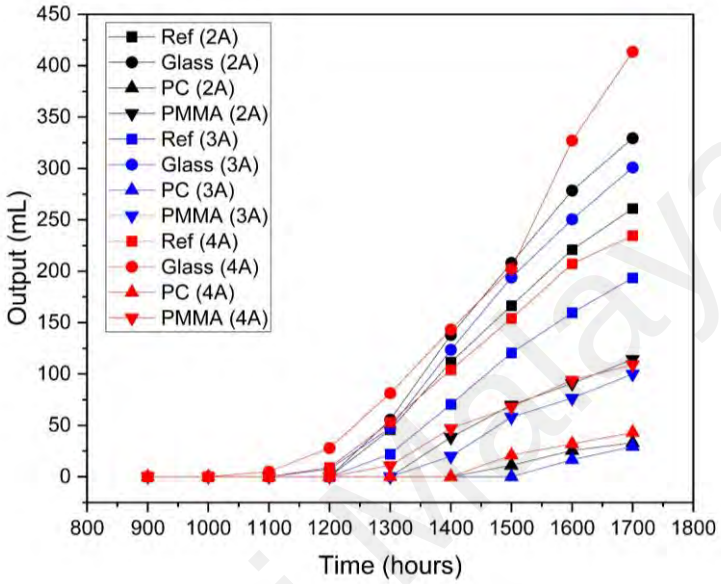


**Figure 5.7: Cumulative freshwater yield for each material with varying $I_{TEC}$.**

The daily cumulative freshwater yield for each material for the experiment days is shown in Table 5.4. The daily freshwater yield was the lowest on 1/6 whereby the recorded output of the reference solar still was 774 mL/m$^2$. The daily freshwater yield recorded was higher on 2/6 than the previous day with a value of 938.4 mL/m$^2$ due to higher solar radiation observed from 10 a.m. to 3 p.m. as shown in Figure 5.3. On 30/5 the output was the highest for reference solar still with a yield of 1044 mL/m$^2$ which corresponds with the solar radiation measured on that day. For TEC cover cooling solar still, glass cover produced the highest yield followed by PMMA and PC for all three experiment days. Contrary to the freshwater yield trend for reference solar still, glass and PC cover obtained the highest yield on 2/6 with applied $I_{TEC}$ of 4 A, thus corresponding with the $I_{TEC}$ applied. However, PMMA cover solar still had the highest yield on 30/5 despite the low applied $I_{TEC}$ of 2 A.

**Table 5.4: Daily productivity of the solar still using various cover materials.**

| Experiment days | I, avg ($W/m^2$) | $T_a$, avg (°C) | Daily freshwater yield ($mL/m^2$) | | | |
|---|---|---|---|---|---|---|
| | | | Reference | Glass | PC | PMMA |
| 30/5 (2 A) | 373.4 | 37.1 | 1044.0 | 1318.0 | 132.0 | 456.8 |
| 1/6 (3 A) | 339 | 37.7 | 774.0 | 1204.0 | 118.0 | 400.0 |
| 2/6 (4 A) | 328.9 | 36.5 | 938.4 | 1654.4 | 172.0 | 436.0 |

The amount of freshwater yield was found to correlate with the cover material surface's wettability where a high wettability results in a faster condensate formation and thus a higher production of freshwater. Besides, it was observed that both glass and PMMA had a higher $T_w$ than PC. A high $T_w$ often results in higher freshwater production and is deemed as one of the most important factors that influence the amount of yield produced by the solar still (Fu et al., 2021; Parsa et al., 2022). It was also revealed in the previous section that the glass cover had a higher rate of evaporative heat transfer followed by PMMA and PC due to the high $T_{w\text{-}c}$. The rate of freshwater productivity is defined by Equation 5.9 and 5.10 (Al-Nimr & Qananba, 2018),

$$\dot{\mathbf{m}}_{\mathbf{ev}} = \frac{\mathbf{Q_{ev}}}{\mathbf{h_{fg}}} \tag{5.9}$$

$$\mathbf{Q_{ev}} = \mathbf{h_{ev}A_w(T_{w-c})} \tag{5.10}$$

where the rate of heat transfer by evaporation, $Q_{ev}$ has a linear relationship with $T_{w\text{-}c}$ as shown in Equation 5.9 thus affecting the freshwater production of the solar still.

#### 5.4.2.2 Productivity comparison between TEC cooled solar still using various cover material and reference solar still.

Figure 5.8 illustrates the comparison in productivity between the reference solar still and solar still with TEC cooling using the different cover materials. As expected, PC had the poorest productivity in comparison to reference solar still ranging from around -87% to -82%. Productivity for PMMA cover solar still was also lower than reference solar ranging between -56% to -48%. The addition of the TEC cooling system was not

sufficient to overcome the difference in productivity compared to the reference, therefore resulting in a negative value for the productivity comparison of the solar still using PC and PMMA cover. On the other hand, glass cover solar still using TEC cooling had a vast improvement in productivity where an increase in $I_{TEC}$ of 2 A, 3 A and 4 A increased the productivity of the solar still by 26%, 56%, and 76%, respectively compared to the reference. This improvement was also shown for PC cover solar still albeit only slightly with only a 3% to 4% difference between the different $I_{TEC}$. However, PMMA showed a different trend with an increase in $I_{TEC}$ where the lowest freshwater yield achieved was using 3 A $I_{TEC}$ followed by 4 A and 2 A. This showed that solar still with PMMA cover was affected by the high cooling power due to the properties of the cover material that is unable to dissipate heat as well as glass and PC cover as mentioned in the previous subsection.

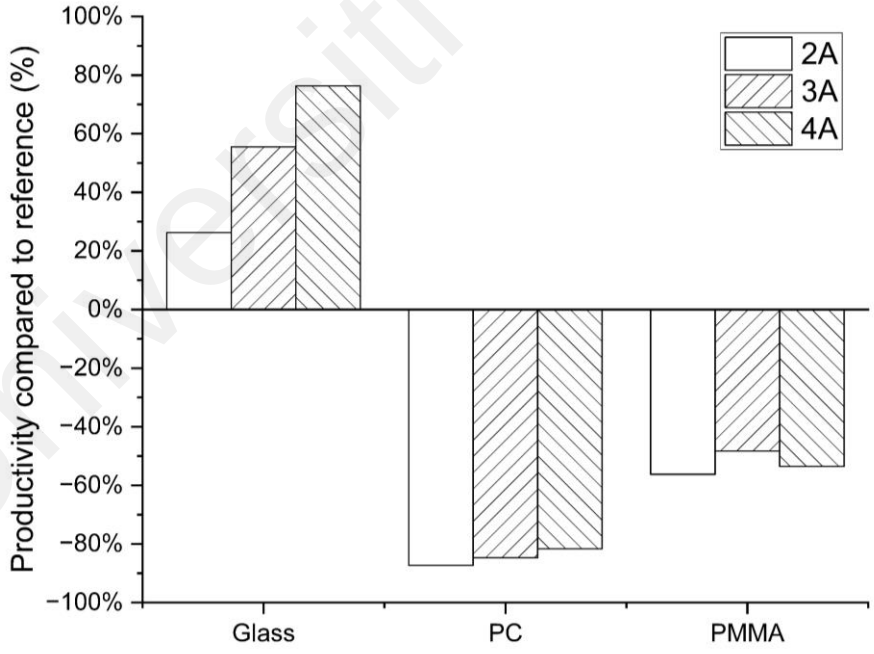


**Figure 5.8: Solar still productivity compared to reference solar still for different $I_{TEC}$.**

### 5.4.3 Efficiency of solar still using different TEC cooling system

#### 5.4.3.1 Energy efficiency

Figure 5.9 illustrates the daily energy efficiency for solar still using various solar still covers. The highest efficiency of the solar still achieved for glass and PC cover was 23.6% and 2.5% on 2/6 using 4 A $I_{TEC}$. Whereas the highest efficiency achieved by PMMA cover solar still was 7.2% on 30/5 using 2 A $I_{TEC}$. The energy efficiency corresponded with the daily yield obtained by the solar still using TEC cover cooling whereby a high freshwater yield resulted in an increase in efficiency. A low energy efficiency was obtained on 1/6 using $I_{TEC}$ of 3 A, due to the low productivity of the solar still as shown previously in Table 5.4. In terms of cover material with TEC cooling, glass cover achieved a slightly better efficiency compared to reference with a range of 18% to 23.6% while reference solar still efficiency ranged between 16.8% to 21% for the three experiments. PMMA and PC achieved an efficiency of less than 10% for all applied $I_{TEC}$ whereby the efficiency of PMMA ranged from 6% to 7.2% and PC ranged from 1.8% to 2.5%. The enhancement in efficiency compared to reference for glass cover with $I_{TEC}$ of 2 A, 3 A and 4 A was 1.8%, 7.5% and 12.5%. While for PMMA and PC cover, the comparison in efficiency to reference solar still for $I_{TEC}$ of 2 A, 3 A and 4 A ranged between -70.4% to -64.3% and -89.8% to -88.3%, respectively.

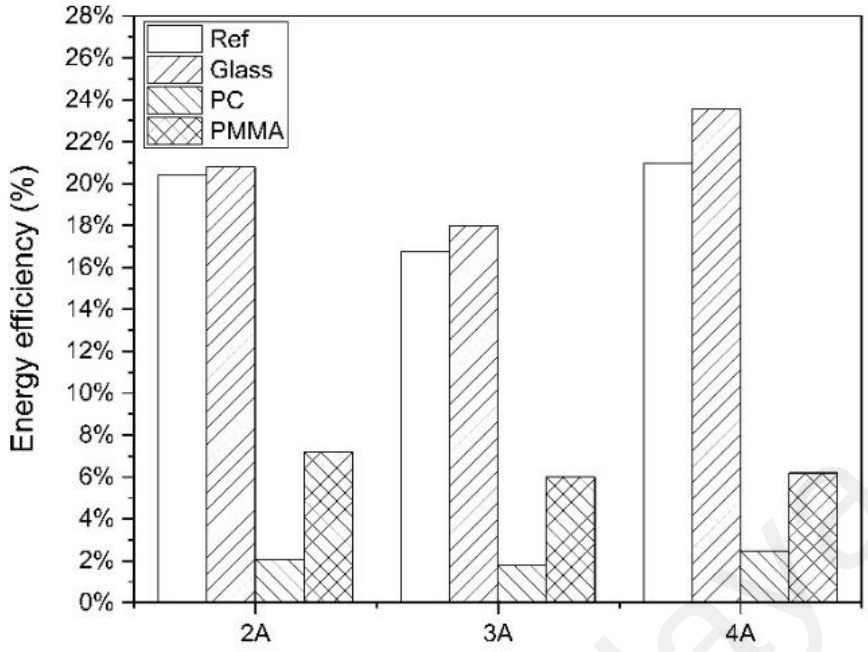


**Figure 5.9: Daily energy efficiency of the solar still on different experiment days using different $I_{TEC}$.**

#### 5.4.3.2 Exergy efficiency

Figure 5.10 illustrates the instantaneous exergy efficiency of the solar stills. Figure 5.10 (a) and 5.10 (c) showed that there was only a slight difference in exergy efficiency between glass cover with TEC cooling and reference solar still for applied $I_{TEC}$ of 2 A and 4 A. The difference in efficiency was more obvious for $I_{TEC}$ of 3 A shown in Figure 5.10 (b), signifying that the amount of work performed by the solar still was better with the addition of cooling compared to the reference solar still.

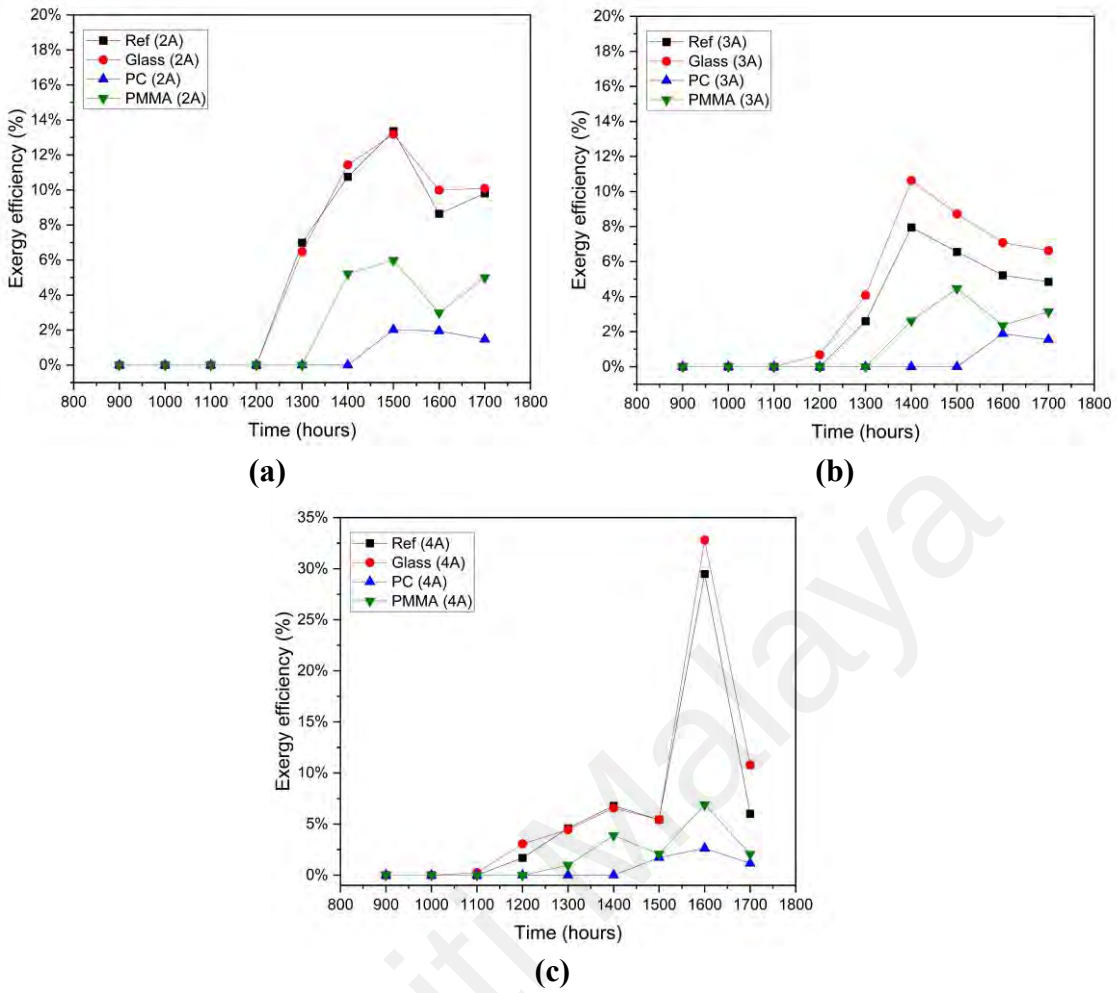


**Figure 5.10: Exergy efficiency for various cover materials with TEC current input of (a) 2 A, (b) 3 A, and (c) 4 A.**

Table 5.5 depicts the average daily exergy efficiency of the solar still. The average exergy efficiency for reference solar still ranged between 3.02% to 6% for the three experimental days. For TEC cooling solar still, solar still using glass cover achieved the highest exergy efficiency followed by PMMA cover and PC cover with a maximum efficiency of 7.04%, 2.13% and 0.61%, respectively. The average exergy efficiency obtained by the glass cover was highest using 4 A $I_{TEC}$, however, PC and PMMA performed similarly and even less using the 4 A $I_{TEC}$ compared to 2 A and 3 A $I_{TEC}$. Therefore, the use of TEC water cooling at higher $I_{TEC}$ for PC and PMMA cover solar still negatively affected the exergy output of the solar still and reduced its quality of work.

**Table 5.5: Average exergy efficiency (%) for different cover materials and $I_{TEC}$.**

| Cover material | Average $\eta ex$ (%) | | |
|---|---|---|---|
| | 2 A | 3 A | 4 A |
| Reference | 5.51 | 3.02 | 6.00 |
| Glass | 5.69 | 4.20 | 7.04 |
| PC | 0.60 | 0.38 | 0.61 |
| PMMA | 2.13 | 1.40 | 1.77 |

### 5.4.4 Economic analysis of solar still

The initial fixed cost for reference solar still without cooling based on the cost given in Table 5.6 was $ 148.7. For the TEC cooling system using glass, PC, and PMMA cover, the fixed cost was $ 232.9, $ 216.8, and $ 214.5, respectively.

**Table 5.6: The cost of each item used to fabricate solar still.**

| Items | Cost of items ($) |
|---|---|
| Galvanized Iron (GI) | 84.8 |
| PE insulator | 10.7 |
| Fabrication of solar still | 23 |
| TEC set (TEC, heatsink, fan, thermal paste, piping, acrylic water container) | 84.1 |
| DC pump | 4 |
| PMMA cover | 23 |
| PC cover | 25.3 |
| Glass cover | 41.4 |

To provide a clear comparison between the different solar stills studied, the annual productivity selected for this analysis was based on the freshwater yield obtained for reference solar still on 30/5. The calculation of annual productivity for various cover materials and TEC input was calculated by the percentage of improvement times the annual productivity of reference solar still of 381.06 L/m$^2$. Based on this calculation, the highest annual productivity obtained by solar still using glass cover followed by PMMA and PC cover as shown in Table 5.7.

**Table 5.7: Annual productivity (L/m$^2$) for solar stills based on freshwater yield obtained on 30/5.**

| $I_{TEC}$ | Reference | Glass | PC | PMMA |
|---|---|---|---|---|
| 2 A | 381.06 | 481.07 | 48.18 | 166.73 |
| 3 A | 381.06 | 592.76 | 90.37 | 196.93 |
| 4 A | 381.06 | 671.81 | 69.84 | 177.05 |

According to Table 5.8, glass cover had a lower CPL compared to other cover materials with cover cooling. However, the cost of solar still using TEC cover cooling was much higher compared to reference solar still without cooling at low $I_{TEC}$ despite having higher productivity. The cost drops when 4 A $I_{TEC}$ was applied for glass cover solar still which shows that it is more cost-effective for solar still with a TEC cooling system to run at a high TEC cooling power. Meanwhile, for PC and PMMA, the CPL was lowest when 3 A $I_{TEC}$ was applied followed by 4 A and the highest CPL was obtained using $I_{TEC}$ of 2 A. PC cover was the least cost-effective material to use for a solar still cover as the CPL is double the amount compared to using PMMA and is six times higher compared to glass cover solar still. Although the initial fixed cost was cheaper using plastic cover material, glass cover produces a solar still with high productivity which resulted in a lower CPL than plastic cover materials. Therefore, a glass cover is more cost-effective than using plastic cover material for single slope solar still regardless of the addition of a TEC cooling system.

**Table 5.8: CPL ($/L/m$^2$) of the solar still calculated from the annual productivity in Table 5.7.**

| $I_{TEC}$ | Reference | Glass | PC | PMMA |
|---|---|---|---|---|
| 2 A | 0.0473 | 0.0587 | 0.5456 | 0.1560 |
| 3 A | 0.0473 | 0.0476 | 0.2909 | 0.1321 |
| 4 A | 0.0473 | 0.0420 | 0.3763 | 0.1469 |

Table 5.9 shows the comparison between the present study and previous studies for solar still using the TEC cooling system.

**Table 5.9: Comparison of the present study with previous studies using TEC cooling systems.**

| Solar still design | Cover material | Daily productivity ($mL/m^2$) | Productivity improvement (%) | Efficiency (%) | | CPL ($/L/m^2) |
|---|---|---|---|---|---|---|
| | | | | Energy | Exergy | |
| Double slope with heating (Shoeibi et al., 2021d) | Glass | 2970 | 103.7 | 28 (max) | 1.45 (max) | 0.1055 |
| Single slope with nanofluid (Nazari et al., 2019a) | Glass | 4400 | 39.6 | 32 | 3.4 | 0.023 |
| Pyramid-shape with nanofluid and turbulator (Parsa et al., 2022) | Glass | 6040 | -78.8 | 22–25.6 | 1–1.5 | 0.023 |
| Single slope with preheating (Pounraj et al., 2018) | Glass | 3355 | 27.1 | 24.7 | – | – |
| Single slope (present study) | Glass | 1654.4 | 76.3 | 23.6 | 7.04 | 0.042 |
| | PC | 172 | -81.7 | 2.5 | 0.61 | 0.376 |
| | PMMA | 436 | -53.5 | 6.2 | 1.77 | 0.147 |

## 5.5 Summary

This study investigated the performance of solar stills with various cover materials subjected to cover cooling using different TEC cooling power. The performance of the solar still was evaluated based on the freshwater productivity, energy and exergy efficiency, and the economic aspect. Findings revealed that glass cover solar still with cover cooling performed significantly better compared to PMMA and PC cover. Increasing the TEC cooling power showed improvement to glass and PC cover solar still

productivity, however, a high TEC cooling power was not beneficial for PMMA cover solar still. The following summarised the results of the present study:

i. Solar still with TEC cooling system improved in freshwater productivity by 26%, 56% and 76% for glass cover and -87%, -84% and -82% for PC cover using $I_{TEC}$ of 2 A, 3 A and 4 A, respectively compared to reference solar still.

ii. PMMA cover solar still productivity improved compared to reference from -56% to -48% with an increase in $I_{TEC}$ from 2 A to 3 A but reduced to -53% when 4 A $I_{TEC}$ was applied.

iii. Glass and PC cover solar still obtained the highest energy and exergy efficiency of 23.6% and 2.5% and 7% and 0.6%, respectively when 4 A $I_{TEC}$ was applied. Whereas PMMA covered solar still had the highest efficiency of 7.2% using 2 A $I_{TEC}$.

iv. Economic analysis showed that the CPL for reference solar still was $ 0.047 whereas the lowest CPL obtained for glass, PC and PMMA with TEC cover cooling was $ 0.042, $ 0.291, and $ 0.132, respectively.

v. The drastic improvement of up to 76% found for using TEC cooling in comparison to 10% for water-cooled glass cover solar still showed the benefits of using TEC cooling with high power for glass covered solar still. Therefore, the TEC cooling method may prove to be beneficial and may produce a higher degree of improvement when applied to the mix wettability covered solar still.

# CHAPTER 6: ENERGY, EXERGY, ECONOMIC, ENVIRONMENTAL ANALYSIS FOR SOLAR STILL USING PARTIALLY COATED CONDENSING COVER WITH THERMOELECTRIC COVER COOLING

The energy, exergy, economic, and environmental analysis of a solar still utilising a mix wettability cover with thermoelectric cover cooling is presented in this chapter. The chapter commences with an introduction, followed by a detailed methodology section that outlines the materials used, experimental setup, procedures, and theoretical considerations employed in the study. The results and discussions subsection thoroughly examines the five key parameters of solar still performance: freshwater productivity, energy, exergy, environmental impact, and economic aspects, as well as related parameters such as enviro-economic, exergo-economic, and energy matrices. Lastly, the chapter concludes by summarizing the findings and insights derived from the study.

## 6.1 Introduction

Freshwater production of solar still varies significantly based on the environment and design of the solar still. Hence, various heating and cooling method has been incorporated in the solar still design for improvement in basin water temperature and condensing cover temperature. Solar still basin water heating is often done using a solar collector combined with the solar still. Among the commonly used solar collectors were flat plate collectors, parabolic troughs, and concentrated parabolic dish (Arunkumar et al., 2019a). Other methods such as using internal heat pipes were also previously investigated (Shoeibi et al., 2022c). Heating of basin water using thermoelectric has also been explored (Parsa et al., 2022). Whereas for cover cooling, techniques such as cooling using flowing air or water and thermoelectric coolers (TEC) were used to decrease the solar still's cover temperature (Omara et al., 2017). Studies on comparison between water and air coolant mediums found that the water-cooling technique resulted in a higher heat transfer rate

that allowed the productivity of the solar still to improve significantly as compared to air cooling (Arunkumar et al., 2013). Improvement in water productivity for a double slope solar still using TEC water-cooled technique resulted in almost doubled the amount of carbon dioxide ($CO_2$) mitigation and a lower cost per litre (CPL) of 0.243 $/L compared to 0.277 $/L for air-cooled (Shoeibi et al., 2021c).

Besides the heating and cooling method, the addition of surface coating has also been shown to produce a favourable outcome by enhancing the properties of the absorber surface to retain and absorb heat better as well as improving the wettability of a condensing cover surface to promote faster condensate removal and collection. The solar still absorber is usually painted matte black to enhance the heat absorption from solar while reducing the reflective effect of a metal-based absorber. Dark-coloured materials such as bitumen were found to raise the productivity of the solar still with an enhancement of 25.4% compared to the conventional solar still (Ouar et al., 2017). Mixing graphite powder with black paint for basin absorber plate coating was shown to improve the freshwater productivity of single slope solar still by 17% using a 40% concentration of graphite powder (Panchal et al., 2021).

Surface coating is also used to alter the cover surface's wettability. Modifying the surface to a low wettability or hydrophobic changes the condensation mode to dropwise condensation whereas modifying the surface to a high wettability or hydrophilic resulted in filmwise condensation mode. Previous studies showed that both condensation modes resulted in improvements to solar still productivity. Zanganeh et al. (2019) examined the use of silicon (Si) nanoparticles to produce dropwise condensation and titanium dioxide ($TiO_2$) nanoparticles to produce filmwise condensation on a solar still glass cover. The authors found that a low tilt angle of 10° resulted in reduced productivity of the solar still by 34%. Whereas the productivity improved by 20% with the increase of tilt angle to 45°

for dropwise condensation (Zanganeh et al., 2020a). However, the opposite was found for filmwise condensation whereby the improvement drops from 5.7% to 2.3% with an increase in tilt angle from 25° to 45° (Zanganeh et al., 2020b). Thakur et al. (2022) explored the synergetic effect of nano-coating both the absorber and condensing cover using nano-silicon for the cover, and rGO for the absorber. The results showed that using nano-coating on the cover only improved the yield by 13.9% (Thakur et al., 2021b). Whereas nano-coating on both absorber and cover resulted in an improved freshwater yield by 58% (Thakur et al., 2022). An improvement to the solar still productivity by 43% was found using a flat solar still due to the enhancement in condensate collection from the application of the ultra-hydrophilic coating and wick material on the solar still cover (Peng et al., 2021b).

The performance of the solar still with the addition of enhancement techniques was often determined based on the productivity of the system i.e., the distillate or freshwater yield. Besides that, the calculation of the energy and exergy efficiency of the modified solar still is crucial to determine the system's ability to perform more efficiently than the conventional solar still. The economic analysis is another method to establish the solar still's performance in terms of the distillate yield CPL and its technology payback time based on the selling price of water in a certain country. Recently, more emphasis has been placed on determining the environmental effect of the use of solar stills for water production. This aligns with the growing concern of minimizing and eliminating carbon footprints that are associated with the life cycle of a technology (Jijakli et al., 2012). A few studies on solar still performance have been analysed based on the five main parameters of productivity, energy, exergy, economics, and environment. Nazari and Daghigh (2022) employed a parabolic dish concentrator and thermoelectric cooling channel for a non-cover solar still. The system improved the yield by 25.6% and produced energy and exergy efficiencies of 22.3% and 4.8%, respectively using 300 L/min fan

speed in the thermoelectric channel. The CPL and $CO_2$ amount mitigated by the solar still was $ 0.0056 and 22 tonnes in a lifetime, respectively. Sharshir et al. (2022) studied the use of an external condenser, evacuated tubes, nanofluid and ultrasonic foggers for pyramid solar still. The enhancement in yield, daily energy and exergy efficiencies, CPL, and $CO_2$ mitigation obtained by the solar still was 162.2%, 66.9%, 7.46%, $ 0.014, and 1.4 tonnes per year, respectively. Utilisation of a spiral solar collector and internal condenser resulted in an improvement in yield by 751.7% with an energy and exergy efficiency of 21.3% and 3.1%, respectively (Abaszadeh Hashemi et al., 2022). The proposed system obtained a CPL of $ 0.012 and $CO_2$ mitigation of 4 tonnes in a lifetime. Passive and active solar still was studied in locations with different altitudes (Parsa et al., 2020b). Both solar stills performed better at lower altitudes with an annual yield of 916.2 L and 2971.8 L for passive and active solar still, respectively. The active solar still had an energy and exergy output, CPL, and $CO_2$ mitigation of 588.7 kWh/year, 81.6 kWh/year, $ 0.014, 30.8 tonnes/year. Water-cooled double slope solar still produced an annual energy and exergy output of 246.3 kWh and 29.25 kWh (Shoeibi et al., 2021c). The CPL and $CO_2$ mitigation obtained by the solar still was $ 0.243 and 14.8 tonnes, respectively.

Previous literature suggests that improvement to the condensation using cover cooling and surface coating benefits the solar still performance. However, the increase in freshwater yield with a higher TEC power input depended on the basin water temperature whereby a low basin water temperature had a negative outcome using higher TEC power (Al-Madhhachi, 2018). Furthermore, results for cover coating showed to produce a negative outcome with the use of a single wettability surface whereby a low wettability surface resulted in reduced freshwater yield due to enhanced dripping effects (Zanganeh et al., 2019). Therefore, the negative effects of both methods can be minimised by combining the use of partial surface coating with cover cooling for further improvement

to the solar still performance. Moreover, recent research showed the importance of analysis encompassing energy, exergy, economic, environmental, and parameters related to the combination of these aspects such as exergo-economic, enviro-economic, and energy matrices in determining the feasibility of the solar still design. Hence, this study aims to investigate the combined effect of using a partially coated condensing cover together with TEC cover cooling on the solar still. The optimal TEC power consumption to produce high-performing solar still was explored by varying the TEC cooling power from 12 W to 36 W. This study also examined the effect of the tropical weather conditions of Malaysia on the modified solar still with TEC cooling. The solar still performance was analysed based on the five main parameters which include freshwater productivity, energy, exergy, environmental and economic. Additional parameters including the relationship between energy and exergy with the environment (enviro-economic) and economic (exergo-economic) as well as energy matrices were also conducted to provide a better perspective of the proposed solar still performance.

## 6.2 Methodology

### 6.2.1 Materials and methods

Solar still with TEC cooling used a partially coated glass cover to form a mix wettability surface on the inner surface of the cover. The mix wettability cover was prepared by spraying a commercial water-based polysiloxane coating on 30% of the glass's surface area. The surface was firstly cleaned using a precoat containing a cleaning agent to remove contaminants from the glass surface to permit sufficient adhesion of the coating to the substrate. Then, the coating was immediately applied upon the surface after the cleaning process was completed to minimise contaminants on the surface. Two layers of coating were applied with 30 minutes of curing period in between the layers at room temperature and the surface treatment was done in a controlled environment without direct exposure to sunlight before and during treatment. The substrate was kept at room

temperature during application and precautions were taken to ensure that the surface treatment was successful. The coating was applied to the collection side of the solar still cover to aid in droplet detachment and minimise the pooling effect at the glass cover's edge. The addition of coating produced a surface with a higher contact angle which allowed condensate to be removed easily. The coated surface was positioned on the front end of the solar still to promote faster condensate removal. The characterisation and selection of the coated surface area have already been given in our previous work. An uncoated glass was used as the cover material for the reference solar still. Both cover materials had a thickness of 3 mm and a dimension of 0.5 m x 0.61 m.

### 6.2.2 Experimental setup and procedure

Both solar stills were fabricated using a galvanized iron sheet of 1.5 mm thickness with a basin area of 0.25 $m^2$. The cover was tilted at a 25° angle. This inclination angle was chosen instead of the optimum inclination angle based on the latitude of location (approximately 3°) to reduce the effect of condensate dripping from an almost zero cover inclination angle. The outer surfaces of the solar still were insulated with polyethylene (PE) foam of a thickness of 5 cm. TEC setup consisted of a single TEC module, two heatsinks placed on the hot and cold side of the TEC module, and two fans to remove heat from the hot side heatsink. A current of 2 A to 4 A was applied to the TEC module to produce a power of 12 W to 36 W using a laboratory DC power source. The TEC cold side was submerged in cooling water and the water flows on the cover at a flow rate of 2 L/hr. The experiment was conducted for three days (29/6 to 1/7/2022) and the location of the experiment was at the Universiti Malaya, Kuala Lumpur, Malaysia (3.118° N latitude/101.656° E longitude). The experiments were conducted from 9 a.m. to 5 p.m. and for water-cooled solar still, cover cooling started at 10 a.m. The solar stills were positioned facing south to receive maximum solar radiation. A 3.5% salinity saline water was placed in the basin with a depth of 1 cm before commencing the experiment. The

basin water was removed after each experiment and the basin was cleaned before repeating each experiment. The temperatures of the basin water, inner cover, and cooling water were measured and recorded using K-type thermocouples. The outdoor ambient temperature and solar irradiance were measured using a temperature sensor (Benetech3016) and a solar power meter (TES-132). A photograph and a schematic diagram of the outdoor experimental setup are shown in Figure 6.1. Range, accuracy, and standard uncertainty of the instruments and sensors used in this experiment are as similarly listed in Table 5.2 in **5.2.2 TEC cover cooling setup**.

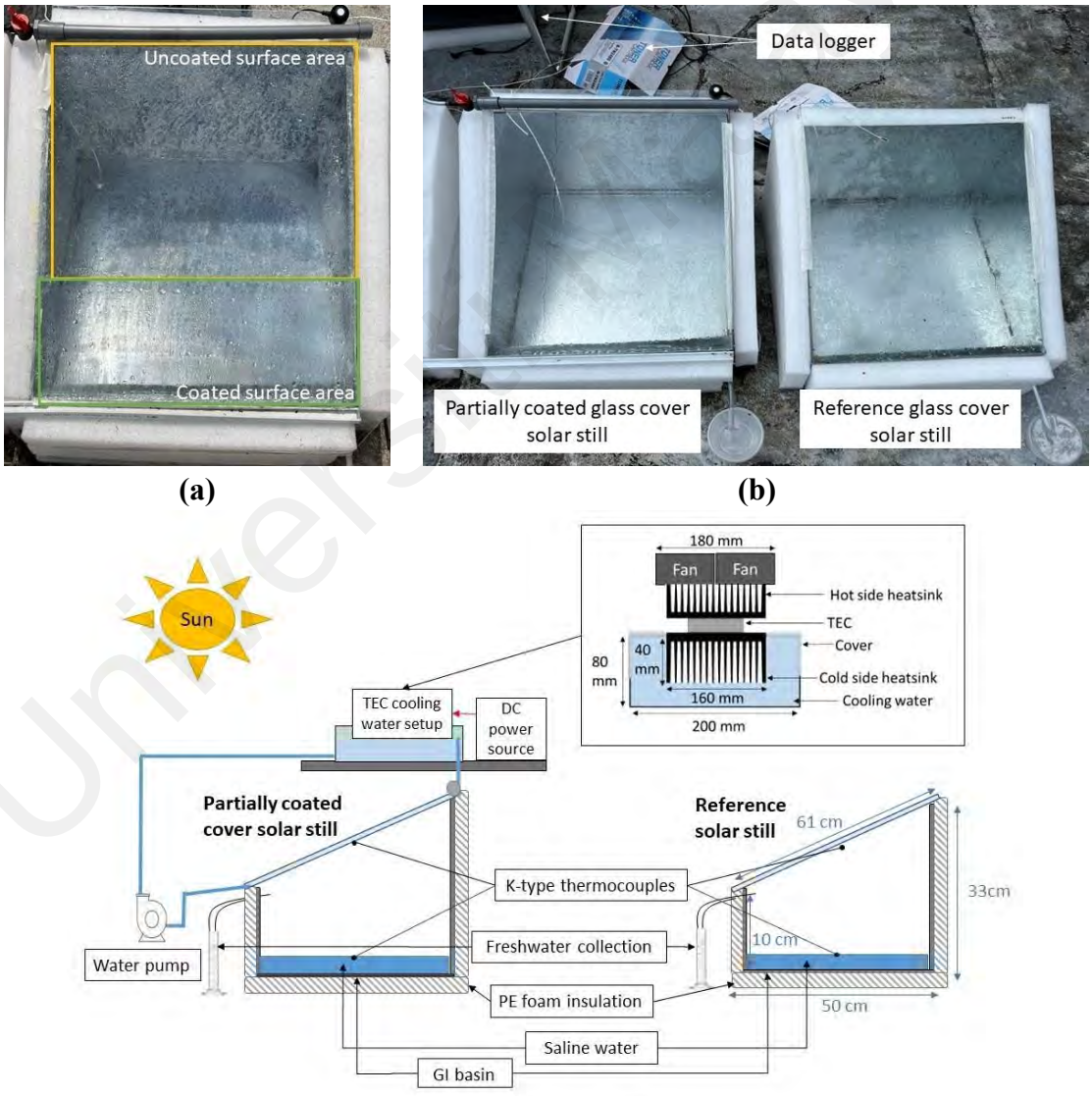


**Figure 6.1: Solar still outdoor experimental setup (a) photograph of the partially coated surface with condensate (b) photograph of the setup (c) schematic diagram of the setup.**

## 6.3 Theoretical analysis

### 6.3.1 Uncertainty analysis

The standard uncertainty of the measured data and the accuracy of the instruments used in measurements are reported in Table 5.2. The uncertainty analysis is calculated using the following Equations 5.1 and 5.2 given in **5.3.1 Uncertainty analysis**. The maximum combined uncertainty for the energy and exergy output of solar still using a partially coated cover with a TEC cooling system based on the above equation was about 2.6%.

### 6.3.2 Efficiency of system

Efficiency is an important parameter when evaluating the application of a system. The efficiency of a system is calculated based on the energy and exergy produced by the solar still system as shown by Equations 5.3 to 5.6 in **5.3.2 Energy efficiency** and **5.3.3 Exergy efficiency** for solar still using TEC cooling system. The energy and exergy efficiency for reference solar still is given by Equation 3.1 and 5.7, respectively.

### 6.3.3 Energy matrices

The energy matrices are used as a decision-making tool to determine the feasibility of a renewable energy-based system in terms of energy by comparing the amount of energy production with the energy consumed by the solar still system. The two energy matrices evaluated in this paper are the energy payback time and the energy production factor.

#### 6.3.3.1 Energy payback time (EPBT)

The duration in which the solar still system output (energy and exergy) makes up for the embodied energy of the components used is known as the energy payback time (EPBT). The embodied energy of a component is obtained based on the amount of energy used to manufacture the component. Table 6.1 gives the embodied energy for each component and material used in the fabrication of solar still. The energy density of the

coating was 174.95 kWh/kg (Liljenström et al., 2013). While the energy density for insulation (PE foam) was taken as 0.63 kWh/kg (Brookes, 2004).

**Table 6.1: The embodied energy of each component used for solar still (Parsa et al., 2020b).**

| Component | Material | Energy density (kWh/kg) | Mass (kg) | Embodied energy, $E_{in}$ (kWh) | | | |
|---|---|---|---|---|---|---|---|
| | | | | Reference | Coated glass | | |
| | | | | | 12 W | 27W | 36 W |
| Body and basin | GI sheet | 13.88 | 8.64 | 119.85 | | 119.85 | |
| Cover | Glass | 4.16 | 2.49 | 10.36 | | 10.36 | |
| Sealant | Silicon | 174.95 | 0.04 | 6.56 | | 6.56 | |
| Fastener (rivets) | Aluminium | 55.28 | $6.6 \times 10^{-4}$ | 0.04 | | 0.04 | |
| Insulation | PE foam | 0.63 | 1.21 | 0.77 | | 0.77 | |
| Coating | Silicon | 174.95 | $7.5 \times 10^{-4}$ | – | | 0.13 | |
| Heat sinks | Aluminium | 55.28 | 1.88 | – | | 103.93 | |
| PVC pump and fan | PVC | 21.4 | 0.05 | – | | 1.07 | |
| Water container and pipe | Acrylic | 28.3 | 0.47 | – | | 13.36 | |
| PV module ($kWh/m^2$) | – | 980 | – | – | 80.36 | 129.36 | 158.76 |
| | | | **Total** | 137.58 | 336.42 | 385.42 | 414.82 |

The embodied energy of the thermoelectric module has not been given due to insufficient information and therefore was not considered in the calculation. A PV module was assumed to be used as the electricity source for the theoretical calculations. The energy payback time based on the energy produced by the solar still, $EPBT_{en}$ is denoted by Equation 6.1 (Joshi & Tiwari, 2018):

$$\mathbf{EPBT_{en}} = \frac{\mathbf{E_{in}}}{\mathbf{(E_{out})_{annual}}} \tag{6.1}$$

whereas the energy payback time based on exergy, $EPBT_{ex}$ is given by Equation 6.2:

$$\mathbf{EPBT_{en}} = \frac{\mathbf{E_{in}}}{\mathbf{(Ex_{out})_{annual}}} \tag{6.2}$$

where $(E_{out})_{annual}$ and $(Ex_{out})_{annual}$ is the annual energy and exergy produced by the solar still, respectively.

#### 6.3.3.2 Energy production factor (EPF)

The energy production factor (EPF) is a crucial parameter in assessing the performance of a solar still system. It is equal to the total energy and exergy output produced by the solar still to the embodied energy of the system. The energy production factor in a year based on the energy produced by the solar still, $EPF_{en}$ is denoted by Equation 6.3 (Joshi & Tiwari, 2018):

$$\mathbf{EPF_{en}} = \frac{\mathbf{(E_{out})_{annual}}}{\mathbf{E_{in}}} \tag{6.3}$$

whereas the energy production factor based on exergy, $EPF_{ex}$ is given by Equation 6.4:

$$\mathbf{EPF_{ex}} = \frac{\mathbf{(Ex_{out})_{annual}}}{\mathbf{E_{in}}} \tag{6.4}$$

### 6.3.4 Environmental analysis

Environmental analysis is critical for determining the amount of carbon dioxide emitted and mitigated by the solar still system. This aspect is important to ensure that the technology used is not contributing to additional $CO_2$ emissions which defeats the purpose of renewable technology application. Besides, this analysis also shows the system's nett $CO_2$ which is crucial in the selection of technology that is carbon neutral. Hence the equations used for calculating both the $CO_2$ emission and mitigation are as presented in the sections below.

#### 6.3.4.1 $CO_2$ emission

The amount of $CO_2$ emitted by the coal power plant to produce electricity taking into account the losses from transmission and distribution was estimated to be about

2 kg $CO_2$/kWh (Joshi & Tiwari, 2018). The lifetime $CO_2$ emission, $CO_2$ of the components used for the solar still is calculated using Equation 6.5 (Parsa et al., 2020b):

$$\mathbf{CO_2 = 2 \times E_{in}} \tag{6.5}$$

#### 6.3.4.2 $CO_2$ mitigation

Tabulation of the nett $CO_2$ mitigation in a lifetime, n based on the energy produced by the solar still, $CO_{2en}$ is given by Equation 6.6 (Shoeibi et al., 2021c):

$$\mathbf{CO_{2en} = \frac{2(E_{out} \times n - E_{in})}{1000}} \tag{6.6}$$

whereas the nett $CO_2$ mitigation based on the exergy of the solar still system, $CO_{2ex}$ is shown in Equation 6.7:

$$\mathbf{CO_{2ex} = \frac{2(Ex_{out} \times n - E_{in})}{1000}} \tag{6.7}$$

### 6.3.5 Economic analysis

An economic analysis is often performed to determine the cost per litre of freshwater produced by the solar desalination method. This analysis allows decision makers to select a system that is advantageous from both a technical and economic standpoint. In addition, this study also evaluates the exergo-economic and enviro-economic aspects to get a better picture of the feasibility of solar desalination in terms of energy and environmental aspects.

#### 6.3.5.1 Cost per litre

The cost per litre, CPL, based on the annual productivity of the solar still, M, is tabulated using Equation 4.3 to 4.9 given in chapter **4.3.6 Economic analysis**.

#### 6.3.5.2 Exergo-economic analysis

The exergo-economic analysis is used to find the relationship between the energy and exergy produced by the solar still and the total annual cost of the solar still system. The

exergo-economic of the solar still based on the energy produced, $R_{ex}$ is given by Shoeibi et al. (2021c) as shown in Equation 6.8:

$$\mathbf{R_{en}} = \frac{\mathbf{E_{out}}}{\mathbf{TAC}} \tag{6.8}$$

whereas the exergo-economic based on exergy, $R_{ex}$ is given by Equation 6.9:

$$\mathbf{R_{ex}} = \frac{\mathbf{Ex_{out}}}{\mathbf{TAC}} \tag{6.9}$$

#### 6.3.5.3 Enviro-economic analysis

The enviro-economic analysis is the amount of carbon credit that can be earned from selling the $CO_2$ mitigated by the solar still system, $ZCO_2$. The relation is calculated using Equation 6.10 (Parsa et al., 2020b):

$$\mathbf{ZCO_2} = \mathbf{XCO_2} \times \mathbf{CO_{2_{mitigate}}} \tag{6.10}$$

Previous studies have used a carbon price, $XCO_2$ of \$14.5/tonnes $CO_2$. However, we have updated the current value of carbon credit in the post-COVID era (the year 2022) based on the California Carbon Allowance which averaged about \$28/tonnes $CO_2$ (CarbonCredits.com, 2022).

## 6.4 Results and discussions

### 6.4.1 Weather condition and temperature of basin water and cover

The solar radiation and ambient temperature observed for the three experiment days are illustrated in Figure 6.2. Usually, Malaysia experienced a high amount of solar radiation and drier weather conditions during the Southwest Monsoon from May to September (MET Malaysia, 2019). However, the La Niña phenomenon has caused a shift in Malaysia's weather which resulted in unprecedented heavy rain, overcasts, and overall cooler weather in June and July 2022 as opposed to previous years (World Meteorological Organization, 2022). This effect was shown by the inconsistent solar radiation measured

during the experiment days, particularly on 30/6. Nonetheless, $T_a$ showed a similar pattern for the three experiment days with a slight drop at 3 p.m. and 4 p.m. on 1/7 and 30/6, respectively. The average solar radiation and $T_a$ observed on 29/6, 30/6 and 1/7 were 342.8 W/m$^2$, 289.1 W/m$^2$, and 345.9 W/m$^2$ and 34.6°C, 35.3°C and 34.9°C, respectively.

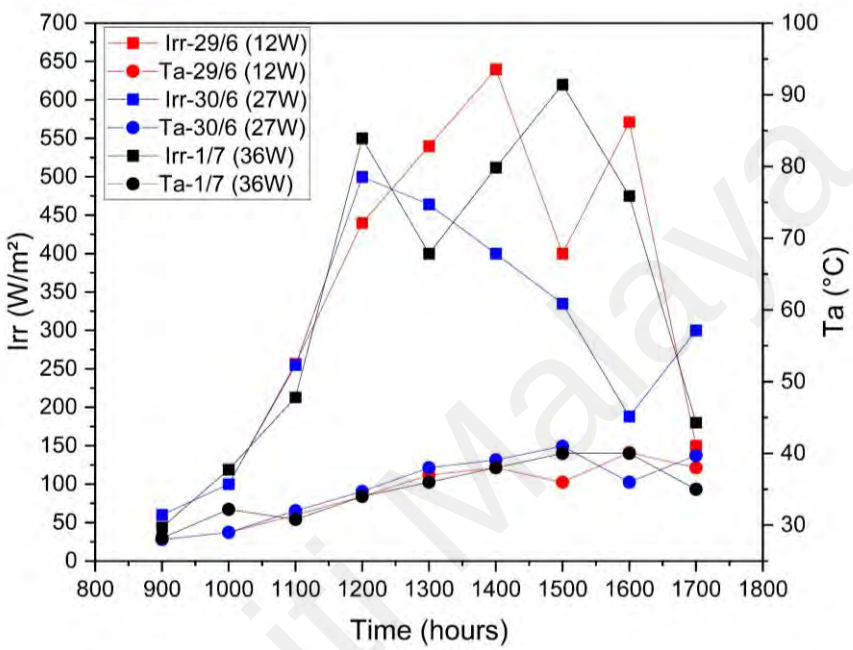


**Figure 6.2: Solar radiation, Irr and ambient temperature, $T_a$ measured during the experiment on 29/6 (12 W), 30/6 (27 W) and 1/7 (36 W).**

Figure 6.3 depicts the cover temperature, $T_c$, and basin water temperature, $T_w$ for both the reference solar still, ref and TEC-cooled solar still, cg. The maximum $T_c$ and $T_w$ for reference solar still and TEC-cooled coated glass solar still on 29/6 was about 49°C and 50°C and 45°C and 53°C, respectively. On 30/6 the maximum $T_c$ and $T_w$ observed for reference solar still was about 45°C and 46°C. For TEC-cooled solar still on 30/6, $T_c$ was lower by 1°C compared to reference but higher by about 4°C for $T_w$. On 1/7, the highest $T_c$ and $T_w$ found for the reference solar still was 49°C and 51.5°C whereas for TEC-cooled coated glass solar still $T_c$ and $T_w$ were higher than reference by 2°C and 4°C, respectively. The results showed that $T_c$ using TEC cooling power of 12 W was lower than the reference by 4°C and reduced by 1°C and -2°C (higher than reference) using TEC cooling power of 27 W and 36 W. Increasing the cooling power of TEC from 12 W to 36 W increased

$T_c$ for the coated glass solar still compared to the reference. In comparison to previous studies on cover cooling, $T_c$ of coated glass did not reduce with higher cooling (Kabeel & Abdelgaied, 2020). This increase in temperature is correlated to the improved rate of condensation whereby a higher amount of heat is absorbed by the glass cover from the latent heat of condensation which in turn increases the $T_c$. This is further exacerbated by the addition of coating which added the thermal resistance of the cover, therefore hindering the heat dissipation of the inner glass to the cooling water. Nonetheless, the difference in $T_c$ and $T_w$ increased with the increase in TEC cooling power and this effect can be seen in the improvement of the solar still productivity.

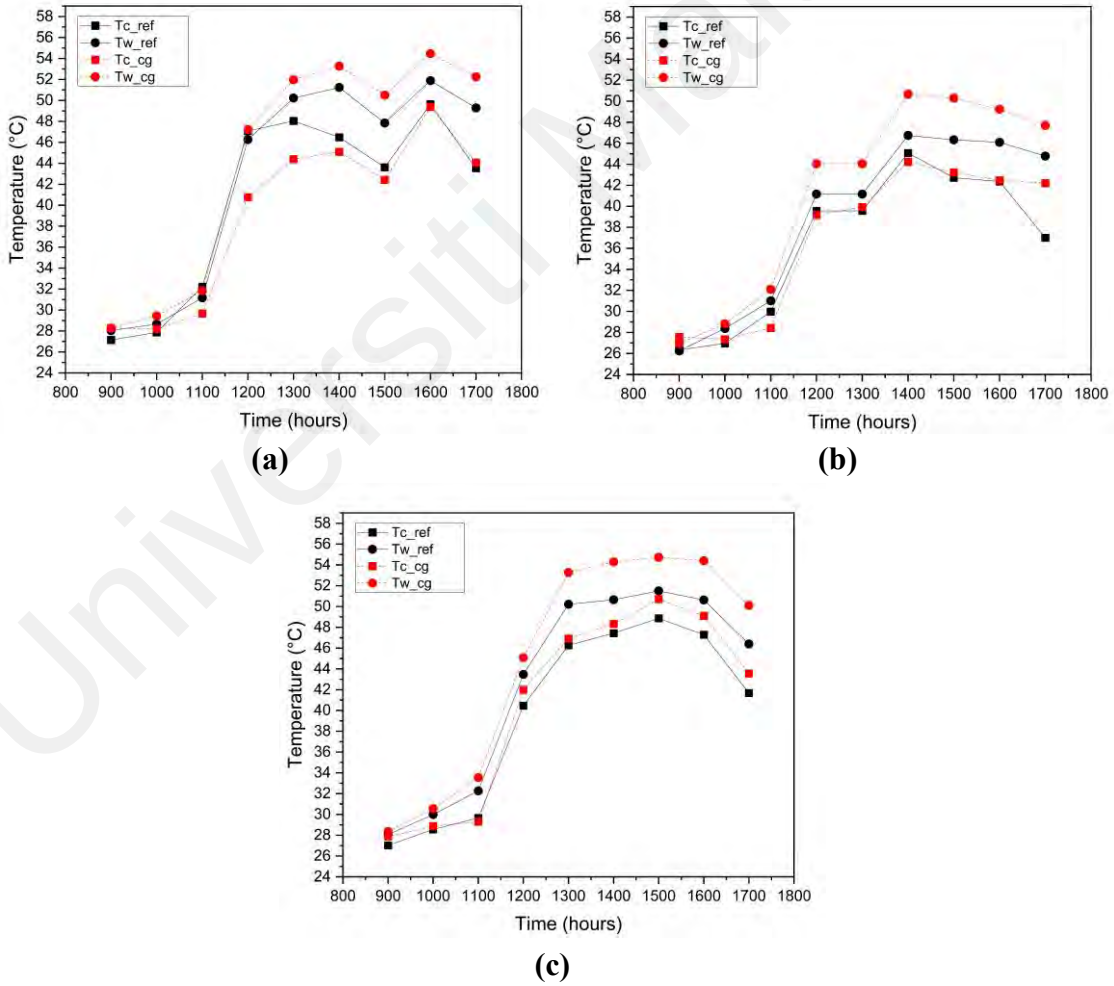


**Figure 6.3: The cover temperature, $T_c$ and basin water temperature, $T_w$ of both solar stills on (a) 29/6 (12 W) (b) 30/6 (27 W) (c) 1/7 (36 W).**

### 6.4.2 Freshwater yield of solar still

Figure 6.4 displays the hourly yield and the total yield of both the solar still. On all the experiment days, the solar still with TEC cooling produced freshwater an hour earlier than the reference solar still. The maximum hourly yield for reference solar still on 29/6, 30/6 and 1/7 was 37 mL, 29 mL, and 34 mL, respectively. Whereas for solar still using coated glass with TEC cooling, the maximum hourly yield on 29/6 (12 W) was 48 mL and on 30/6 (27 W) the maximum hourly yield was 45 mL. An even more drastic increase in hourly yield of 59.5 mL was found on 1/7 for coated glass with a TEC cooling power of 36 W. The cumulative yield for the reference solar still and coated glass with TEC cooling on 29/6 (12 W), 30/6 (27 W) and 1/7 (36 W) was 536 mL/$m^2$ and 800 mL/$m^2$, 486 mL/$m^2$ and 780 mL/$m^2$, and 466 mL/$m^2$ and 1052 mL/$m^2$, respectively. Increasing the TEC cooling power from 12 W to 36 W showed to increase in the yield of the coated glass cover solar still by 49%, 60%, and 126% as compared to the reference solar still.

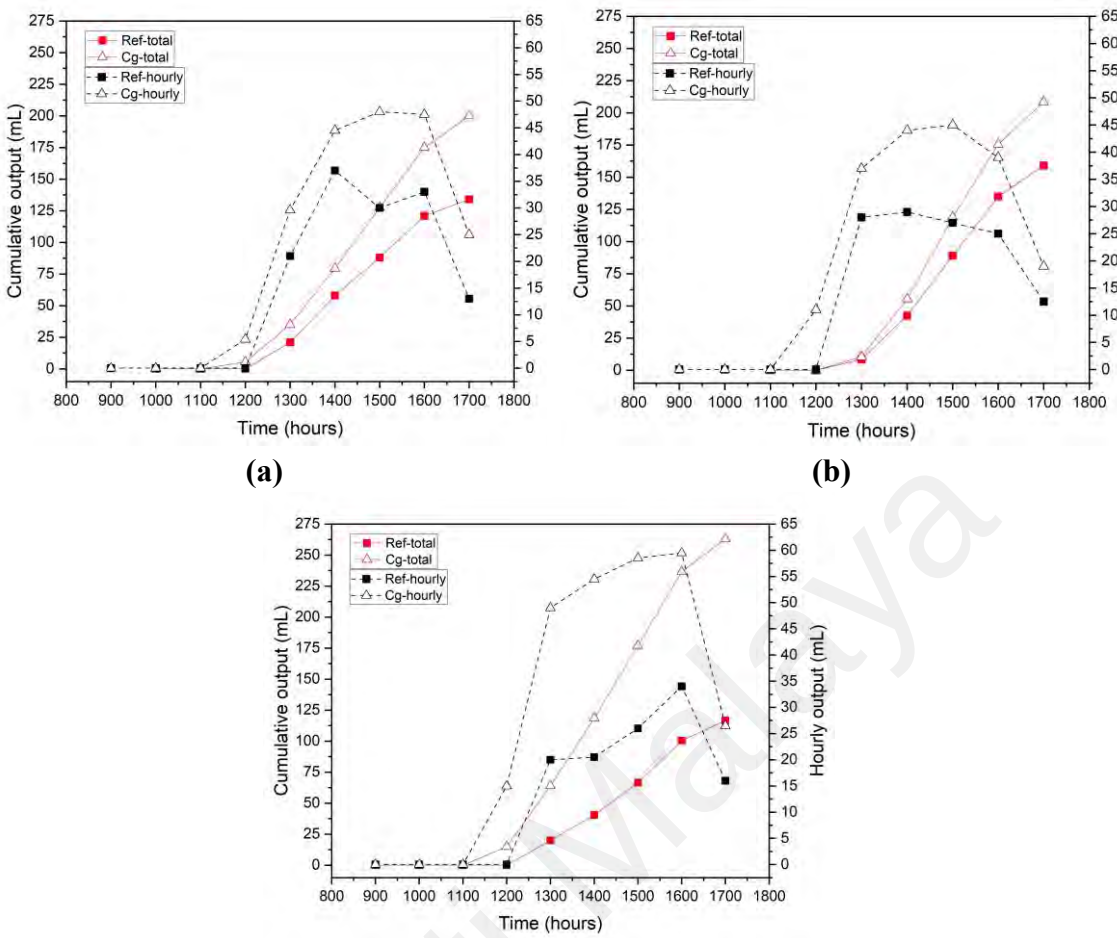


**Figure 6.4: Solar stills freshwater output for reference solar still, Ref and coated glass solar still with TEC cooling, Cg on (a) 29/6 (12 W) (b) 30/6 (27 W) (c) 1/7 (36 W).**

### 6.4.3 Efficiency of the solar still

Figure 6.5 shows the daily energy and exergy efficiency of the reference and coated glass with TEC cooling solar still. The energy efficiency of reference solar still differs each experiment day with the highest efficiency of 12.4% obtained on 30/6 followed by 11.5% and 9.9% on 29/6 and 1/7, respectively. The variation in the energy efficiency of the reference solar still was due to the difference in the freshwater productivity and the amount of solar radiation obtained on the experimental days. In contrast to the energy efficiency of reference, the highest efficiency of 14.3% was found for the coated glass solar still with 36 W TEC cooling (1/7) followed by 13.3% and 12.8% on 29/6 and 30/6, respectively. The enhancement in energy efficiency for the coated glass solar still with

TEC cooling of 12 W, 27 W and 36 W was 16%, 3% and 44%, respectively. A drop in the energy efficiency enhancement using TEC with 27 W cooling power was due to the low solar radiation observed on 30/6. For exergy efficiency, reference solar still had an efficiency of 3% to 5.7%. Whereas the exergy efficiency of solar still with TEC cooling power of 12 W, 27 W, and 36 W was 3.9%, 2.7% and 4.3%, respectively. Regardless of the TEC cooling power, the TEC-cooled coated glass solar still observed a decrease in exergy efficiency by 10% to 25% compared to the reference. This shows the adverse effect of using cover cooling during days with intermittent solar radiation.

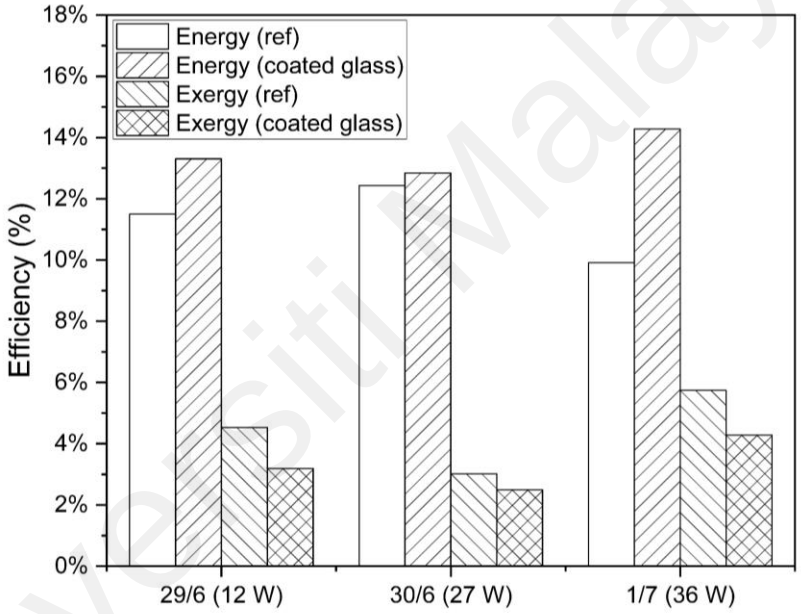


**Figure 6.5: Energy and exergy efficiency for reference and TEC cooled solar still at different cooling power.**

### 6.4.4 Energy matrices

Table 6.2 shows the energy payback time (EPBT) and energy production factor (EPF) of the solar stills on the two experiment days. The total embodied energy given in this table refers to the value taken in Table 6.2. The embodied energy of a solar still using a TEC cooling system is more than twice the embodied energy of a reference solar still. The yield, energy, and exergy output are calculated based on the results obtained on the different experiment days. The highest energy and exergy output obtained was with

coated glass solar still using 36 W TEC cooling. The result shows that the payback time based on both energies, $EPBT_{en}$ and exergy, $EPBT_{ex}$ is lower for reference solar still ranging between 4.25 years to 4.89 years based on energy and 9.06 years and 20.6 years based on exergy. The difference between reference and coated glass solar still using 36 W power decreased for $EPBT_{en}$ and $EPBT_{ex}$. The highest payback time of 40.57 years was found for solar still using coated glass with 27 W TEC cooling. Although the value seems high, previous studies showed similar results obtained modified the solar still whereby the $EPBT_{ex}$ ranged between 10 years (Shoeibi et al., 2021c) to 50 years (Parsa et al., 2020b). The energy production factor based on energy, $EPF_{en}$ and exergy, $EPF_{ex}$ for reference was higher than the solar still with TEC cooling. The largest decrease in $EPF_{en}$ of 43% was found for solar still using 27 W TEC cooling. A reduction in $EPF_{ex}$ by as high as 60% was found for solar still using 36 W TEC cooling.

**Table 6.2: Energy payback time (EPBT) and energy production factor (EPF) for the three experiment days based on energetic and exergetic points of view.**

| Parameter | Ref (29/6) | Coated glass (12 W) | Ref (30/6) | Coated glass (27W) | Ref (1/7) | Coated glass (36 W) |
|---|---|---|---|---|---|---|
| Embodied energy (kWh) | 137.58 | 336.42 | 137.58 | 385.42 | 137.58 | 414.82 |
| Yield, annual ($L/m^2$) | 195.64 | 292.00 | 177.39 | 284.70 | 170.09 | 383.98 |
| $E_{out}$, annual (kWh) | 32.38 | 48.22 | 29.51 | 47.21 | 28.15 | 63.36 |
| $Ex_{out}$, annual (kWh) | 11.87 | 13.47 | 6.68 | 9.50 | 15.19 | 18.17 |
| $EPBT_{en}$ | 4.25 | 6.98 | 4.66 | 8.19 | 4.89 | 6.55 |
| $EPBT_{ex}$ | 11.59 | 24.98 | 20.60 | 40.57 | 9.06 | 22.83 |
| $EPF_{en}$ | 0.24 | 0.14 | 0.21 | 0.12 | 0.20 | 0.15 |
| $EPF_{ex}$ | 0.09 | 0.04 | 0.05 | 0.02 | 0.11 | 0.04 |

### 6.4.5 $CO_2$ emission and mitigation

Table 6.3 depicts the amount of $CO_2$ emitted and mitigated for reference and coated glass with TEC cooling solar still. The amount of $CO_2$ emitted in a lifetime (30 years) by

the solar still with a TEC cooling system was 3 times compared to the reference solar still. However, the amount of $CO_2$ mitigated by the solar still with 36 W TEC cooling based on the energy produced, $CO_{2en}$ was twice the amount compared to the reference solar still. For solar still using 12 W and 27 W, the increase in $CO_{2en}$ compared to reference was 33.2% and 37.8%, respectively. However, the amount of exergy produced was insufficient to make up for the amount of $CO_2$ produced from the embodied energy. Hence, the reduction of carbon dioxide mitigated based on exergy, $CO_{2ex}$ by 260% was found for TEC-cooled solar still using 27 W power compared to the reference. The $CO_{2ex}$ mitigated for coated glass solar still using 36 W TEC cooling power was higher than using 12 W TEC cooling power with an amount of 0.26 tonnes $CO_2$.

**Table 6.3: $CO_2$ emission and mitigation for the different applied power TEC.**

| Parameter | Ref (29/6) | Coated glass (12 W) | Ref (30/6) | Coated glass (27 W) | Ref (1/7) | Coated glass (36 W) |
|---|---|---|---|---|---|---|
| Embodied energy (kWh) | 137.58 | 336.42 | 137.58 | 385.42 | 137.58 | 414.82 |
| Emitted $CO_2$, lifetime (tonnes $CO_2$) | 275.15 | 672.84 | 275.15 | 770.84 | 275.15 | 829.64 |
| Yield, annual ($L/m^2$) | 195.64 | 292.00 | 177.39 | 284.70 | 170.09 | 383.98 |
| $E_{out}$, annual (kWh) | 32.38 | 48.22 | 29.51 | 47.21 | 28.15 | 63.36 |
| $Ex_{out}$, annual (kWh) | 11.87 | 13.47 | 6.68 | 9.50 | 15.19 | 18.17 |
| Mitigated $CO_{2en}$, lifetime (tonnes $CO_2$) | 1.67 | 2.22 | 1.50 | 2.06 | 1.41 | 2.97 |
| Mitigated $CO_{2ex}$, lifetime (tonnes $CO_2$) | 0.44 | 0.14 | 0.13 | -0.20 | 0.64 | 0.26 |

### 6.4.6 Cost per litre of distilled yield

Table 6.4 lists the cost of items used in the solar still fabrication. The capital cost of reference and TEC cooling solar still was $ 148 and $ 232.6, respectively. Table 6.5 gives the economic parameters calculated for the present study. The total annual cost of

reference solar still and solar still using coated glass with TEC cooling was $ 8.68 and $ 13.64, respectively. Table 6.6 shows the CPL of reference and coated glass solar still with TEC cooling on the different experiment days. The highest CPL of $ 0.051 was obtained by reference solar still on 1/7, while the lowest CPL was obtained by solar still with TEC cooling with a cost of $ 0.036. The CPL for solar still using 12 W TEC cooling power was slightly higher than the reference by 5%. Increasing the TEC cooling power to 36 W reduced the CPL by 30% compared to the reference solar still. Increasing the TEC cooling power from 12 W to 36 W also reduced the cost of coated glass solar still by 24%.

**Table 6.4: Cost of items used in solar still.**

| Item | Price ($) |
|---|---|
| GI sheet (basin) | 73.6 |
| Coated glass | 42.0 |
| Glass | 41.4 |
| PE foam | 10.0 |
| TEC set | 70.0 |
| DC power source | 10.0 |
| DC pump | 4.0 |
| Fabrication service | 23.0 |
| Total (reference) | 148.0 |
| Total (TEC cooled) | 232.6 |

**Table 6.5: Total annual cost (TAC) for reference and coated glass with TEC cooling solar still.**

| Solar still | Reference | Coated glass with TEC cooling |
|---|---|---|
| Capital cost, C ($) | 148.00 | 232.60 |
| Capital recovery factor, CRF | 0.054 | 0.054 |
| First annual cost, FAC ($) | 8.05 | 12.65 |
| Salvage value, S ($) | 29.60 | 46.52 |
| Sinking fund factor, SFF | 0.019 | 0.019 |
| Annual salvage value, ASV ($) | 0.573 | 0.901 |
| Annual maintenance coefficient, MC | 0.15 | 0.15 |
| Annual maintenance cost, AMC ($) | 1.21 | 1.90 |
| Total annual cost ($) | 8.68 | 13.64 |

**Table 6.6: Annual yield and cost per litre (CPL) for different experiment days.**

| Solar still | M (L/m$^2$.year) | CPL ($/L/m$^2$) |
|---|---|---|
| Reference (29/6) | 195.64 | 0.044 |
| Coated glass (12 W) | 292.00 | 0.047 |
| Reference (30/6) | 177.39 | 0.049 |
| Coated glass (27 W) | 284.70 | 0.048 |
| Reference (1/7) | 170.09 | 0.051 |
| Coated glass (36 W) | 383.98 | 0.036 |

### 6.4.7 Exergo and enviro-economic analysis

Table 6.7 compares the exergo-economic and enviro-economic of the reference solar still and the coated glass solar still with TEC cooling. In the exergo-economic analysis based on energy, $R_{en}$ showed that the increase in TEC cooling power increased the result by 43% compared to reference solar still. The exergo-economic analysis based on exergy, $R_{ex}$ for solar still using TEC cooling was lower compared to the reference. The result was particularly unfavourable for coated glass solar still using low TEC cooling power whereby a decrease of 5% and 27.8% for both $R_{en}$ and $R_{ex}$ was found, respectively. The enviro-economic analysis shows that the highest cost was given by the coated glass solar

still using 36 W TEC cooling power of $ 83.21. Due to the negative $CO_2$ mitigated by the solar still using 27 W TEC power from the low exergetic output, the enviro-economic cost also becomes a negative value.

**Table 6.7: Exergo and enviro-economic results for reference and TEC cooled solar still.**

| Parameter | Ref (29/6) | Coated glass (12 W) | Ref (30/6) | Coated glass (27 W) | Ref (1/7) | Coated glass (36 W) |
|---|---|---|---|---|---|---|
| $E_{out}$, annual (kWh) | 32.38 | 48.22 | 29.51 | 47.21 | 28.15 | 63.36 |
| $Ex_{out}$, annual (kWh) | 11.87 | 13.47 | 6.68 | 9.50 | 15.19 | 18.17 |
| TAC ($) | 8.72 | 13.64 | 8.72 | 13.64 | 8.72 | 13.64 |
| $R_{en}$ (kWh/$) | 3.73 | 3.53 | 3.40 | 3.46 | 3.24 | 4.64 |
| $R_{ex}$ (kWh/$) | 1.37 | 0.99 | 0.77 | 0.70 | 1.75 | 1.33 |
| Mitigated $CO_{2en}$, lifetime (tonnes $CO_2$) | 1.67 | 2.22 | 1.50 | 2.06 | 1.41 | 2.97 |
| Mitigated $CO_{2ex}$, lifetime (tonnes $CO_2$) | 0.44 | 0.14 | 0.13 | -0.20 | 0.64 | 0.26 |
| $ZCO_2$, energy ($) | 46.69 | 62.17 | 41.88 | 57.73 | 39.59 | 83.21 |
| $ZCO_2$, exergy ($) | 12.24 | 3.79 | 3.51 | -5.62 | 17.81 | 7.29 |

Table 6.8 illustrates the comparison between the present study and the previous study using the TEC water cooling system for the analysed parameters. The embodied energy for the present study was half of that of the previous study due to the size and materials used to fabricate the solar still. The annual yield obtained was similar to the previous study, however, the energy output was significantly lower than the previous study using the TEC water cooling system. Therefore, the parameters calculated based on energy output were poorer compared to the previous study. Although the exergy output was also lower than in the previous study, the system was shown to perform better based on the parameters calculated in terms of exergy compared to the previous study. The current solar still design was shown to be more cost-effective compared to the previous study with a CPL value of about 7 times lower than the previous solar still design.

**Table 6.8: Comparison between the present study and previous study with TEC cooling (n= 30 years).**

| Parameter | Ref (1/7) | Coated glass (36 W) | Water-cooled (Shoeibi et al., 2021c) |
|---|---|---|---|
| Embodied energy (kWh) | 137.58 | 414.82 | 843.5 |
| Annual yield, M ($L/m^2$.year) | 170.09 | 383.98 | 385.5 |
| $E_{out}$, annual (kWh) | 28.15 | 63.36 | 246.25 |
| $Ex_{out}$, annual (kWh) | 15.19 | 18.47 | 29.28 |
| $EPBT_{en}$ | 4.89 | 6.55 | 3.42 |
| $EPBT_{ex}$ | 9.06 | 22.83 | 28.79 |
| $EPF_{en}$ | 0.20 | 0.15 | 0.29 |
| $EPF_{ex}$ | 0.11 | 0.04 | 0.03 |
| Mitigated $CO_{2en}$, lifetime (tonnes $CO_2$) | 1.41 | 2.97 | 13.09 |
| Mitigated $CO_{2ex}$, lifetime (tonnes $CO_2$) | 0.64 | 0.26 | 0.07 |
| Emitted $CO_2$, lifetime (tonnes $CO_2$) | 275.15 | 829.64 | 1687.0 |
| CPL ($/L/m^2$) | 0.051 | 0.036 | 0.243 |
| $R_{en}$ (kWh/$) | 3.24 | 4.64 | 2.62 |
| $R_{ex}$ (kWh/$) | 1.75 | 1.33 | 0.31 |
| $ZCO_2$, energy ($) | 39.59 | 83.21 | 189.79 |
| $ZCO_2$, exergy ($) | 17.81 | 7.29 | 1.03 |

## 6.5 Summary

The present study investigated the effect of the condensation enhancement method using partial cover coating and TEC cover cooling with varied input power (12 W to 36 W) on the solar still performance. Comparison between the reference solar still and the solar still with varying TEC cooling power was conducted to elucidate the impact of the TEC cover cooling utilisation together with partially coated condensing cover on various major parameters which includes the freshwater productivity, energy, exergy, economic, environmental, energy-matrices, and related parameters such as exergo-economic and enviro-economic. The following are the summarised results of the present study:

i. The annual freshwater yield obtained for reference solar still ranged between 170.1 L/$m^2$.year to 195.6 L/$m^2$.year.

ii. For coated glass solar still using TEC cooling power of 12 W, 27 W, and 36 W, the annual freshwater yield obtained was 292 L/$m^2$.year, 284.7 L/$m^2$.year, and 384 L/$m^2$.year, respectively.

iii. The productivity of coated glass solar still was enhanced by 49%, 60%, and 126% with the increase in TEC cooling power from 12 W to 36 W compared to reference solar still.

iv. The energy and exergy efficiency obtained for the coated glass cover solar still with TEC cooling power 12 W, 27 W, and 36 W was 13.3%, 12.8%, and 14.3%, and 3.9%, 2.7%, and 4.3%, respectively.

v. The energy efficiency improved by 3% to 44% but the exergy efficiency decreased by 10% to 25% compared to reference solar still.

vi. The energy matrices found that the energy payback time based on energy and exergy production for coated glass solar still ranged between 6.6 years to 8.2 years and 22.8 years to 40.6 years which was higher than reference solar still by 57.7% to 121.5%.

vii. The energy production factor for coated glass solar still with TEC cover cooling based on energy and exergy ranged between 0.12 to 0.15 and 0.02 to 0.04, respectively.

viii. The highest amount of $CO_2$ emission and nett mitigation was 829.64 tonnes $CO_2$ and 2.97 tonnes $CO_2$, respectively for the coated glass solar still using 36 W TEC cooling power.

ix. The lowest CPL obtained for the coated glass cover solar still was with 36 W TEC power of $ 0.036 which was lower than the reference by 30%.

x. The exergo-economic analysis based on energy and exergy of the solar still was 3.46 kWh/$ to 4.64 kWh/$, and 0.7 kWh/$ to 1.33 kWh/$ for coated glass solar still using TEC cooling, whereas for reference solar still was 3.24 kWh/$ to 3.73 kWh/$, and 0.77 kWh/$ to 1.75 kWh/$, respectively.

xi. The enviro-economic results revealed the highest amount of carbon credit earned with coated glass solar still using 36 W TEC cooling power based on energy production was $ 83.21 whereas based on exergy, the highest cost was earned by the reference solar still on 1/7 with a value of $ 17.81.

Taking into consideration all the results summarised in the context of pricing, environment, and tropical weather conditions of Malaysia, using a partially coated glass cover with TEC cooling at high cooling power (36 W) positively affected the performance of the solar still in the majority of the aspects as compared to using lower TEC cooling power. The use of TEC cooling with mix wettability covered solar still also showed the best performance in comparison to the passive and water-cooling method as well as compared to the use of the three other cover materials, glass, PMMA and PC.

# CHAPTER 7: CONCLUSION AND FUTURE WORK

This chapter concludes the study and the achieved research objectives are summarised. The novelty and significance of the work are also outlined. Finally, a recommendation for future works on improvement to the solar still performance is given.

## 7.1 Conclusion

In conclusion, this research investigated the effect of incorporating mix wettability cover as well as the use of TEC cover cooling on the solar still performance. The overall results presented in previous chapters revealed that the use of mix wettability cover together with TEC cooling had a highly positive effect on the solar still performance as compared to other cover materials including bare glass cover. The following concludes the objectives of this study:

1. The optimum surface area coating of below 30% was found to improve the performance of the solar still in terms of productivity, efficiency and cost-effectiveness by enabling the condensate formation and minimised condensate loss for a low cover tilt angle.
2. The performance of the mix wettability cover compared to other cover materials (glass, PC, and PMMA) under passive mode solar still and water-cooled solar still has been evaluated and results showed the superiority of mix wettability cover for both solar still modes.
3. Analysis of the effect of various TEC cooling power on the different cover materials showed that a high TEC cooling power of 36 W resulted in improved performance for glass and PC covered solar still, however, PMMA cover performed better using lower cooling power.
4. The ideal TEC cooling power application on the mix wettability on solar still cover has been established to be 36 W based on the improvement in the performance of

the following factors: freshwater productivity, energy, and exergy output, economic viability, and environmental impact.

## 7.2 Novelty and significance of research

Solar desalination using the solar still method and improvement of the system predates almost 80 years of research. Growth of new technologies and materials opens new possibilities for further improvement to the current solar still design hence allowing this method to achieve an even higher performance than previous designs. However, most of the proposed solar still enhancement methods do not consider the effect of condensate dripping from the cover which is an important factor in determining the solar still freshwater productivity. Therefore, this research is the first of its kind to introduce the usage of mix wettability surface concept for the solar still application which tackled the issue regarding the dripping effects from hydrophobic coating on solar still with a low tilt angle. Mix wettability surface combines both the ability of the surface to form condensate and minimized dripping in the high wetting region while also facilitating higher condensate removal in the lower wetting region.

This research also provided new insights on the relationship between different cover materials with thermoelectric cooling as there have been no known studies done to correlate the use of cover cooling and the solar still performance using different commonly used cover materials. Although cover cooling using thermoelectric showed a positive outcome in enhancing the solar still performance, common solar still cover materials have different wettability and thermal properties which resulted in varied solar still performance. Hence it is imperative to understand the role the effect that cover materials have on solar still using thermoelectric cover cooling. Besides that, this research explored the use of different thermoelectric cooling power on a solar still to determine the optimum power for a solar still subjected to the variation of weather

conditions. Previous studies on optimal thermoelectric parameters used for solar still have been limited and the effect of weather variations has not been considered despite the importance of weather parameters on the performance of the solar still performance.

## 7.3 Future works

Currently, the focus of the study has been on improving the condensation formation and collection to improve the current solar still performance. Future studies should focus on including methods to simultaneously enhance the evaporation process together with the condensation process such as using steam generation interfacial materials, novel heat storage materials or thermally stable nanofluids. Furthermore, focusing on the environmental aspect of the solar still application is crucial to ensure that the technology does not add to the carbon emissions and instead mitigates greenhouse gases. Analysis such as performing a cradle-to-grave or cradle-to-cradle life cycle assessment to further assess the environmental impact of using solar still compared to other thermal desalination method should be considered. Moreover, polymer-based materials should continue to be explored for utilisation as a solar still cover due to its advantages over glass of having lower initial cost and lighter weight. Modification to the surface of the polymer-based materials to produce a mix wettability or a biphilic surface should also be introduced to improve the performance of the material for the solar still application.

## REFERENCES


Abaszadeh Hashemi, S., Kazemi, M., & Passandideh-Fard, M. (2022). Experimental characterization of a solar still integrated with a spiral collector using energy, exergy, economic, and environmental (4E) analyses. *Sustainable Energy Technologies and Assessments*, *53*, 102521. https://doi.org/10.1016/j.seta.2022.102521

Abbasiasl, T., Chehrghani, M. M., Sadaghiani, A. K., & Koşar, A. (2021). Gradient mixed wettability surfaces for enhancing heat transfer in dropwise flow condensation. *International Journal of Heat and Mass Transfer*, *179*, 121664. https://doi.org/10.1016/j.ijheatmasstransfer.2021.121664

Abdelgaied, M., Zakaria, Y., Kabeel, A. E., & Essa, F. A. (2021). Improving the tubular solar still performance using square and circular hollow fins with phase change materials. *Journal of Energy Storage*, *38*, 102564. https://doi.org/10.1016/j.est.2021.102564

Abo-Elfadl, S., Yousef, M. S., & Hassan, H. (2021). Energy, exergy, economic and environmental assessment of using different passive condenser designs of solar distiller. *Process Safety and Environmental Protection*, *148*, 302–312. https://doi.org/10.1016/j.psep.2020.10.022

Abu-Arabi, M., Al-harahsheh, M., Ahmad, M., & Mousa, H. (2020). Theoretical modeling of a glass-cooled solar still incorporating PCM and coupled to flat plate solar collector. *Journal of Energy Storage*, *29*, 101372. https://doi.org/10.1016/j.est.2020.101372

Abu-Arabi, M., Zurigat, Y., Al-Hinai, H., & Al-Hiddabi, S. (2002). Modeling and performance analysis of a solar desalination unit with double-glass cover cooling. *Desalination*, *143*(2), 173–182. https://doi.org/10.1016/S0011-9164(02)00238-2

Abu-Hiljeh, B. A. K. (1996). Enhanced solar still performance using water film cooling of the glass cover. *Desalination*, *107*(3), 235–244. https://doi.org/10.1016/S0011-9164(96)00165-8

Ahmed, M. M. Z., Alshammari, F., Abdullah, A. S., & Elashmawy, M. (2021). Basin and tubular solar distillation systems: A review. *Process Safety and Environmental Protection*, *150*, 157–178. https://doi.org/10.1016/j.psep.2021.04.015

Ahsan, A., Islam, Kh. M. S., Fukuhara, T., & Ghazali, A. H. (2010). Experimental study on evaporation, condensation and production of a new Tubular Solar Still. *Desalination*, *260*(1), 172–179. https://doi.org/10.1016/j.desal.2010.04.044

Alarifi, I. M., Abo-Khalil, A. G., Al-Qawasmi, A.-R., Alharbi, W., & Alobaid, M. (2021). On the effects of nanomaterials on the performance of solar distillation systems-A comprehensive review. *Solar Energy*, *218*, 596–610. https://doi.org/10.1016/j.solener.2021.03.018

Al-Hayeka, I., & Badran, O. O. (2004). The effect of using different designs of solar stills on water distillation. *Desalination*, *169*(2), 121–127. https://doi.org/10.1016/j.desal.2004.08.013

Al-Hilphy, A. R. S. (2013). Development of basin solar still by adding magnetic treatment unit and double glass cover provided with water. *Computers and Chemical Engineering*, *6*(3), 286–296. https://doi.org/10.3844/ajeassp.2013.286.296

Al-Karaghouli, A., & Kazmerski, L. L. (2013). Energy consumption and water production cost of conventional and renewable-energy-powered desalination processes. *Renewable and Sustainable Energy Reviews*, *24*, 343–356. https://doi.org/10.1016/j.rser.2012.12.064

Al-Maddhachi, H., & Smaisim, G. F. (2021). Experimental and numerical investigation with environmental impacts of affordable square pyramid solar still. *Solar Energy*, *216*, 303–314. https://doi.org/10.1016/j.solener.2020.12.051

Al-Madhhachi, H. (2018). Effective thermal analysis of using peltier module for desalination process. *Advances in Science, Technology and Engineering Systems*, *3*(1), 191–197. https://doi.org/10.25046/aj030122

Al-Madhhachi, H., & Min, G. (2017). Effective use of thermal energy at both hot and cold side of thermoelectric module for developing efficient thermoelectric water distillation system. *Energy Conversion and Management*, *133*, 14–19. https://doi.org/10.1016/j.enconman.2016.11.055

Al-Madhhachi, H., & Min, G. (2018). Key factors affecting the water production in a thermoelectric distillation system. *Energy Conversion and Management*, *165*, 459–464. https://doi.org/10.1016/j.enconman.2018.03.080

Al-Nimr, M. A., & Qananba, K. S. (2018). A solar hybrid system for power generation and water distillation. *Solar Energy*, *171*, 92–105. https://doi.org/10.1016/j.solener.2018.06.019

Altarawneh, I., Rawadieh, S., Batiha, M., Al-Makhadmeh, L., Alrowwad, S., & Tarawneh, M. (2017). Experimental and numerical performance analysis and optimization of single slope, double slope and pyramidal shaped solar stills. *Desalination*, *423*, 124–134. https://doi.org/10.1016/j.desal.2017.09.023

Arunkumar, T., Ao, Y., Luo, Z., Zhang, L., Li, J., Denkenberger, D., & Wang, J. (2019). Energy efficient materials for solar water distillation—A review. *Renewable and Sustainable Energy Reviews*, *115*, 109409. https://doi.org/10.1016/j.rser.2019.109409

Arunkumar, T., Jayaprakash, R., Ahsan, A., Denkenberger, D., & Okundamiya, M. S. (2013). Effect of water and air flow on concentric tubular solar water desalting system. *Applied Energy*, *103*, 109–115. https://doi.org/10.1016/j.apenergy.2012.09.014

Arunkumar, T., Jayaprakash, R., Ahsan, A., & Technology, S. (2012). A comparative experimental testing in enhancement of the efficiency of pyramid solar still and hemispherical solar still. *International Journal of Renewable Energy*, *7*(2), 1–7.

Arunkumar, T., Jayaprakash, R., Denkenberger, D., Ahsan, A., Okundamiya, M. S., kumar, S., Tanaka, H., & Aybar, H. Ş. (2012). An experimental study on a hemispherical solar still. *Desalination*, *286*, 342–348. https://doi.org/10.1016/j.desal.2011.11.047

Arunkumar, T., Raj, K., Dsilva Winfred Rufuss, D., Denkenberger, D., Tingting, G., Xuan, L., & Velraj, R. (2019). A review of efficient high productivity solar stills. *Renewable and Sustainable Energy Reviews*, *101*, 197–220. https://doi.org/10.1016/j.rser.2018.11.013

Attia, M. E. H., Kabeel, A. E., Abdelgaied, M., El-Maghlany, W. M., & Bellila, A. (2021). Comparative study of hemispherical solar distillers iron-fins. *Journal of Cleaner Production*, *292*, 126071. https://doi.org/10.1016/j.jclepro.2021.126071

Attia, M. E. H., Kabeel, A. E., Abdelgaied, M., El-Maghlany, W. M., & Driss, Z. (2021). Enhancement of the performance of hemispherical distiller via phosphate pellets as energy storage medium. *Environmental Science and Pollution Research, 28*, 32386–32395. https://doi.org/10.1007/s13204-021-01677-y

Attia, M. E. H., Kabeel, A. E., Abdelgaied, M., Essa, F. A., & Omara, Z. M. (2021). Enhancement of hemispherical solar still productivity using iron, zinc and copper trays. *Solar Energy*, *216*, 295–302. https://doi.org/10.1016/j.solener.2021.01.038

Attia, M. E. H., Kabeel, A. E., Bellila, A., Muthu Manokar, A., Sathyamurthy, R., Driss, Z., & Muthusamy, S. (2021). A comparative energy and exergy efficiency study of hemispherical and single-slope solar stills. *Environmental Science and Pollution Research, 28*, 35649–35659. https://doi.org/10.1007/s11356-021-13161-9

Attia, M. E. H., Kabeel, A. E., Elaloui, E., Abdelgaied, M., & Abdullah, A. (2022). Experimental study on improving the yield of hemispherical distillers using CuO nanoparticles and cooling the glass cover. *Solar Energy Materials and Solar Cells*, *235*, 111482. https://doi.org/10.1016/j.solmat.2021.111482

Badran, O. O. (2007). Experimental study of the enhancement parameters on a single slope solar still productivity. *Desalination*, *263*(1-3), 136–143. https://doi.org/10.1016/j.desal.2007.04.022

Baggio, G., Qadir, M., & Smakhtin, V. (2021). Freshwater availability status across countries for human and ecosystem needs. *Science of The Total Environment*, *792*, 148230. https://doi.org/10.1016/j.scitotenv.2021.148230

Bell, S. (1999). *Good Practice Guide No. 11 The Beginner's Guide to Uncertainty of Measurement*. National Physical Laboratory.

Bellila, A., Attia, M. E. H., Kabeel, A. E., Abdelgaied, M., Harby, K., & Soli, J. (2021). Productivity enhancement of hemispherical solar still using Al2O3-water-based nanofluid and cooling the glass cover. *Applied Nanoscience*, *11*, 1127–1139. https://doi.org/10.1007/s13204-021-01677-y

Bhardwaj, R., ten Kortenaar, M. V., & Mudde, R. F. (2013). Influence of condensation surface on solar distillation. *Desalination*, *326*, 37–45. https://doi.org/10.1016/j.desal.2013.07.006

Bhardwaj, R., ten Kortenaar, M. V., & Mudde, R. F. (2015). Maximized production of water by increasing area of condensation surface for solar distillation. *Applied Energy*, *154*, 480–490. https://doi.org/10.1016/j.desal.2015.05.060

Boutriaa, A., & Rahmani, A. (2017). Thermal modeling of a basin type solar still enhanced by a natural circulation loop. *Computers and Chemical Engineering*, *101*, 31–43. https://doi.org/10.1016/j.compchemeng.2017.02.033

Brookes, C. K. (2004). *A comparative life cycle assessment: Polyethylene and starch foam.* Michigan States University.

Central California Area Office (CCAO). (2022, October). *Water Facts—Worldwide Water Supply*. Bureau of Reclamation.

Chauhan, V. K., Shukla, S. K., & Rathore, P. K. S. (2022). A systematic review for performance augmentation of solar still with heat storage materials: A state of art. *Journal of Energy Storage*, *47*, 103578. https://doi.org/10.1016/j.est.2021.103578

Chauhan, V. K., Shukla, S. K., Tirkey, J. V., & Singh Rathore, P. K. (2020). A comprehensive review of direct solar desalination techniques and its advancements. *Journal of Cleaner Production, 284*, 124719. https://doi.org/10.1016/j.jclepro.2020.124719

Das, D., Bordoloi, U., Kalita, P., Boehm, R. F., & Kamble, A. D. (2020). Solar still distillate enhancement techniques and recent developments. *Groundwater for Sustainable Development*, *10*, 100360. https://doi.org/10.1016/j.gsd.2020.100360

de Paula, A. C. O., & Ismail, K. A. R. (2021). Comprehensive investigation of water film thickness effects on the heat and mass transfer of an inclined solar still. *Desalination*, *500*, 114895. https://doi.org/10.1016/j.desal.2020.11.114895

Deng, Z., Gao, S., Wang, H., Liu, X., & Zhang, C. (2022). Visualization study on the condensation heat transfer on vertical surfaces with a wettability gradient. *International Journal of Heat and Mass Transfer*, *184*, 122331. https://doi.org/10.1016/j.ijheatmasstransfer.2021.122331

Dhivagar, R., Mohanraj, M., Hidouri, K., & Belyayev, Ye. (2021). Energy, exergy, economic and enviro-economic (4E) analysis of gravel coarse aggregate sensible heat storage-assisted single-slope solar still. *Journal of Thermal Analysis and Calorimetry*, *145*(2), 475–494. https://doi.org/10.1007/s10973-020-09766-w

Dimri, V., Sakar, B., Singh, U., & Tiwari, G. N. (2008). Effect of condensing cover material on yield of an active solar still: An experimental validation. *Desalination*, *227*, 178–189. https://doi.org/10.1016/j.desal.2007.06.024

Ding, H., Peng, G., Mo, S., Ma, D., Sharshir, S. W., & Yang, N. (2017). Ultra-fast vapor generation by a graphene nano-ratchet: A theoretical and simulation study. *Nanoscale*, *9*(48), 19066–19072. https://doi.org/10.1039/C7NR05304E

Dwivedi, V. K., & Tiwari, G. N. (2009). Comparison of internal heat transfer coefficients in passive solar stills by different thermal models: An experimental validation. *Desalination*, *246*, 304–318. https://doi.org/10.1016/j.desal.2008.06.024

Edalatpour, M., Liu, L., Jacobi, A. M., Eid, K. F., & Sommers, A. D. (2018). Managing water on heat transfer surfaces: A critical review of techniques to modify surface wettability for applications with condensation or evaporation. *Applied Energy*, *222*, 967–992. https://doi.org/10.1016/j.apenergy.2018.03.178

Elashmawy, M. (2019). Effect of surface cooling and tube thickness on the performance of a high temperature standalone tubular solar still. *Applied Thermal Engineering*, *156*, 276–286. https://doi.org/10.1016/j.applthermaleng.2019.04.068

Elashmawy, M. (2020). Improving the performance of a parabolic concentrator solar tracking-tubular solar still (PCST-TSS) using gravel as a sensible heat storage material. *Desalination*, *473*, 114182. https://doi.org/10.1016/j.desal.2019.114182

Elmaadawy, K., Kandeal, A. W., Khalil, A., Elkadeem, M. R., Liu, B., & Sharshir, S. W. (2021). Performance improvement of double slope solar still via combinations of low cost materials integrated with glass cooling. *Desalination*, *500*, 114856. https://doi.org/10.1016/j.desal.2020.114856

El-Said, E. M. S., Elshamy, S. M., & Kabeel, A. E. (2020). Performance enhancement of a tubular solar still by utilizing wire mesh packing under harmonic motion. *Desalination*, *474*, 114165. https://doi.org/10.1016/j.desal.2019.114165

Elsaid, K., Kamil, M., Sayed, E. T., Abdelkareem, M. A., Wilberforce, T., & Olabi, A. (2020). Environmental impact of desalination technologies: A review. *Science of the Total Environment*, *748*, 141528. https://doi.org/10.1016/j.scitotenv.2020.141528

El-Samadony, Y. A. F., & Kabeel, A. E. (2014). Theoretical estimation of the optimum glass cover water film cooling parameters combinations of a stepped solar still. *Energy*, *68*, 744–750. https://doi.org/10.1016/j.energy.2014.01.080

El-Sebaii, A., & Khallaf, A. E.-M. (2020). Mathematical modeling and experimental validation for square pyramid solar still. *Environmental Science and Pollution Research, 27*, 32283–32295. https://doi.org/10.1007/s11356-019-07587-5

Esfahani, J. A., Rahbar, N., & Lavvaf, M. (2011). Utilization of thermoelectric cooling in a portable active solar still—An experimental study on winter days. *Desalination*, *269*(1–3), 198–205. https://doi.org/10.1016/j.desal.2010.10.062

Faegh, M., & Shafii, M. B. (2017). Experimental investigation of a solar still equipped with an external heat storage system using phase change materials and heat pipes. *Desalination*, *409*, 128–135. https://doi.org/10.1016/j.desal.2017.01.023

Fallahzadeh, R., Aref, L., Gholamiarjenaki, N., Nonejad, Z., & Saghi, M. (2020). Experimental investigation of the effect of using water and ethanol as working fluid on the performance of pyramid-shaped solar still integrated with heat pipe solar collector. *Solar Energy*, *207*, 10–21. https://doi.org/10.1016/j.solener.2020.06.032

Fang, S., Mu, L., & Tu, W. (2021). Application design and assessment of a novel small-decentralized solar distillation device based on energy, exergy, exergoeconomic, and enviroeconomic parameters. *Renewable Energy*, *164*, 1350–1363. https://doi.org/10.1016/j.renene.2020.09.075

Feng, W., & Bhushan, B. (2020). Multistep wettability gradient in bioinspired triangular patterns for water condensation and transport. *Journal of Colloid and Interface Science*, *560*, 866–873. https://doi.org/10.1016/j.jcis.2019.10.113

Fernández, JoséL., & Chargoy, N. (1990). Multi-stage, indirectly heated solar still. *Solar Energy*, *44*(4), 215–223. https://doi.org/10.1016/0038-092X(90)90150-B

Food and Agriculture Organization. (2011). *The state of the world's land and water resources for food and agriculture (SOLAW) – Managing systems at risk.* The Food and Agriculture Organization of the United Nations.

Fu, H., Dai, M., Song, H., Hou, X., Riaz, F., Li, S., Yang, K., Ali, I., Peng, C., & Sultan, M. (2021). Updates on Evaporation and Condensation Methods for the Performance Improvement of Solar Stills. *Energies*, *14*(21), 7050. https://doi.org/10.3390/en14217050

Gad, H. E., Shams El-Din, Sh., Hussien, A. A., & Ramzy, Kh. (2015). Thermal analysis of a conical solar still performance: An experimental study. *Solar Energy*, *122*, 900–909. https://doi.org/10.1016/j.solener.2015.10.016

Han, T., Choi, Y., Na, K. M., Kim, M. H., & Jo, H. J. (2021). Enhanced condensation on a biphilic-zigzag surface due to self-arrangement of crystals on a micro-structured surface. *International Journal of Heat and Mass Transfer*, *179*, 121710. https://doi.org/10.1016/j.ijheatmasstransfer.2021.121710

Hassan, H., & Yousef, M. S. (2021). An assessment of energy, exergy and CO2 emissions of a solar desalination system under hot climate conditions. *Process Safety and Environmental Protection*, *145*, 157–171. https://doi.org/10.1016/j.psep.2020.07.043

Hassan, H., Yousef, M. S., Fathy, M., & Ahmed, M. S. (2020). Assessment of parabolic trough solar collector assisted solar still at various saline water mediums via energy, exergy, exergoeconomic, and enviroeconomic approaches. *Renewable Energy*, *155*, 604–616. https://doi.org/10.1016/j.renene.2020.03.126

He, W., Zhang, G., Zhang, X., Ji, J., Li, G., & Zhao, X. (2015). Recent development and application of thermoelectric generator and cooler. *Applied Energy*, *143*, 1–25. https://doi.org/10.1016/j.apenergy.2014.12.075

Hou, J., Yang, J., Chang, Z., Zheng, H., & Su, Y. (2018). The mass transfer coefficient assessment and productivity enhancement of a vertical tubular solar brackish water still. *Applied Thermal Engineering*, *128*, 1446–1455. https://doi.org/10.1016/j.applthermaleng.2017.09.129

Ismail, B. I. (2009). Design and performance of a transportable hemispherical solar still. *Renewable Energy*, *34*(1), 145–150. https://doi.org/10.1016/j.renene.2008.03.013

Jijakli, K., Arafat, H., Kennedy, S., Mande, P., & Theeyattuparampil, V. V. (2012). How green solar desalination really is? Environmental assessment using life-cycle analysis (LCA) approach. *Desalination*, *287*, 123–131. https://doi.org/10.1016/j.desal.2011.09.038

Jin, Y., Zhang, L., & Wang, P. (2017). Atmospheric Water Harvesting: Role of Surface Wettability and Edge Effect. *Global Challenges*, *1*(4), 1700019. https://doi.org/10.1002/gch2.201700019

Jones, E., Qadir, M., van Vliet, M. T. H., Smakhtin, V., & Kang, S. (2019). The state of desalination and brine production: A global outlook. *Science of The Total Environment*, *657*, 1343–1356. https://doi.org/10.1016/j.scitotenv.2018.12.076

Joshi, P., & Tiwari, G. N. (2018). Energy matrices, exergo-economic and enviro-economic analysis of an active single slope solar still integrated with a heat exchanger: A comparative study. *Desalination*, *443*, 85–98. https://doi.org/10.1016/j.desal.2018.05.012

Kabeel, A. E., & Abdelgaied, M. (2020). Enhancement of pyramid-shaped solar stills performance using a high thermal conductivity absorber plate and cooling the glass cover. *Renewable Energy*, *146*, 769–775. https://doi.org/10.1016/j.renene.2019.07.020

Kabeel, A. E., Abdelgaied, M., Harby, K., & Eisa, A. (2020). Augmentation of diurnal and nocturnal distillate of modified tubular solar still having copper tubes filled with PCM in the basin. *Journal of Energy Storage*, *32*, 101992. https://doi.org/10.1016/j.est.2020.101992

Kabeel, A. E., Attia, M. E. H., El-Maghlany, W. M., Abdelgaied, M., & Elharidi, A. M. (2022). Finest concentration of phosphate grains as energy storage medium to improve hemispherical solar distillate: An experimental study. *Alexandria Engineering Journal*, *61*(7), 5573–5583. https://doi.org/10.1016/j.aej.2021.11.014

Kabeel, A. E., Harby, K., Abdelgaied, M., & Eisa, A. (2020a). A comprehensive review of tubular solar still designs, performance, and economic analysis. *Journal of Cleaner Production*, *246*, 119030. https://doi.org/10.1016/j.jclepro.2019.119030

Kabeel, A. E., Harby, K., Abdelgaied, M., & Eisa, A. (2020b). Performance of the modified tubular solar still integrated with cylindrical parabolic concentrators. *Solar Energy*, *204*, 181–189. https://doi.org/10.1016/j.solener.2020.04.080

Kabeel, A. E., Harby, K., Abdelgaied, M., & Eisa, A. (2021). Performance improvement of a tubular solar still using V-corrugated absorber with wick materials: Numerical and experimental investigations. *Solar Energy*, *217*, 187–199. https://doi.org/10.1016/j.solener.2021.02.008

Kabeel, A. E., Sharshir, S. W., Abdelaziz, G. B., Halim, M. A., & Swidan, A. (2019). Improving performance of tubular solar still by controlling the water depth and cover cooling. *Journal of Cleaner Production*, *233*, 848–856. https://doi.org/10.1016/j.jclepro.2019.06.104

Kaushal, A. & Varun. (2010). Solar stills: A review. *Renewable and Sustainable Energy Reviews*, *14*(1) , 446–453. https://doi.org/10.1016/j.rser.2009.05.011

Khalifa, A. J. N. (2011). On the effect of cover tilt angle of the simple solar still on its productivity in different seasons and latitudes. *Energy Conversion and Management*, *52*, 431–436. https://doi.org/10.1016/j.enconman.2010.07.018

Khanmohammadi, S., & Khanjani, S. (2021). Experimental study to improve the performance of solar still desalination by hydrophobic condensation surface using cold plasma technology. *Sustainability Energy Technologies and Assessments*, *45*, 101129. https://doi.org/10.1016/j.seta.2021.101129

Khechekhouche, A., Benhaoua, B., A.M.Manokar, Kabeel, A. E., & Sathyamurthy, R. (2019). Exploitation of an insulated air chamber as a glazed cover of a conventional solar still. *Heat Transfer-Asian Research*, *48*(5), 1563–1574. https://doi.org/10.1002/htj.21446

Lee, A., Moon, M. W., Lim, H., Kim, W. D., & Kim, H. Y. (2012). Water harvest via dewing. *Langmuir*, *28*(27), 10183–10191. https://doi.org/10.1021/la3013987

Lee, J., Lee, S., & Lee, J. (2020). Improved humid air condensation heat transfer through promoting condensate drainage on vertically stripe patterned bi-philic surfaces. *International Journal of Heat and Mass Transfer*, *160*, 120206. https://doi.org/10.1016/j.ijheatmasstransfer.2020.120206

Liljenström, C., Lazarevic, D., & Finnveden, G. (2013). *Silicon-based nanomaterials in a life-cycle perspective, including a case study on self-cleaning coatings*. KTH - Royal Institute of Technology. https://www.kth.se/abe/om-skolan/organisation/inst/see/om/avd/fms

Maheswari, K. S., Mayandi, K., Joe Patrick Gnanaraj, S., & Appadurai, M. (2022). Effect of transparent glass cover material on double slope solar still productivity. *Materials Today: Proceedings*, *62*, 5415–5419. https://doi.org/10.1016/j.matpr.2022.03.702

Mamlook, R., & Badran, O. (2007). Fuzzy sets implementation for the evaluation of factors affecting solar still production. *Desalination*, *203*(1–3), 394–402. https://doi.org/10.1016/j.desal.2006.02.024

Manokar, A. M., Kalidasa Murugavel, K., & Esakkimuthu, G. (2014). Different parameters affecting the rate of evaporation and condensation on passive solar still—A review. *Renewable and Sustainable Energy Reviews*, *38*, 309–322. https://doi.org/10.1016/j.rser.2014.05.092

Manokar, A. M., Prince Winston, D., Sathyamurthy, R., Kabeel, A. E., & Rama Prasath, A. (2018). Experimental investigation on pyramid solar still in passive and active mode. *Heat and Mass Transfer, 55*, 1045–1058. https://doi.org/10.1007/s00231-018-2483-3

Manokar, A. M., Taamneh, Y., Kabeel, A. E., Prince Winston, D., Vijayabalan, P., Balaji, D., Sathyamurthy, R., Padmanaba Sundar, S., & Mageshbabu, D. (2020). Effect of water depth and insulation on the productivity of an acrylic pyramid solar still

– An experimental study. *Groundwater for Sustainable Development*, *10*, 100319. https://doi.org/10.1016/j.gsd.2019.100319

MET Malaysia. (2019). *Annual Report 2019*. Malaysian Meteorological Department, Ministry of Environment and Water.

Mishra, A. K., Meraj, M., Tiwari, G. N., & Ahmad, A. (2021). Effect of inclination on internal heat and mass transfer of active solar still having conical condensing cover. *Materials Today: Proceedings*, *38*, 105–111. https://doi.org/10.1016/j.matpr.2020.06.105

Mishra, A. K., Meraj, Md., Nath Tiwari, G., Ahmad, A., & Zaheen Khan, M. (2021). Parametric studies of PVT-CPC active conical solar still. *Materials Today: Proceedings, 46*, 6660–6664. https://doi.org/10.1016/j.matpr.2021.04.115

Mohaisen, H. S., Esfahani, J. A., & Ayani, M. B. (2021). Improvement in the performance and cost of passive solar stills using a finned-wall/built-in condenser: An experimental study. *Renewable Energy*, *168*, 170–180. https://doi.org/10.1016/j.renene.2020.12.056

Mohsenzadeh, M., Aye, L., & Christopher, P. (2021). A review on various designs for performance improvement of passive solar stills for remote areas. *Solar Energy*, *228*, 594–611. https://doi.org/10.1016/j.solener.2021.09.086

Morad, M. M., El-Maghawry, H. A. M., Wasfy, K. I., Faegh, M., Shafii, M. B., Arunkumar, T., Ao, Y., Luo, Z., Zhang, L., Li, J., Denkenberger, D., Wang, J., Al-Madhhachi, H., Min, G., Al-Nimr, M. A., Qananba, K. S., Remeli, M. F., Singh, B., Amirah, N., … Bahiraei, M. (2015). Improving the double slope solar still performance by using flat-plate solar collector and cooling glass cover. *Desalination*, *373*(1), 1–9. https://doi.org/10.1016/j.desal.2015.06.017

Mousa, H., & Arabi, M. A. (2013). Desalination and hot water production using solar still enhanced by external solar collector. *Desalination and Water Treatment*, *51*(4–6), 1296–1301. https://doi.org/10.1080/19443994.2012.699237

Mu, L., Chen, L., Lin, L., Park, Y. H., Wang, H., Xu, P., Kota, K., & Kuravi, S. (2021). An overview of solar still enhancement approaches for increased freshwater production rates from a thermal process perspective. *Renewable and Sustainable Energy Reviews*, *150*, 111458. https://doi.org/10.1016/j.rser.2021.111458

Nayi, K. H., & Modi, K. V. (2018). Pyramid solar still: A comprehensive review. *Renewable and Sustainable Energy Reviews*, *81*, 136–148. https://doi.org/10.1016/j.rser.2017.07.004

Nazari, S., & Daghigh, R. (2022). Techno-enviro-exergo-economic and water hygiene assessment of non-cover box solar still employing parabolic dish concentrator and thermoelectric peltier effect. *Process Safety and Environmental Protection*, *162*, 566–582. https://doi.org/10.1016/j.psep.2022.04.006

Nazari, S., Safarzadeh, H., & Bahiraei, M. (2019a). Experimental and analytical investigations of productivity, energy and exergy efficiency of a single slope solar

still enhanced with thermoelectric channel and nanofluid. *Renewable Energy*, *135*, 729–744. https://doi.org/10.1016/j.renene.2018.12.059

Nazari, S., Safarzadeh, H., & Bahiraei, M. (2019b). Performance improvement of a single slope solar still by employing thermoelectric cooling channel and copper oxide nanofluid: An experimental study. *Journal of Cleaner Production*, *208*, 1041–1052. https://doi.org/10.1016/j.jclepro.2018.10.194

Nguyen-Tri, P., Tran, H. N., Plamondon, C. O., Tuduri, L., Vo, D.-V. N., Nanda, S., Mishra, A., Chao, H.-P., & Bajpai, A. K. (2019). Recent progress in the preparation, properties and applications of superhydrophobic nano-based coatings and surfaces: A review. *Progress in Organic Coatings*, *132*, 235–256. https://doi.org/10.1016/j.porgcoat.2019.03.042

Omara, Z. M., Abdullah, A. S., Kabeel, A. E., & Essa, F. A. (2017). The cooling techniques of the solar stills' glass covers – A review. *Renewable and Sustainable Energy Reviews*, *78*, 176–193. https://doi.org/10.1016/j.rser.2017.04.085

Ouar, M. L. A., Sellami, M. H., Meddour, S. E., Touahir, R., Guemari, S., & Loudiyi, K. (2017). Experimental yield analysis of groundwater solar desalination system using absorbent materials. *Groundwater for Sustainable Development*, *5*, 261–267. https://doi.org/10.1016/j.gsd.2017.08.001

Panchal, H. N., & Patel, S. (2017). An extensive review on different design and climatic parameters to increase distillate output of solar still. *Renewable and Sustainable Energy Reviews*, *69*, 750–758. https://doi.org/10.1016/j.rser.2016.09.001

Panchal, H. N., Sadasivuni, K. K., Ahmed, A. A. A., Hishan, S. S., Doranehgard, M. H., Essa, F. A., Shanmugan, S., & Khalid, M. (2021). Graphite powder mixed with black paint on the absorber plate of the solar still to enhance yield: An experimental investigation. *Desalination*, *520*, 115349. https://doi.org/10.1016/j.desal.2021.115349

Panchal, H. N., Sadasivuni, K. K., Israr, M., & Thakar, N. (2019). Various techniques to enhance distillate output of tubular solar still: A review. *Groundwater for Sustainable Development*, *9*, 100268. https://doi.org/10.1016/j.gsd.2019.100268

Panchal, H. N., Sadasivuni, K. K., Prajapati, C., Khalid, M., Essa, F. A., Shanmugan, S., Pandya, N., Suresh, M., Israr, M., Dharaskar, S., & Khechekhouche, A. (2020). Productivity enhancement of solar still with thermoelectric modules from groundwater to produce potable water: A review. *Groundwater for Sustainable Development*, *11*, 100429. https://doi.org/10.1016/j.gsd.2020.100429

Parsa, S. M., Rahbar, A., Javadi Y, D., Koleini, M. H., Afrand, M., & Amidpour, M. (2020). Energy-matrices, exergy, economic, environmental, exergoeconomic, enviroeconomic, and heat transfer (6E/HT) analysis of two passive/active solar still water desalination nearly 4000m: Altitude concept. *Journal of Cleaner Production*, *261*, 121243. https://doi.org/10.1016/j.jclepro.2020.121243

Parsa, S. M., Rahbar, A., Koleini, M. H., Aberoumand, S., Afrand, M., & Amidpour, M. (2020). A renewable energy-driven thermoelectric-utilized solar still with external condenser loaded by silver/nanofluid for simultaneously water disinfection and

desalination. *Desalination*, *480*, 114354. https://doi.org/10.1016/j.desal.2020.114354

Parsa, S. M., Yazdani, A., Javadi, D., Afrand, M., Karimi, N., & Ali, H. M. (2022). Selecting efficient side of thermoelectric in pyramid-shape solar desalination units incorporated phase change material (PCM), nanoparticle, turbulator with battery storage powered by photovoltaic. *J. Energy Storage*, *51*, 104448. https://doi.org/10.1016/j.est.2022.104448

Patel, S. K., & Modi, K. V. (2020). Techniques to improve the performance of enhanced condensation area solar still: A critical review. *Journal of Cleaner Production*, *268*, 122260. https://doi.org/10.1016/j.jclepro.2020.122260

Peng, G., Sharshir, S. W., Hu, Z., Ji, R., Ma, J., Kabeel, A. E., Liu, H., Zang, J., & Yang, N. (2021). A compact flat solar still with high performance. *International Journal of Heat and Mass Transfer*, *179*, 121657. https://doi.org/10.1016/j.ijheatmasstransfer.2021.121657

Peng, G., Sharshir, S. W., Wang, Y., An, M., Ma, D., Zang, J., Kabeel, A. E., & Yang, N. (2021). Potential and challenges of improving solar still by micro/nano-particles and porous materials—A review. *Journal of Cleaner Production*, *311*, 127432. https://doi.org/10.1016/j.jclepro.2021.127432

Pounraj, P., Prince Winston, D., Kabeel, A. E., Praveen Kumar, B., Manokar, A. M., Sathyamurthy, R., & Christabel, S. C. (2018). Experimental investigation on Peltier based hybrid PV/T active solar still for enhancing the overall performance. *Energy Conversion and Management*, *168*, 371–381. https://doi.org/10.1016/j.enconman.2018.05.011

Pourkiaei, S. M., Ahmadi, M. H., Sadeghzadeh, M., Moosavi, S., Pourfayaz, F., Chen, L., Pour Yazdi, M. A., & Kumar, R. (2019). Thermoelectric cooler and thermoelectric generator devices: A review of present and potential applications, modeling and materials. *Energy*, *186*, 115849. https://doi.org/10.1016/j.energy.2019.07.179

Rahbar, N., Asadi, A., & Fotouhi-Bafghi, E. (2018). Performance evaluation of two solar stills of different geometries: Tubular versus triangular: Experimental study, numerical simulation, and second law analysis. *Desalination*, *443*, 44–55. https://doi.org/10.1016/j.desal.2018.05.015

Rahbar, N., & Esfahani, J. A. (2012). Experimental study of a novel portable solar still by utilizing the heatpipe and thermoelectric module. *Desalination*, *284*, 55–61. https://doi.org/10.1016/j.desal.2011.08.036

Rahbar, N., & Esfahani, J. A. (2013). Productivity estimation of a single-slope solar still: Theoretical and numerical analysis. *Energy*, *49*, 289–297. https://doi.org/10.1016/j.energy.2012.10.023

Rahbar, N., Esfahani, J. A., & Asadi, A. (2016). An experimental investigation on productivity and performance of a new improved design portable asymmetrical solar still utilizing thermoelectric modules. *Energy Conversion and Management*, *118*, 55–62. https://doi.org/10.1016/j.enconman.2016.03.052

Rahbar, N., Gharaiian, A., & Rashidi, S. (2017). Exergy and economic analysis for a double slope solar still equipped by thermoelectric heating modules—An experimental investigation. *Desalination*, *420*, 106–113. https://doi.org/10.1016/j.desal.2017.07.005

Raluy, R. G., Serra, L., & Uche, J. (2005). Life Cycle Assessment of Water Production Technologies—Part 1: Life Cycle Assessment of Different Commercial Desalination Technologies (MSF, MED, RO) (9 pp). *The International Journal of Life Cycle Assessment*, *10*(4), 285–293. https://doi.org/10.1065/lca2004.09.179.1

Remeli, M. F., Singh, B., Amirah, N., Meon, M. S., & Fadilla, W. N. (2019). Solar Distillation Thermoelectric Power Generation. *IOP Conference Series: Earth and Environmental Science*, *268*(1), 012022. https://doi.org/10.1088/1755-1315/268/1/012022

Sadeghi, G., & Nazari, S. (2021). Retrofitting a thermoelectric-based solar still integrated with an evacuated tube collector utilizing an antibacterial-magnetic hybrid nanofluid. *Desalination*, *500*, 114871. https://doi.org/10.1016/j.desal.2020.114871

Saini, V., L.Sahota, Jain, V. K., & Tiwari, G. N. (2019). Performance and cost analysis of a modified built-in-passive condenser and semitransparent photovoltaic module integrated passive solar distillation system. *Journal of Energy Storage*, *24*, 100809. https://doi.org/10.1016/j.est.2019.100809

Sardarabadi, M., Passandideh-Fard, M., & Zeinali Heris, S. (2014). Experimental investigation of the effects of silica/water nanofluid on PV/T (photovoltaic thermal units). *Energy*, *66*, 264–272. https://doi.org/10.1016/j.energy.2014.01.102

Sathyamurthy, R., Kennady, H. J., Nagarajan, P. K., & Ahsan, A. (2014). Factors affecting the performance of triangular pyramid solar still. *Desalination*, *344*, 383–390. https://doi.org/10.1016/j.desal.2014.04.005

Serrano, M., & Moreno, J. C. (2020). Spectral transmission of solar radiation by plastic and glass material. *Journal of Photochemistry & Photobiology, B: Biology*, *208*, 111894. https://doi.org/10.1016/j.jphotobiol.2020.111894

Sharma, K., Hooda, A., Goyat, M. S., Rai, R., & Mittal, A. (2022). A review on challenges, recent progress and applications of silica nanoparticles based superhydrophobic coatings. *Ceramics International*, *48*(5), 5922–5938. https://doi.org/10.1016/j.ceramint.2021.11.239

Sharon, H., & Reddy, K. S. (2015). A review of solar driven desalination technologies. *Renewable and Sustainable Energy Reviews*, *41*, 1080–1118. https://doi.org/10.1016/j.rser.2014.09.002

Sharshir, S. W., Ellakany, Y. M., Algazzar, A. M., Elsheikh, A. H., Elkadeem, M. R., Edreis, E. M. A., Waly, A. S., Sathyamurthy, R., Panchal, H., & Elashry, M. S. (2019). A mini review of techniques used to improve the tubular solar still performance for solar water desalination. *Process Safety and Environmental Protection*, *124*, 204–212. https://doi.org/10.1016/j.psep.2019.02.020

Sharshir, S. W., Kandeal, A. W., Algazzar, A. M., Eldesoukey, A., El-Samadony, M. O. A., & Hussien, A. A. (2022). 4-E analysis of pyramid solar still augmented with external condenser, evacuated tubes, nanofluid and ultrasonic foggers: A comprehensive study. *Process Safety and Environmental Protection*, *164*, 408–417. https://doi.org/10.1016/j.psep.2022.06.026

Sharshir, S. W., Peng, G., Wu, L., Essa, F. A., Kabeel, A. E., & Yang, N. (2017). The effects of flake graphite nanoparticles, phase change material, and film cooling on the solar still performance. *Applied Energy*, *191*, 358–366. https://doi.org/10.1016/j.apenergy.2017.01.067

Sharshir, S. W., Yang, N., Peng, G., & Kabeel, A. E. (2016). Factors affecting solar stills productivity and improvement techniques: A detailed review. *Applied Thermal Engineering*, *100*, 267–284. https://doi.org/10.1016/j.applthermaleng.2015.11.041

Shen, C., Liu, L., Wu, S., Yao, F., & Zhang, C. (2020). Lattice Boltzmann simulation of droplet condensation on a surface with wettability gradient. *Proceedings of the Institution of Mechanical Engineers, Part C: Journal of Mechanical Engineering Science*, *234*(7), 1403–1413. https://doi.org/10.1177/0954406219898220

Shoeibi, S., Kargarsharifabad, H., Mirjalily, S. A. A., Sadi, M., & Arabkoohsar, A. (2022). A comprehensive review of nano-enhanced phase change materials on solar energy applications. *Journal of Energy Storage*, *50*, 104262. https://doi.org/10.1016/j.est.2022.104262

Shoeibi, S., Kargarsharifabad, H., & Rahbar, N. (2021). Effects of nano-enhanced phase change material and nano-coated on the performance of solar stills. *Journal of Energy Storage*, *42*, 103061. https://doi.org/10.1016/j.est.2021.103061

Shoeibi, S., Kargarsharifabad, H., Rahbar, N., Khosravi, G., & Sharifpur, M. (2022). An integrated solar desalination with evacuated tube heat pipe solar collector and new wind ventilator external condenser. *Sustainable Energy and Technologies Assessments*, *50*, 101857. https://doi.org/10.1016/j.seta.2021.101857

Shoeibi, S., Rahbar, N., Abedini Esfahlani, A., & Kargarsharifabad, H. (2020). Application of simultaneous thermoelectric cooling and heating to improve the performance of a solar still: An experimental study and exergy analysis. *Applied Energy*, *263*, 114581. https://doi.org/10.1016/j.apenergy.2020.114581

Shoeibi, S., Rahbar, N., Abedini Esfahlani, A., & Kargarsharifabad, H. (2021a). A comprehensive review of Enviro-Exergo-economic analysis of solar stills. *Renewable and Sustainable Energy Reviews*, *149*, 111404. https://doi.org/10.1016/j.rser.2021.111404

Shoeibi, S., Rahbar, N., Abedini Esfahlani, A., & Kargarsharifabad, H. (2021b). A review of techniques for simultaneous enhancement of evaporation and condensation rates in solar stills. *Solar Energy*, *225*, 666–693. https://doi.org/10.1016/j.solener.2021.07.028

Shoeibi, S., Rahbar, N., Abedini Esfahlani, A., & Kargarsharifabad, H. (2022). Energy matrices, economic and environmental analysis of thermoelectric solar

desalination using cooling fan. *Journal of Thermal Analysis and Calorimetry*, *147*(17), 9645–9660. https://doi.org/10.1007/s10973-022-11217-7

Shoeibi, S., Rahbar, N., Esfahlani, A. A., & Kargarsharifabad, H. (2021a). Energy matrices, exergoeconomic and enviroeconomic analysis of air-cooled and water-cooled solar still: Experimental investigation and numerical simulation. *Renewable Energy*, *171*, 227–244. https://doi.org/10.1016/j.renene.2021.02.081

Shoeibi, S., Rahbar, N., Esfahlani, A. A., & Kargarsharifabad, H. (2021b). Improving the thermoelectric solar still performance by using nanofluids– Experimental study, thermodynamic modeling and energy matrices analysis. *Sustainable Energy Technologies and Assessments*, *47*, 101339. https://doi.org/10.1016/j.seta.2021.101339

Singh, S. K., Kaushik, S. C., Tyagi, V. V., & Tyagi, S. K. (2021). Comparative Performance and parametric study of solar still: A review. *Sustainable Energy Technologies and Assessments*, *47*, 101541. https://doi.org/10.1016/j.seta.2021.101541

Sohani, A., Hoseinzadeh, S., & Berenjkar, K. (2021). Experimental analysis of innovative designs for solar still desalination technologies; An in-depth technical and economic assessment. *Journal of Energy Storage*, *33*, 101862. https://doi.org/10.1016/j.est.2020.101862

Som, C., Wick, P., Krug, H., & Nowack, B. (2011). Environmental and health effects of nanomaterials in nanotextiles and façade coatings. *Environment International*, *37*(6), 1131–1142. https://doi.org/10.1016/j.envint.2011.02.013

Song, J. W., & Fan, L. W. (2021). Temperature dependence of the contact angle of water: A review of research progress, theoretical understanding, and implications for boiling heat transfer. *Advances in Colloid and Interface Science*, *288*, 102339. https://doi.org/10.1016/j.cis.2020.102339

Tang, X., Huang, J., Guo, Z., & Liu, W. (2021). A combined structural and wettability gradient surface for directional droplet transport and efficient fog collection. *Journal of Colloid and Interface Science*, *604*, 526–536. https://doi.org/10.1016/j.jcis.2021.07.033

Thakur, A. K., Sathyamurthy, R., Velraj, R., Saidur, R., & Hwang, J.-Y. (2021). Augmented performance of solar desalination unit by utilization of nano-silicon coated glass cover for promoting drop-wise condensation. *Desalination*, *515*, 115191. https://doi.org/10.1016/j.desal.2021.115191

Thakur, A. K., Sathyamurthy, R., Velraj, R., Saidur, R., Lynch, I., Chaturvedi, M., & Sharshir, S. W. (2022). Synergetic effect of absorber and condenser nano-coating on evaporation and thermal performance of solar distillation unit for clean water production. *Solar Energy Materials and Solar Cells*, *240*, 111698. https://doi.org/10.1016/j.solmat.2022.111698

Tiwari, A. Kr., & Tiwari, G. N. (2005). Effect of the condensing cover's slope on internal heat and mass transfer in distillation: An indoor simulation. *Desalination*, *180*, 73–88. https://doi.org/10.1016/j.desal.2004.12.029

Tiwari, G. N., Dimri, V., & Chel, A. (2009). Parametric study of an active and passive solar distillation system: Energy and exergy analysis. *Desalination*, *242*(1–3), 1–18. https://doi.org/10.1016/j.desal.2008.03.027

Tiwari, G. N., Mishra, A. K., Meraj, Md., Ahmad, A., & Khan, M. E. (2020). Effect of shape of condensing cover on energy and exergy analysis of a PVT-CPC active solar distillation system. *Solar Energy*, *205*, 113–125. https://doi.org/10.1016/j.solener.2020.04.084

Tokunaga, A., & Tsuruta, T. (2020). Enhancement of condensation heat transfer on a microstructured surface with wettability gradient. *International Journal of Heat and Mass Transfer*, *156*, 119839. https://doi.org/10.1016/j.ijheatmasstransfer.2020.119839

Tuly, S. S., Rahman, M. S., Sarker, M. R. I., & Beg, R. A. (2021). Combined influence of fin, phase change material, wick, and external condenser on the thermal performance of a double slope solar still. *Journal of Cleaner Production*, *287*, 125458. https://doi.org/10.1016/j.jclepro.2020.125458

United Nations. (2022a). *Goal 6: Ensure availability and sustainable management of water and sanitation for all*.

United Nations. (2022b). *The Sustainable Development Goals Report*. United Nations Publications.

World Meteorological Organization. (2022). *Stubborn La Niña persists*. https://public.wmo.int/en/media/press-release/stubborn-la-nina-persists

Wu, S., Yu, C., Yu, F., & Chen, Y. (2018). Lattice Boltzmann simulation of co-existing boiling and condensation phase changes in a confined micro-space. *International Journal of Heat and Mass Transfer*, *126*, 773–782. https://doi.org/10.1016/j.ijheatmasstransfer.2018.05.139

Xie, J., She, Q., Xu, J., Liang, C., & Li, W. (2020). Mixed dropwise-filmwise condensation heat transfer on biphilic surface. *International Journal of Heat and Mass Transfer*, *150*, 119273. https://doi.org/10.1016/j.ijheatmasstransfer.2019.119273

Yousef, M. S., & Hassan, H. (2020). Energy payback time, exergoeconomic and enviroeconomic analyses of using thermal energy storage system with a solar desalination system: An experimental study. *Journal of Cleaner Production*, *270*, 122082. https://doi.org/10.1016/j.jclepro.2020.122082

Yousef, M. S., Hassan, H., & Sekiguchi, H. (2019). Energy, exergy, economic and enviroeconomic (4E) analyses of solar distillation system using different absorbing materials. *Applied Thermal Engineering*, *150*, 30–41. https://doi.org/10.1016/j.applthermaleng.2019.01.005

Zanganeh, P., Goharrizi, A. S., Ayatollahi, S., & Feilizadeh, M. (2019). Productivity enhancement of solar stills by nano-coating of condensing surface. *Desalination*, *454*, 1–9. https://doi.org/10.1016/j.desal.2018.12.007

Zanganeh, P., Goharrizi, A. S., Ayatollahi, S., & Feilizadeh, M. (2020). Nano-coated condensation surfaces enhanced the productivity of the single-slope solar still by changing the condensation mechanism. *Journal of Cleaner Production*, *265*, 121758. https://doi.org/10.1016/j.jclepro.2020.121758

Zanganeh, P., Goharrizi, A. S., Ayatollahi, S., Feilizadeh, M., & Dashti, H. (2020). Efficiency improvement of solar stills through wettability alteration of the condensation surface: An experimental study. *Applied Energy*, *268*, 114923. https://doi.org/10.1016/j.apenergy.2020.114923